Engineering Sciences Innovative Approaches

ISBN: 978-2-38236-178-8

LIVRE DE LYON

livredelyon.com
livredelyon
livredelyon
livredelyon

ENGINEERING SCIENCES
Innovative Approaches

Editor
Prof. Dr. Yeliz AŞÇI

LIVRE DE LYON
Lyon 2021

Editor • Prof. Dr. Yeliz AŞÇI • Orcid: 0000-0001-5618-058X

Cover Design • Mirajul Kayal

Book Layout • Clarica Consulting

First Published • September 2021, Lyon

ISBN: 978-2-38236-178-8

Publisher • Livre de Lyon
Address • 37 rue marietton, 69009, Lyon France
website • http://www.livredelyon.com
e-mail • livredelyon@gmail.com

PREFACE

Engineering is a discipline that is a bridge between science and technology and has an important place in the construction of the modern world. This book, titled “ENGINEERING SCIENCES: Innovative Approaches”, brings together study topics from different disciplines in the field of engineering. For this reason, it is aimed that this book will create a different perspective by recognizing each other's work by scientists doing research in the field of engineering. At the same time, this book will be an important resource for academics, researchers and students in line with this goal. I would like to express my endless thanks to all the authors who supported the book with their studies and shared the information, to the referees who contributed to the evaluation of the studies, and to Livre de Lyon publishing house, who made the studies turn into a book...

Prof. Dr. Yeliz AŞÇI

CONTENTS

CHAPTER I

CHARACTERISTICS OF ELECTROMAGNETIC WAVES PROPAGATING IN 2D PHOTONIC CRYSTALS

Ayse Nihan Basmaci

(Asst. Prof Dr.), *Tekirdag Namik Kemal University*, *Vocational School of Technical Sciences, Tekirdag, 59030, Turkey*
e-mail:anbasmaci@nku.edu.tr
Orcid: 0000-0003-3737-3751

1. Introduction

According to the rapid advances in fiber optics and satellite communication systems, the requirement for variable designs of photonic structures increases more and more. The design of photonic structures can be performed artificially in different ways (Barrientos-Garcia et al., 2016; Han et al., 2021; Li et al., 2016; Shalaev et al., 2019). The designs are generally made by combining at least two structures with different material properties by positioning them side by side (Basmaci, 2020; Hao et al., 2020; Hayrapetyan et al., 2016). These artificially designed structures are basically treated in two different ways, namely photonic structures using optic waves and phononic structures using acoustic waves. The propagation of optical waves basically takes place in line with the principles of electromagnetic wave propagation (Napolskii et al., 2020; Yang et al. 2008; Yablonovitch, 1994; Chen et al., 2017;

Yıldırım and Çelebi, 2015). On the other hand, wave propagation is also possible in phononic structures using acoustic principles (Arayantinos-Zafiris et al., 2021; Lu et al., 2017; Wang et al., 2015).

In order to determine the electromagnetic wave propagation behavior, the reflection and transmission conditions of the electromagnetic wave should also be investigated (Delihacıoğlu, 2014; Pandev and Suthar, 2021; Wei et al., 2021). In the literature, there are studies on the absorption of waves as well as studies on the transmission of waves (Hassan et al., 2019; Elakkiya et al., 2020; Kang et al., 2018; Wu and Gao, 2021). Studies on wave absorption have an important place, especially in defense industry applications. Stealthy technology is among the applications where absorption can be maximized by minimizing the reflection of electromagnetic waves. Carbon nanotube-based (CNT) radar absorption material (RAM) is used to provide electromagnetic wave absorption (Chen et al., 2011; Jeong et al., 2018; Zhang et al., 2015; Zohuri, 2020; Zou et al., 2015). In the case of electromagnetic wave reflection, when determining the propagation characteristic of the wave within the photonic structure, the angle of the wave when entering the structure is also taken into account (Chen et al., 2011; Kaya and Delihacioglu, 2014; Ge et al., 2018; Panyaev et al., 2021).

In this study, the behaviors of electromagnetic wave propagation in two-dimensional (2D), inhomogeneous photonic crystals, divided into different mediums, are investigated. It is assumed that the electromagnetic waves entering the 2D photonic crystals make certain angles with the normals while entering the photonic crystals. The electromagnetic waves that travel through the 2D photonic crystals encounter different mediums throughout the photonic crystals and each medium that the electromagnetic waves encounter has a homogeneous feature.

2. Theoretical Analysis

Figure 1 depicts an incident electromagnetic (EM) wave travelling at a certain angle with respect to the x-axis.

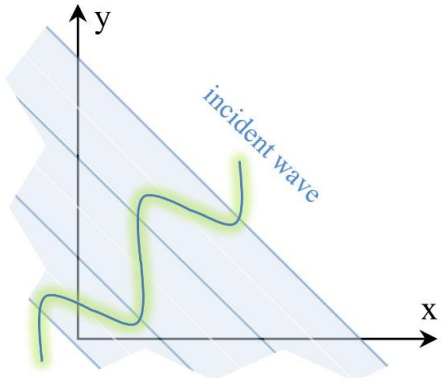

Figure. 1. An EM wave propagating in a vacuum

Figure 2 shows an inhomogeneous 2D photonic crystal. The 2D photonic crystal is divided into four different mediums, ensuring that each medium is isotropic and homogeneous. Besides, each medium of the photonic crystal has different material property parameters (ε, μ). Although each medium is isotropic and homogeneous, the whole of the photonic crystal is artificially in an inhomogeneous manner. The electromagnetic wave starts from the first medium of the 2D photonic crystal and travels through all the mediums of the 2D photonic crystal without loss.

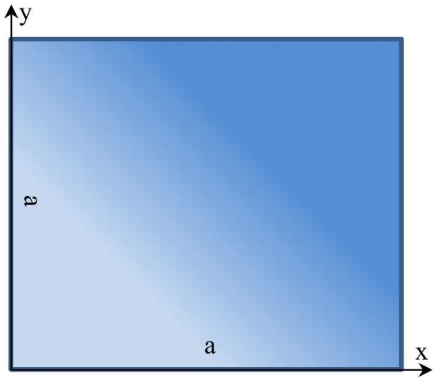

Figure 2. The inhomogeneous 2D photonic crystal

In a source free, linear, isotropic, and homogenous region, the first-order Maxwell's curl equations are as follows (Pozar, 2012):

$$\nabla x\vec{E} = -jf\mu\vec{H} \quad (1a)$$

$$\nabla x\vec{H} = -jf\epsilon\vec{E} \quad (1b)$$

where μ is the permeability, ϵ is the permittivity, $\vec{E}$ is the electrical field and $\vec{H}$ is the magnetic field.

In this study, the behaviors of the incident electromagnetic waves that enter the 2D photonic crystals at a certain angle and then travel through the 2D photonic crystals are examined. For this purpose, when $\vec{E}$ and $\vec{H}$ are expressed with the $u_i(x,y,t)$ function in the two-dimensional electromagnetic wave equation obtained after Equation (1a) and Equation (1b) are solved together, Equation (2) is obtained as in the following form:

$$\frac{\partial^2 u_i(x,y,t)}{\partial x^2} + \frac{\partial^2 u_i(x,y,t)}{\partial y^2} - \frac{1}{c^2}\frac{\partial^2 u_i(x,y,t)}{\partial t^2} = 0 \quad (2)$$

Equation (2) is an electromagnetic wave equation and equations for the incident and transmitted electromagnetic waves are required for the solution of Equation (2). Therefore, equations for the incident and transmitted waves are given by Equation (3a) and Equation (3b), respectively:

$$u_i(x,y,t) = U_1 e^{\mathrm{j}(f_i t - k_1 x - k_1 y)} + U_1 e^{\mathrm{j}(f_r t + k_1 x + k_1 y)} \quad (3a)$$

$$u_t(x,y,t) = U_2 e^{\mathrm{j}(f_t t - k_2 x - k_2 y)} \quad (3b)$$

where $\mathrm{j} = \sqrt{-1}$ is a fixed value, c is the speed of light, f is the angular frequency, f_i is the frequency of the incident electromagnetic wave, f_r is the frequency of the reflected electromagnetic wave, f_t is the frequency of the transmitted electromagnetic wave, k is the wavenumber, k_1 is the number of incident waves, k_2 is the number of the transmitted waves, u_i is the incident electromagnetic wave, and u_t is the transmitted electromagnetic wave.

By substituting the expressions given in Equation (3) in Equation (2), the frequencies of electromagnetic wave propagation in the homogeneous, isotropic 2D photonic crystal are obtained as follows:

$$k_m{}^2 + k_n{}^2 - (\varepsilon\mu)^2 f_{mn}{}^2 = 0 \tag{4a}$$

$$k_m{:}\frac{m\pi}{\mathrm{a}}, k_n{:}\frac{n\pi}{\mathrm{b}}\ and\ m{:}\ 0,1,2\ \ldots, n{:}\ 0,1,2\ \ldots, \tag{4b}$$

$$f_{mn} = \frac{\sqrt{\left(\frac{m\pi}{\mathrm{a}}\right)^2 + \left(\frac{n\pi}{\mathrm{b}}\right)^2}}{\varepsilon\mu} \tag{4c}$$

where k_m represents the traveling electromagnetic wave for the x-axis, k_n represents the traveling electromagnetic wave for the y-axis, f_{mn} represents the electromagnetic wave propagation frequencies, and both a and b represent the dimensions of the 2D photonic crystal.

The incident electromagnetic wave propagating at a certain angle to the first medium (Medium 1) of the 2D photonic crystal and then propagating through the second medium (Medium 2) at another angle is depicted in Figure 3.

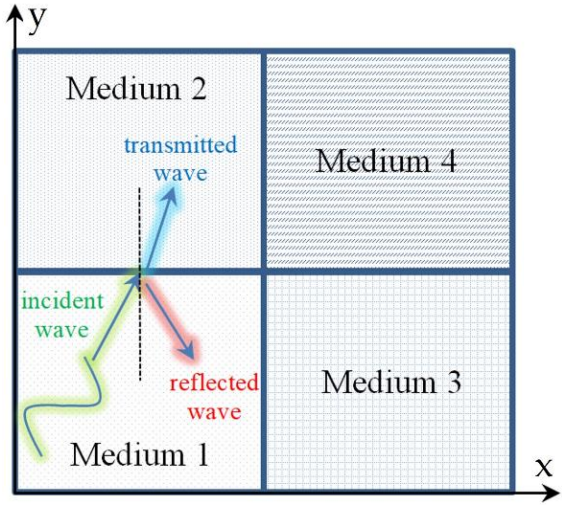

Figure 3. The EM wave propagation in different mediums of the 2D photonic crystal

As in Figure 3, the wavenumber of the electromagnetic wave traveling in medium 1 with a certain angle is expressed with k, while the wavenumbers of the incident, reflected, and transmitted waves are expressed as k_1, k_r, and k_t, respectively. The expressions regarding the wavenumbers of the incident, reflected, and transmitted waves are as follows:

$$k_1{}^2 = \frac{f_i{}^2 \beta_1{}^2}{c^2} \quad (5a)$$

$$k_r{}^2 = \frac{f_r{}^2 \beta_1{}^2}{c^2} \quad (5b)$$

$$k_t{}^2 = \frac{f_t{}^2 \beta_2{}^2}{c^2} \quad (5c)$$

where $\beta=\varepsilon\mu$ is the material property parameter. The value of β differs for each medium through which the electromagnetic wave propagates.

Figure 4 illustrates the incident electromagnetic wave traveling from the first medium to the second medium of the 2D photonic crystal at a certain angle of α_i. As seen in Figure 4, the transmitted electromagnetic wave that can propagate in the second medium continues to travel with a certain angle of α_t, and the electromagnetic wave that cannot propagate in the second medium is reflected with the α_r angle, which has the same value as the angle of α_i.

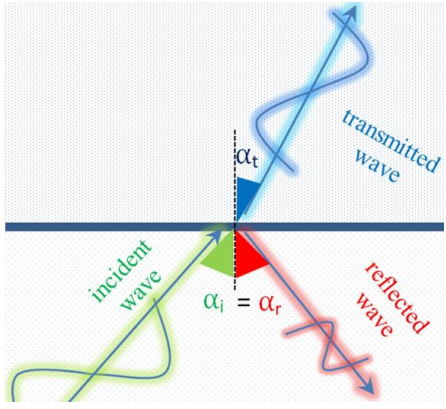

Figure 4. Angles of the EM waves traveling from the first medium to the second medium of the 2D photonic crystal

When 2D photonic crystal's material property parameter of the first medium (β_{m1}) and the material property parameter of the second medium (β_{m2}) are equal to each other, the reflection will not be observed and the electromagnetic wave would be completely transmitted. The value of the reflected wave energy given in Equation (6a) is obtained by expressing the number of waves given in Equation (5a) as k_n for medium number n, and as k_{n+1} for the next medium through which the electromagnetic wave can be propagated. Accordingly, the values of the transmission (*Γ)* and reflection (*Ψ)* of the electromagnetic waves are as follows:

$$\Gamma = \left(\frac{k_{n+1}\cos(\alpha_t) - k_n\cos(\alpha_i)}{k_{n+1}\cos(\alpha_t) + k_n\cos(\alpha_i)}\right)^2 \quad (6a)$$

$$\Psi = 1 - \Gamma \quad (6b)$$

where α_i and α_t represent the angle between the traveling wave and the normal and the angle between the transmitted wave and the normal, respectively.

The angles regarding the electromagnetic wave, which is transmitted from the first medium to the second medium of the 2D photonic crystal, are obtained by the Snell's law, as in the following form:

$$\beta_{m1}\sin(\alpha_i) = \beta_{m2}\sin(\alpha_t) \quad (7)$$

where β_{m1} and β_{m2} represent material property parameters of the first and second mediums of the 2D photonic crystal, respectively.

3. Results and Discussion

Depending on the material property parameters in each medium of 2D photonic crystals, the behaviors of the transmitted or absorbed electromagnetic waves change. In this section, the propagation and

the waveforms of the electromagnetic waves in each medium of two 2D photonic crystals with different material property parameters (β) are examined. These two 2D photonic crystals with different material property parameters are named S_1 and S_2 and can be seen in Figure 5 and Figure 6, respectively. Besides, as also seen in Figure 5 and Figure 6, the first medium, the second medium, the third medium, and the fourth medium for 2D photonic crystals are named M1, M2, M3, and M4, respectively. The values of the material property parameters of each medium of the 2D photonic crystals are given in Table 1. Accordingly, the transmission angles of the electromagnetic waves propagating through the first mediums of the two 2D photonic crystals are obtained for six different cases with respect to the incident electromagnetic waves' traveling angles. Figure 5a shows the first case named S_{1a} which the incident electromagnetic wave travels through M1 of S_1 with an α_i angle of 30°. Figure 5b shows the second case named S_{1b} which the incident electromagnetic wave travels through M1 of S_1 with an α_i angle of 45°. Figure 5c shows the third case named S_{1c} which the incident electromagnetic wave travels through M1 of S_1 with an α_i angle of 60°.

Table 1. Variation of material property parameters (β) in two 2D photonic crystal structures (S_1, S_2) with respect to the different mediums.

Structure	***Medium 1*** **(β_{m1})**	***Medium 2*** **(β_{m2})**	***Medium 3*** **(β_{m3})**	***Medium 4*** **(β_{m4})**
S_1	4.00	4.50	4.75	5.00
S_2	5.00	4.75	4.50	4.00

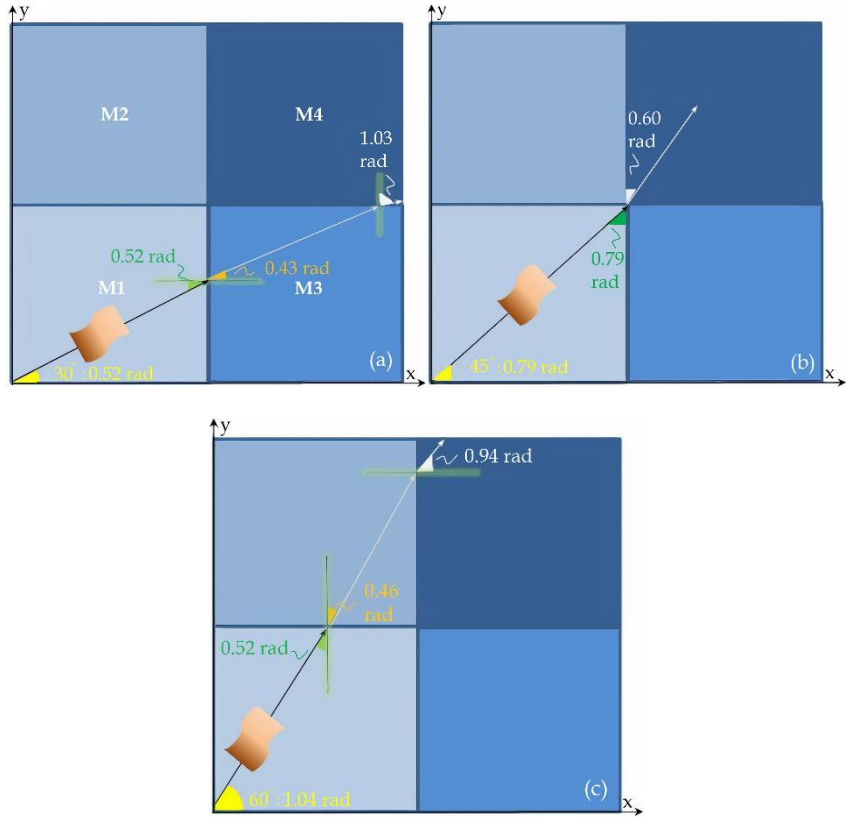

Figure 5. The transmitted electromagnetic wave angles for (a) Case S_{1a}, (b) Case S_{1b}, and (c) Case S_{1c}

It is assumed that the incident electromagnetic waves that enter the 2D photonic crystals named S_1 and S_2, whose material property parameters of the mediums can be seen in Table 1, always enter from M1. Figure 5 and Figure 6 show the travel of the transmitted electromagnetic waves. As can be seen from the figures, the reflected electromagnetic waves also travel. However, it is assumed that the travels of the reflected electromagnetic waves are limited only to the mediums in which they are reflected. In the 2D photonic crystal named S1, the incident electromagnetic waves travel from the mediums with the low-value material property parameters to the mediums with the high-value material property parameters.

In the 2D photonic crystal named S2, the mediums are arranged with the opposite logic of the S1 structure in terms of material property parameters. In other words, the travels of the electromagnetic waves in S2 are from the mediums with the high-material property parameters to the mediums with the low-material property parameters. Figure 6a shows the fourth case named S_{2a} which the incident electromagnetic wave travels through M1 of S_2 with an α_i angle of 30˚. Figure 6b shows the fifth case named S_{2b} which the incident electromagnetic wave travels through M1 of S_2 with an α_i angle of 45˚. Figure 6c shows the sixth case named S_{2c} which the incident electromagnetic wave travels through M1 of S_2 with an α_i angle of 60˚. It should be noted that, for S2, the refraction is greater in the mediums where the material property parameters have the highest values.

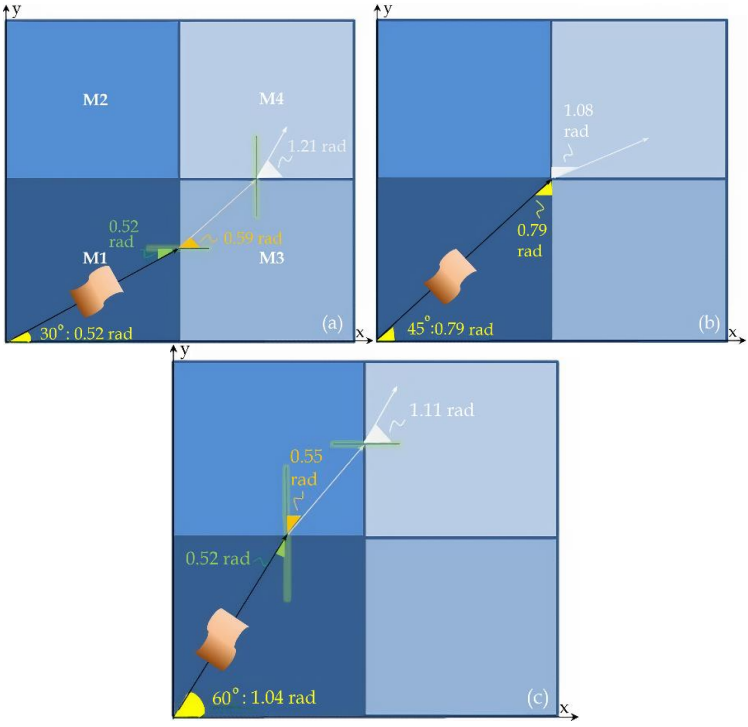

Figure 6. The transmitted EM wave angles for
(a) Case S_{2a}, (b) Case S_{2b}, and (c) Case S_{2c}

In Case S_{1a}, the incident wave is transmitted from M1 to M3 and then from M3 to M4. Since the incident angle is 45˚ in Case S_{1b}, the incident wave only is transmitted from M1 to M3. In Case S_{1c}, the incident wave is transmitted from M1 to M2 and then from M2 to M4. Figure 7 shows the reflection and transmission values for all S_{1a}, S_{1b}, S_{1c} cases.

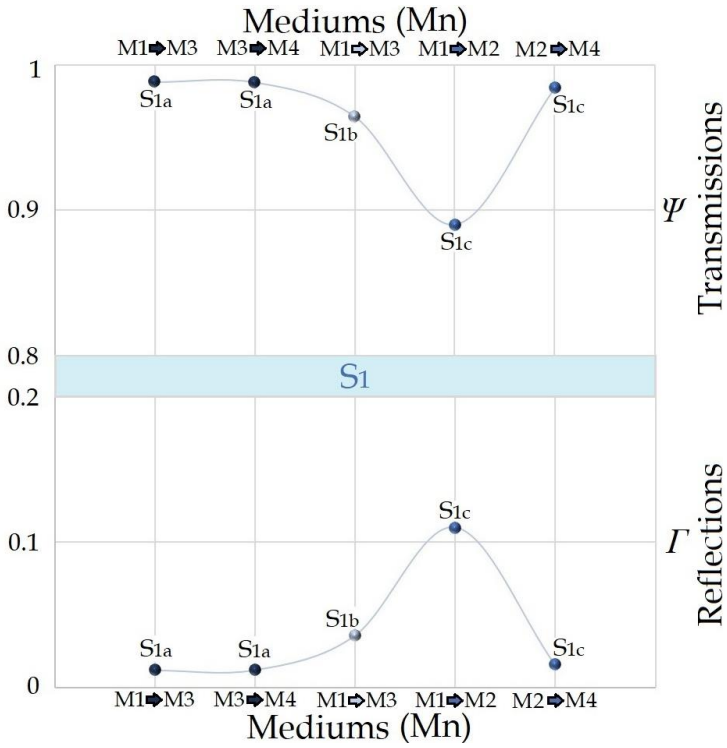

Figure 7. The values of reflection and transmission for S_{1a}, S_{1b}, S_{1c} cases

In Case S_{2a}, the incident wave is transmitted from M1 to M3 and then from M3 to M4. Since the incident angle is 45˚ in Case S_{1b}, the incident wave is only transmitted from M1 to M4. In Case S_{1c}, the incident wave is transmitted from M1 to M2 and then from M2 to M4. Figure 7 shows the reflection and transmission values for all S_{2a}, S_{2b}, S_{2c} cases.

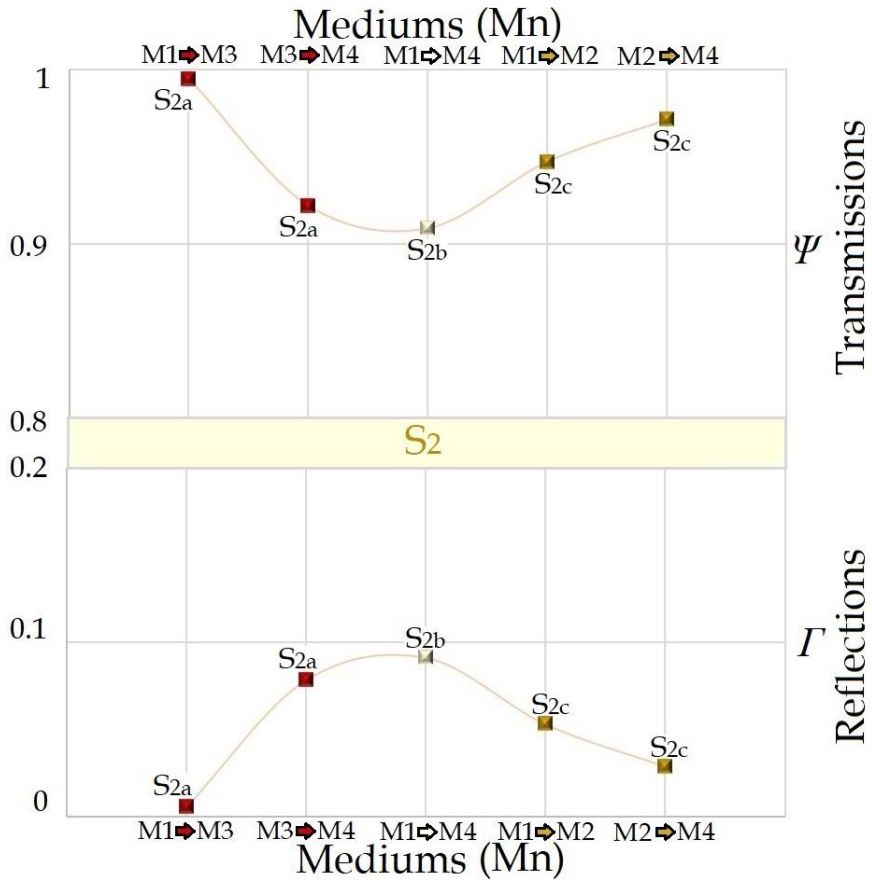

Figure 8. The values of reflection and transmission for S_{2a}, S_{2b}, S_{2c} cases

In Figures 9-13, the waveforms of the transmitted and the reflected electromagnetic waves obtained for the S_{1a}, S_{1b}, S_{1c} cases are shown. Waveforms of the transmitted and the reflected electromagnetic waves obtained for cases S_{2a}, S_{2b}, S_{2c} are shown in Figures 14-18. While amplitudes related to the transmission values of the waveforms of the transmitted and the reflected electromagnetic waves are obtained by using Equation (6), the frequencies related to the waveforms of the electromagnetic waves are obtained by using Equation (4) and Equation (5).

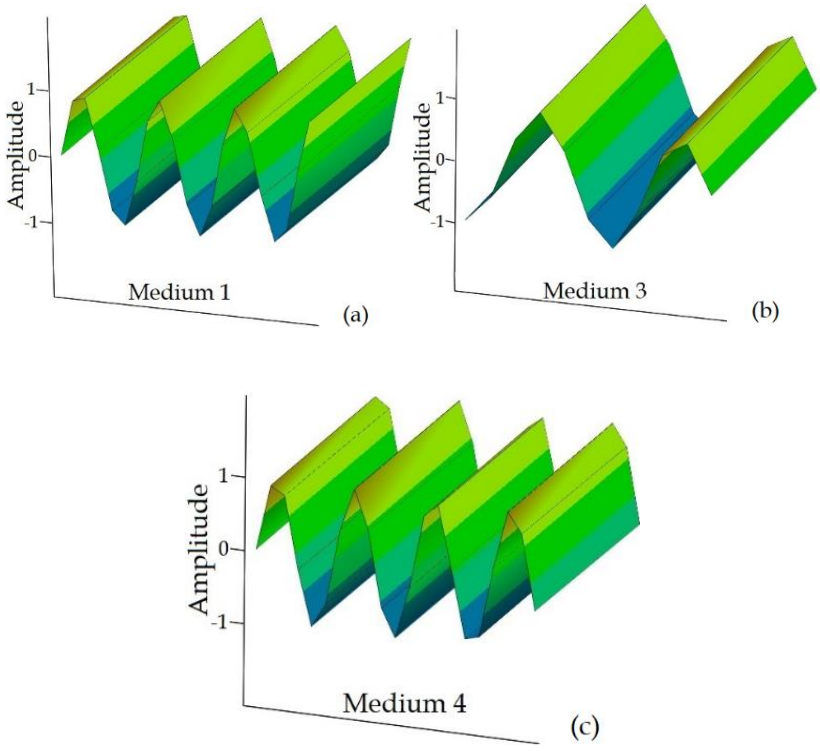

Figure 9. The EM waveforms of the transmitted waves for case S_{1a} in (a) M1, (b) M3, and (c) M4

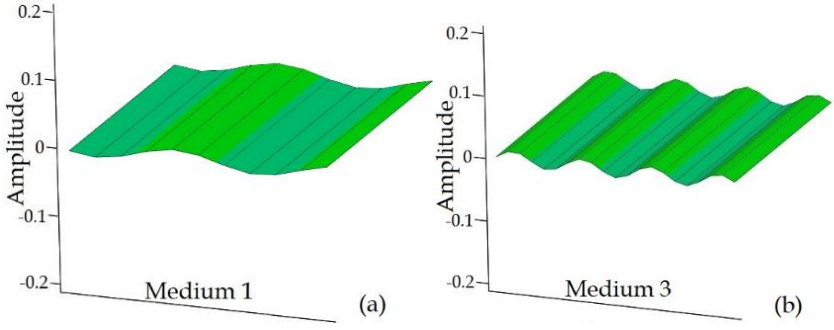

Figure 10. The EM waveforms of the reflected waves for case S_{1a} in (a) M1 and (b) M3

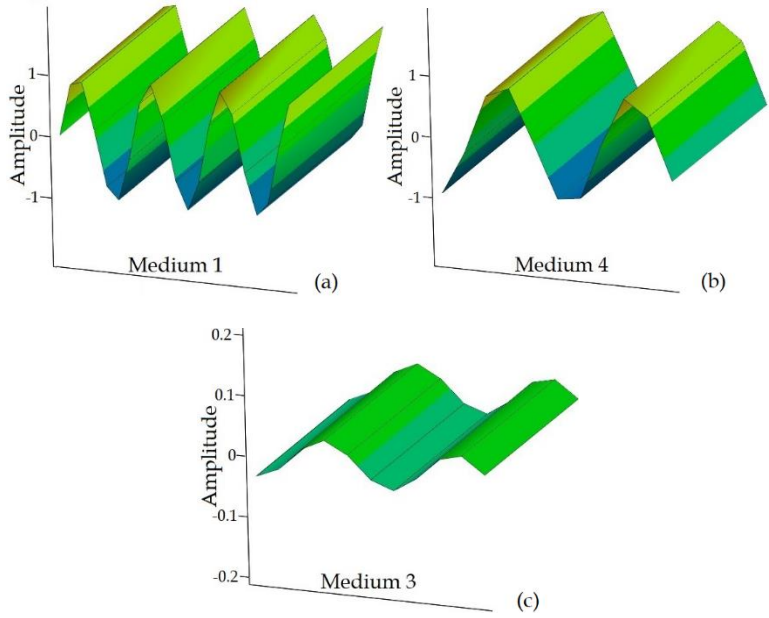

Figure 11. For case S_{1b}, (a) the EM waveform of the transmitted wave in M1, (b) the EM waveform of the transmitted wave in M4, and (c) the EM waveform of the reflected wave in M3

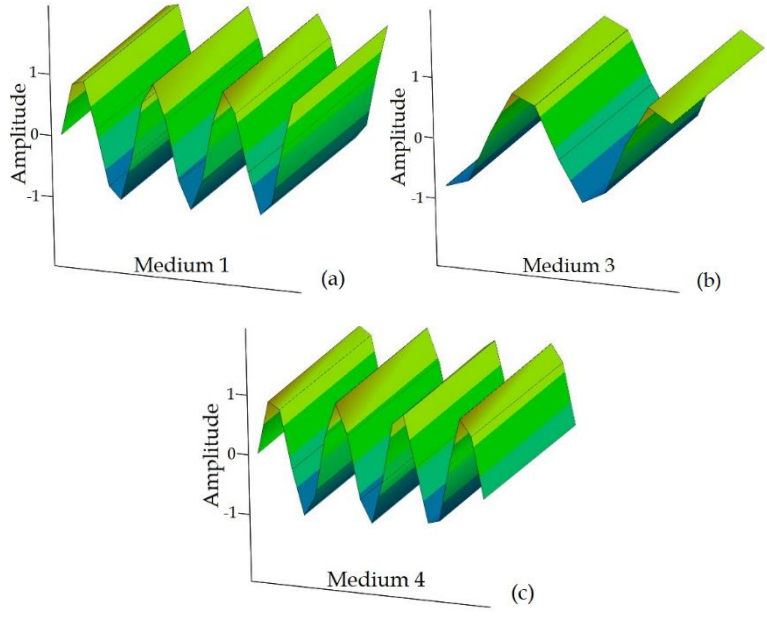

Figure 12. The EM waveforms of the transmitted waves for case S_{1c} in (a) M1, (b) M3, and (c) M4

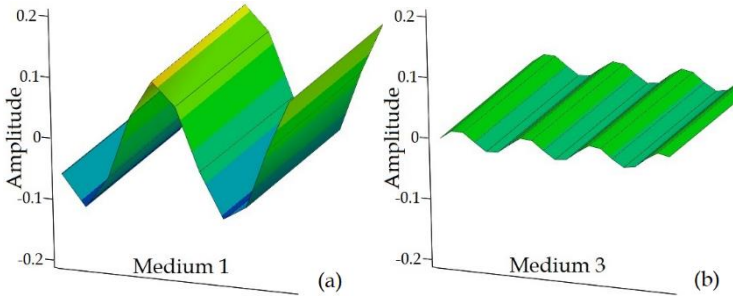

Figure 13. The EM waveforms of the reflected waves for case S_{1c} in (a) M1 and (b) M3

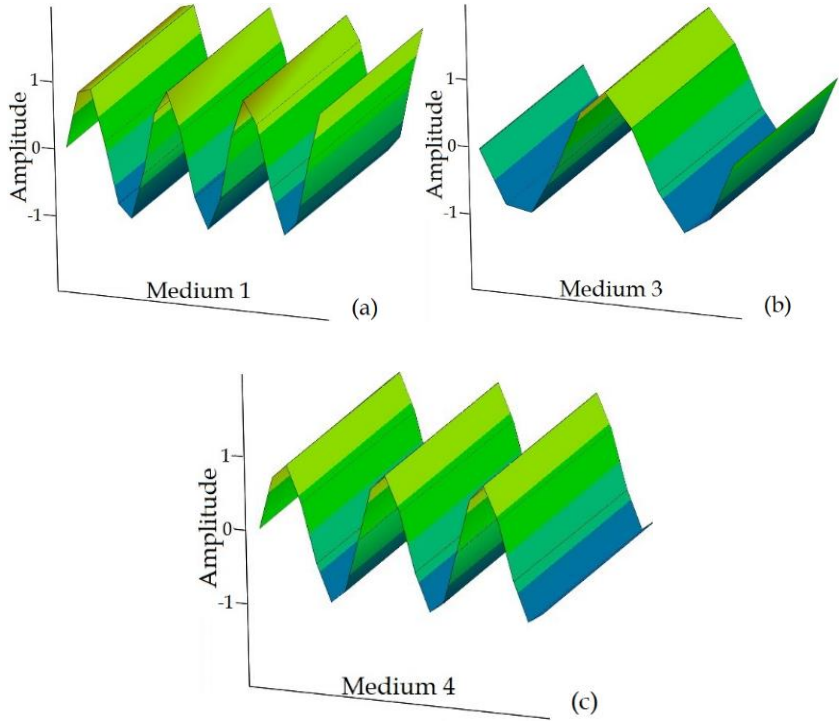

Figure 14. The EM waveforms of the transmitted waves for case S_{2a} in (a) M1, (b) M3, and (c) M4

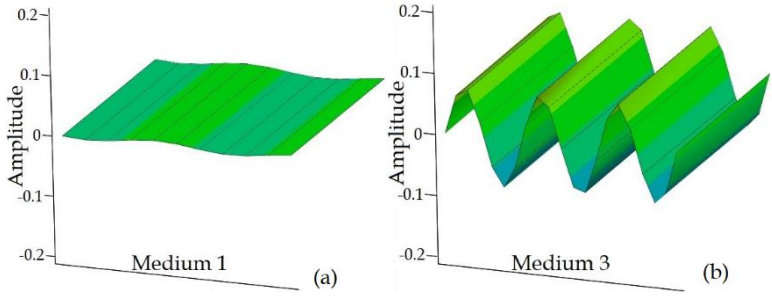

Figure 15. The EM waveforms of the reflected waves for case S_{2a} in (a) M1 and (b) M3

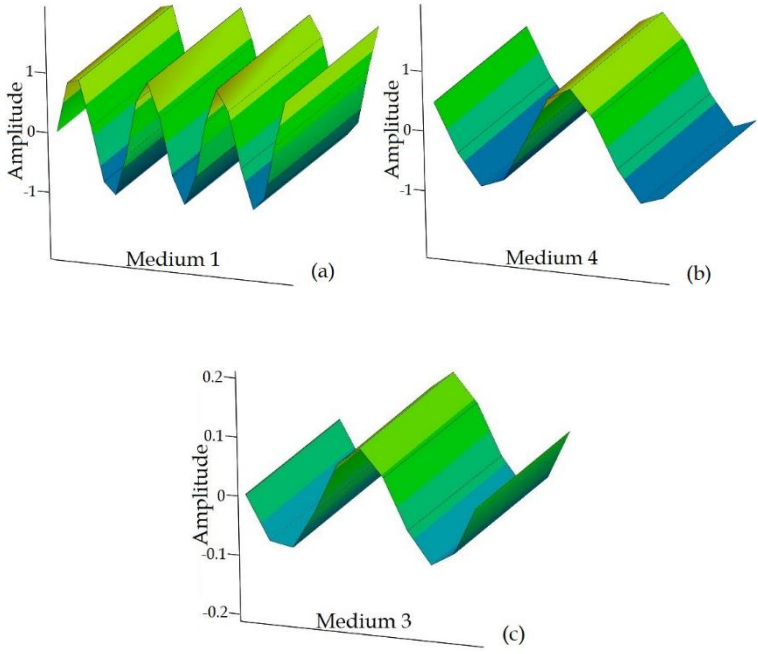

Figure 16. For case S_{2b}, (a) the EM waveform of the transmitted wave in M1, (b) the EM waveform of the transmitted wave in M4, and (c) the EM waveform of the reflected wave in M3

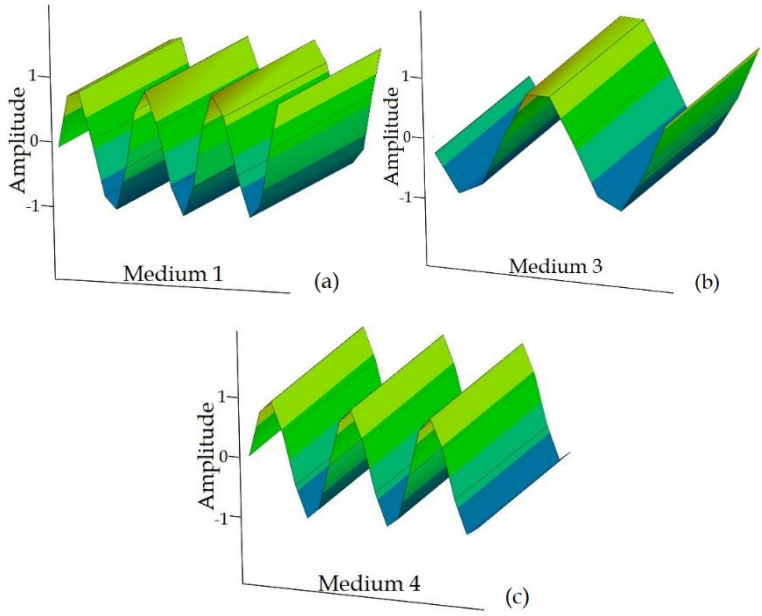

Fig. 17. The EM waveforms of the transmitted waves for case S_{2c} in (a) M1, (b) M3, and (c) M4

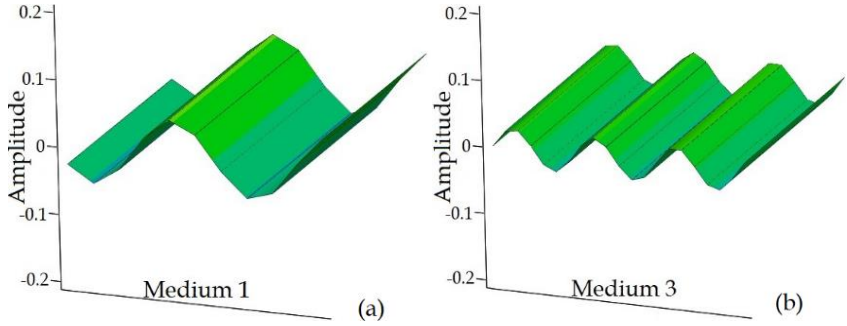

Figure 18. The EM waveforms of the reflected waves for case S_{2c} in (a) M1 and (b) M3

Since the material property parameters of each medium of the examined 2D photonic crystals have close values, all transmission values obtained for six different cases of two 2D photonic crystals are obtained at greater than 0.89. When the reflected electromagnetic waves are examined, the least transmission value among the three different cases

of S_1 is obtained for the case S_{1c}, whereas the least transmission value among the three different cases of S_2 is obtained for case S_{2b}. Accordingly, while the transmission value for S_1 is obtained at a minimum 0.89; for S_2, this value is obtained at 0.90. The highest transmission values for S_1 and S_2 are obtained at 0.99 and 0.98 for the S_{1a} and S_{2a} cases, respectively.

4. Conclusions

In this study, electromagnetic wave propagation behaviors of two 2D photonic crystal structures, named S_1 and S_2, each of which is divided into four different mediums, are investigated. The mediums of the photonic crystal named S_1 are arranged from the medium with the low-value material property parameter to the medium with the high-value material property parameter. In the mediums of the photonic crystal named S_2, this sequence is from the medium with a high-value material property parameter to the medium with the low-value material property parameter. When electromagnetic wave propagation is examined in 2D photonic crystals, transmission is obtained at a value in the range of 0.89 to 0.99. The reason why the transmission is obtained at high values is that the values of the material property parameters of the mediums of 2D photonic crystals are close to each other.

In future studies, with a different approach, it is possible that a similar analysis can be applied to 2D photonic crystals with anisotropic material characteristics and three-dimensional (3D) photonic crystals.

References

Aravantinos-Zafiris N., Lucklum F. & Sigalas M. M. (2021). Complete phononic band gaps in the 3D Yablonovite structure with spheres. *Ultrasonics*, *110*, 106265.

https://doi.org/10.1016/j.ijleo.2020.164794

Barrientos-Garcia A., Sukhoivanov I. A., Andre-Lucio J. A., Hernandez-Garcia J. C., Ramos-Ortiz G., Ibarra-Manzano O. G. & Guryev I. V. (2016). Numerical analysis of supercontinuum generation in photonic-crystal fibers with zero dispersion wavelengths in telecommunication Windows. *Optik, 127*, 10981-10990.
https://doi.org/10.1016/j.ijleo.2016.08.111

Basmaci A. N. (2020). Characteristics of electromagnetic wave propagation in a segmented photonic waveguide. *Journal of Optoelectronics and Advanced Materials*, *22*, 452-460.
https://joam.inoe.ro/articles/characteristics-of-electromagnetic-wave-propagation-in-a-segmented-photonic-waveguide/fulltext

Chen M., Zhu Y., Pan Y., Kou H., Xu H. & Guo J. (2011). Gradient multilayer structural design of CNTs/SiO_2 composites for improving microwave absorbing properties. *Materials & Design*, *32*, 3013-3016.
https://doi.org/10.1016/j.matdes.2010.12.043

Chen X.-D., Zhao F.-L., Chen M. & Dong J.-W. (2017). Valley-contrasting physics in all-dielectric photonic crystals: Orbital angular momentum and topological propagation. *Physical Review B*, *96*, 020202(R).
https://doi.org/10.1103/PhysRevB.96.020202

Chen Y., Wang Y., Leung C. W., Hu M. & Chan H. L. W. (2011). Photonic gap vanishing in one-dimensional photonic crystals with single-negative metamaterials. *Physics Letter A*, *375*, 2465-2470.
https://doi.org/10.1016/j.physleta.2011.04.045

Delihacıoğlu K. (2014). Chiral frequency selective surfaces comprised of multiple conducting strips per unit cell. *IET*

Microwaves, Antennas & Propagation, *8*, 621-626. https://doi.org/10.1049/iet-map.2013.0146

Elakkiya A., Radha S., Sreeja B.S. & Manikandan E. (2020). Terahertz metamaterial absorber with sensing capabilities. *Journal of Optoelectronics and Advanced Materials, 22*, 360-364. http://joam2.inoe.ro/articles/terahertz-metamaterial-absorber-with-sensing-capabilities/fulltext

Ge Z., Zhao D. & Wu J.-W. (2018). Spectral properties of one-dimensional $(AB)^N$ $(BA)^N$ photonic crystal containing double-negative and single-negative metamaterials. *Optoelectronics Advanced Materials – Rapid Communications*, *12*, 495-501. https://oam-rc.inoe.ro/articles/spectral-properties-of-one-dimensional-ab-n-ba-n-photonic-crystal-containing-double-negative-and-single-negative-metamaterials/fulltext

Han Y., Fei H., Lin H., Zhang Y., Zhang M. & Yang Y. (2021). Design of broadband all-dielectric valley photonic crystals at telecommunication wavelength. *Optics Communications*, *488*, 126847. https://doi.org/10.1016/j.optcom.2021.126847

Hao K., Wang X., Zhou L., Yang S., Zhang J., Wang Y. & Li Z. (2020). Design of one-dimensional composite photonic crystal with high infrared reflectivity and low microwave reflectivity. *Optik*, *216*, 164794. https://doi.org/10.1016/j.ijleo.2020.164794

Hassan S., Alnasser K., Lowell D. & Lin Y. (2019). Effects of photonic band structure and unit super-cell size in graded photonic super-crystal on broadband light absorption in silicon. Photonics, 6, 50. https://doi.org/10.3390/photonics6020050

Hayrapetyan A. G., Götte J. B., Grigoryan K. K., Fritzsche S. & Petrosyan R. G. (2016). Electromagnetic wave propagation in

spatially homogeneous yet smoothly time-varying dielectric media. *Journal of Quantitative Spectroscopy & Radiative Transfer*, *178*, 158-166. https://doi.org/10.1016/j.jqsrt.2015.12.007

Jeong H., Nguyen T. T. & Lim S. (2018). Meta-Dome for broadband radar absorbing structure. *Scientific Reports*, *8*, 17893. https://doi.org/10.1038/s41598-018-36273-8

Kang Y., Liu H. & Cao Q. (2018). Enhanced absorption in heterostructure composed of graphene and a doped photonic crystals. *Optoelectronics and Advanced Materials – Rapid Communications*, *12*, 665-669. https://oam-rc.inoe.ro/articles/enhanced-absorption-in-heterostructure-composed-of-graphene-and-a-doped-photonic-crystal/fulltext

Kaya N. & Delihacioglu K. (2014). Reflection and transmission coefficients from chiral nihility slab. *Journal of Optoelectronics and Advanced Materials*, *16*, 859-863. https://joam.inoe.ro/articles/reflection-and-t-ransmission-c-oefficients-from-c-hiral-n-ihility-s-lab/fulltext

Li K., Lim J. L., Xu, Z., Hu, D.J. J., Wong R. Y.-N., Shum P. P., Hao E. J., Wang Y., Sun Q. & Jiang M. (2016). Investigation of temperature sensitivity under the influence of coupling strength between a silica core and a satellite waveguide in a photonic crystal fiber with selective infiltration of glycerin. *Procedia Engineering*, *140*, 72-76. https://doi.org/10.1016/j.proeng.2015.08.1115

Lu J., Qiu C., Ye L., Fan X., Ke M., Zhang F. & Liu Z. (2017). Observation of topological valley transport of sound in sonic crystals, *Nature Physics*, *13*, 369-375. https://doi.org/10.1038/nphys3999

Napolskii K. S., Noyan A. A. & Kushnir S. E. (2020). Control of high-order photonic band gaps in one-dimensional anodic alümina photonic crystals. *Optical Materials*, *109*, 110317. https://doi.org/10.1016/j.optmat.2020.110317

Pandey G. N. & Suthar B. (2021). Transmittance properties of superconductor-dielectric photonic crystal. *Materials Today*, (In press). https://doi.org/10.1016/j.matpr.2020.12.082

Panyaev I. S., Sannikov D. G., Dadoenkova N. N. & Dadoenkova Y. S. (2021). Energy flux optimization in 1D multiperiodic four-component photonic crystals. *Optics Communications*, *489*, 126875. https://doi.org/10.1016/j.optcom.2021.126875

Pozar D. (2012). *Microwave Engineering*, Massachusetts: John Wiley & Sons. https://www.wiley.com/en-au/Microwave+ Engineering %2C+4th+Edition-p-9780470631553

Shalaev, M.I., Walasik, W., Tsukernik, A., Xu, Y. & Litchinitser, N.M. (2019). Robust topologically protected transport in photonic crystals at telecommunication wavelengths. *Nature Nanotechnology*, *14*, 31-34. https://doi.org/10.1038/s41565-018-0297-6

Wang Q., Yang Y., Ni X., Xu Y.-L., Sun X.-C., Chen Z.-G., Feng L., Liu X.-P., Lu M.-H. & Chen Y.-F. (2015). Acoustic asymmetric transmission based on time-dependent dynamical scattering. *Scientific Reports*, *5*, 10880. https://doi.org/10.1038/srep10880

Wei D., Cao F., Wu Z., Liu Y., Wang J., Wang Q., Liu X. & Zhang Q. (2021). Enhanced spectral splitting in a novel solar spectrum optical splitter based on one dimensional photonic crystal heterostructure. *Journal of Materiomics*, *7*, 648-655. https://doi.org/10.1016/j.mat.2020.10.014

Wu J.-J. & Gao J.-X. (2021). Multi-band absorption characteristics of a metal-loaded graphene-based photonic crystal. *Physica E: Low-dimensional Systems and Nanostructures*, *129*, 114675. https://doi.org/10.1016/j.physe.2021.114675

Yablonovitch E. (1994). Photonic crystals. *Journal of Modern Optics*, *41*, 173-194. https://doi.org/10.1080/09500349414550261

Yang T.-J., Shen L.-F., Chau Y.-F., Sung M.-J., Chen D. & Tsai D. P. (2008). High birefringence and low loss circular air-holes photonic crystal fiber using complex unit cells in cladding. *Optics Communications*, *281*, 4334-4338. https://doi.org/10.1016/j.optcom.2008.05.008

Yıldırım R. & Çelebi, F.V. (2015). Semiconductor laser beam bending, Turkish Journal of Electrical Engineering & Computer Sciences, 23, 1257-1262. https://doi.org/10.3906/elk-1303-143

Zhang Y., Xia S., Li L., Ren G., Chen Q., Quan H. & Wu Q. (2015). Microwave absorption enhancement of rectangular activated carbon fibers screen composites. *Composite Part B: Engineering*, *77*, 371-378. https://doi.org/10.1016/j.compositesb.2015.03.059

Zohuri B. (2020). *Radar Energy Warfare and the Challenges of Stealth Technology*, Albuquerque: Springer. https://doi.org/10.1007/978-3-030-40619-6

Zou C., Yao Y., Wei N., Gong Y., Fu W., Wang M., Jiang L., Liao X., Yin G., Huang Z. & Chen X. (2015). Electromagnetic wave absorption properties of mesoporous Fe_3O_4/C nanocomposites. *Composite Part B: Engineering*, *77*, 209-214. https://doi.org/10.1016/j.compositesb.2015.03.030

CHAPTER II

THE USE OF PULSED ELECTRIC FIELD (PEF) TECHNIQUE IN MEAT INDUSTRY

Berkay Kopuk[1] & Harun Uran[2]

[1]*(MSc Student), Tekirdag Namik Kemal University, e-mail: berkay_kopuk@hotmail.com*
Orcid: 0000-0001-7321-9642

[2] *(Asst. Prof. Dr.), Kirklareli University, e-mail: harunuran@klu.edu.tr*
Orcid: 0000-0002-3161-6698

1. Introduction

Pasteurization and sterilization, which are two of the heat treatment applications, can be specified as the two most common methods used in the processing and preservation of foods. The main objective of these processes is to inactivate pathogenic microorganisms and spores, which can be found in foods, and to offer a microbially safe product to the consumer. However, despite these benefits, classical heat treatments can cause changes that negatively affect the sensory, textural and nutritional quality of the final product. In terms of the technologies used to process food and food safety, in recent years, consumers have started to know more about the products they buy and consume. In parallel with this, today's consumers seek freshness-like qualities in their food along with high

sensory quality and nutritional content, and prefer more natural products. In this context, the need for minimal product processing alternatives, which enable microbial inactivation and thus preserve the nutrient content of the food before it is processed and enable the production of environmentally friendly products, is the focus of many food scientists (Bolado-Rodriguez et al., 2000; Zhang et al., 2011).

Pulsed Electric Field (PEF) is a method in which short-term electrical pulses at high voltages (0.1-80 kV/cm, 0.1-100 μs) are applied to the food placed between two electrodes in order to increase the quality of food production and ensure food safety. It is defined as one of the non-thermal electrical-based food processing methods that have a minimal effect on the physical and sensory properties of foods compared to traditional heat treatments (Buckow et al., 2013; Barba et al., 2018; Zhao and Yang, 2019). PEF technology ensures that the application of short-term electrical pulses at high voltages keeps the thermal effect at low levels, and also increases cell membrane breakdown or cell membrane permeability of biological materials in the food matrix without causing adverse effects on food products, making this technology a promising technique. Gomez et al., 2019). Since PEF applications cause changes on cell membranes in food, they can also modify the microstructure and texture of foods by triggering the release of cellular fluid out of the cell or affecting water retention properties (Toepfl et al., 2014a). In this respect, since its discovery, PEF technology has been tried in many foods for various purposes as well as in different industrial applications, and the valuable information obtained has contributed to the literature (Dziadek et al., 2019; Oliveira et al., 2019). However, although the processing of various foods with PEF in laboratory or pilot scale facilities has been studied in detail, information on the use of this application in the production of foods, such as meat and fish, is limited.

In recent studies conducted by different researchers on the subject, it has been reported that the application of PEF improves functional properties, such as tenderness, protein digestibility and water retention capacity, in meat and meat products, while processes such as drying, brining/curing and freezing are faster (Khan et al., 2018a; Alahakoon et al., 2019; Bhat et al., 2019a, b, c, d; Chian et al., 2019; Bhat et al., 2020).

However, there are some factors that hinder the integration of PEF technology into industrial applications. These include factors such as the inability to develop an industrial-grade reliable high-intensity electric field pulse generator, high investment costs, and extensive changes that need to be applied to existing traditional layouts of meat and seafood processing plants (Khan et al., 2018b). In addition, it is known that various factors such as temperature, humidity, pH, nutrient composition, parameters of production conditions, and other techniques applied to the product before and after processing (cooling, freezing, ageing, marination, etc.) in the food industry are also very effective on the safety and quality of the product. In this respect, it is clear that more detailed studies are required for the industrial transfer of PEF technology. This review, therefore, aims to provide information about the general working mechanism of PEF technology through the consideration of the findings of the studies on the use of PEF technology in meat and seafood products

2. Electroporation Mechanism

After Doevenspeck proved the destructive effect of electric field applications on biological cells in the 1960s, the dielectric breakdown theory was proposed by Neumann and Rosenheck (1972) and Zimmermann et al. (1974). According to this theory, the cell membrane, exposed to a high-intensity electric field, may be

temporarily destabilized or irreversibly ruptured. However, there is no direct evidence of pore formation in the cell membrane, that is, visualization at membrane levels. Current knowledge is phenomenological and is based on measurements of electric current through planar bilayer membranes under a surface electric field. These measurements show a significant increase in electrical conductivity of cellular tissues exposed to electric field pulses. This observed phenomenon is called electropermeabilization of the membrane and is hypothetically explained by the electroporation of the membrane (Bouzrara and Vorobiev, 2003). The electrical breakdown theory postulates the cell membrane as a capacitor filled with dielectric material. The accumulation of charges of opposite polarity on either side of the membrane causes the accumulation of a naturally occurring transmembrane potential. In this context, during PEF application, food is placed between two electrodes and a superficial electric field is applied, which triggers the movement of ions inside or outside the cells along the force direction of the applied electric field. This causes ions to accumulate on the cell membranes, leading to cell polarization, which causes a decrease in membrane thickness due to the attractive forces between oppositely charged ions on both sides of the membrane. For a spherical cell with radius a in an electric field, the transmembrane potential ($\Delta\varphi g$) between the inner and outer surfaces of the cell membrane is expressed by the following equation:

$$\Delta\varphi_g = F \times a \times E \times \cos\alpha \qquad (1)$$

In this equation, F is a factor determined by the form (length/radius) of the cells; a is the radius; E is the applied electric field strength; and $\cos\alpha$ is the angle between the electric field and the poles of the cells (Grahl and Markl, 1996). If the transmembrane potential reaches a critical or threshold value higher than the natural potential of a cell, electroporation or pore formation occurs in the membrane, thereby

increasing cell membrane permeability. In order to create primary membrane pores with a minimum radius of ~1 nm, it is assumed that electrical pulses must be used to ensure that the transmembrane voltage of the liquid lipid layer reaches at least 0.2 V, usually 0.5-1.0 V. In the formation of transmembrane pores, if the amount and size of the pores are large enough, irreversible membrane fragmentation occurs. However, the increase in membrane permeability is reversible if the applied surface electric field strength is equal to or around the critical value (Martin-Belloso and Soliva-Fortuny, 2010; Weaver, 2000; Bhat et al., 2018a). In this context, the process of fragmentation and pore formation consists of 3 different stages: (1) opening and formation of pores, (2) growth of pores, and (3) reclosing if reversible, and fragmentation if irreversible. While pore formation occurs within microseconds, it takes about 4 seconds for the pores to close (Chang, 1992). Based on this theory, the electric field intensity must exceed the critical value for electroporation or pore formation to occur (Barbosa-Canovas and Sepulveda, 2005). The electric field strength required to induce electroporation depends on factors such as properties of the food (liquid, viscoelastic or solid dielectric properties), processing parameters (temperature, pulse length, density, pulse number), cell properties (type, size, shape), and membrane characteristic (ionic strength, thickness and structure) (Toepfl et al. et al., 2014b). After electroporation has occurred, the structure of the cell membrane, which acts as a semipermeable barrier responsible for mass transfer, changes significantly. As a result, membrane permeability increases and various processes such as extraction and microbial inactivation occur more easily (Korma et al., 2016).

3. Effect of PEF Applications on Meat and Meat Products

Although there are studies which detailedly investigate the effect of PEF application on industrial pasteurization and sterilization of liquid

foods such as milk, dairy products, liquid eggs, fruit juice, wine, beer, and other alcoholic beverages, studies on solid foods, especially meat and meat products, started in the early 2010s. In this context, PEF applications can improve functional properties and quality by causing microstructural changes; therefore, interest in its use in the processing of meat and meat products has recently increased significantly. However, the effect of PEF applications on such foods is quite complex due to differences in the structure and composition of meat and meat products. These differences in meat structure depend on many factors such as type of animal, age, breed, way of rearing, pre- or post-rigor state of the meat, meat ageing method, and freeze-thaw processes (Farouk et al., 2014; Khan et al., 2015; Choe et al., 2016). The effect of PEF applications on meat quality and functionality is the result of combined and complex interactions between physical microstructural changes due to electroporation, and chemical and biochemical reactions occurring during and after PEF application (Alahakoon et al., 2017). According to McDonnell et al. (2014), since PEF causes permeabilization of the cell membrane, PEF can modify meat quality parameters, such as texture, color, and water retention capacity, and improve mass transfer processes such as curing and brine absorption. On the other hand, it is known that traditional methods used for meat preservation, such as drying, freeze storage, and salting, cause negative effects on the microstructure of the product (Gudmundsson and Hafsteinsson, 2001). In this respect, it can be said that PEF technology has a significant potential in this field. However, it should not be forgotten that some negative factors, such as the conversion of some of the electrical energy into heat due to the thermo-electric effect during application, which affects the physical and quality properties of the product, should also be taken into account (Gomez et al., 2019).

3.1. Effect of PEF on Ageing and Tenderness of Meat

Molecular changes continue in animal muscles after slaughter, and this process is divided into three: (I) pre-rigor phase, where mainly collagen content causes stiffness, (II) rigor phase, where stiffness is due to muscle contraction, and (III) tenderisation phase, in which the muscles undergo some changes and a visible tenderisation takes place. The tenderisation phase largely depends on factors such as ageing time, temperature, muscle type, and animal species (Longo et al., 2015). Important quality parameters of meat occur during ageing, and it is known that the most important feature, tenderness, increases with ageing time. Flesh tenderness is determined by the amount and solubility of connective tissues, sarcomere shortening during rigor development, and post-mortem proteolysis of myofibrillar proteins (Koohmaraie and Geesink, 2006). Since PEF technology is similar to the electrical stimulation technique used in the meat industry to stimulate the carcass during early post-mortem and improve tenderness, it is stated that some of the mechanisms suggested in this regard may also be valid for PEF (Bekhit et al., 2014). Three important mechanisms have been proposed to explain the effect of electrical stimulation on shear force: (I) faster onset of rigor, (II) weakening of muscle fibers as a result of the physical breakdown of sarcomeres from severe muscle contractions, and (III) the acceleration of proteolysis as a result of the release of calcium ions and various enzymes activated by calcium (Hwang et al., 2003; Bekhit et al., 2014).

The formation of tenderness in meat is closely related to the changes shaped in myofibrillar proteins. Many of these changes are shaped by proteolytic enzymes (cathepsins, calpains, and caspases). Calpains (calpains 1 and 2) are known to be major proteases responsible for post-mortem proteolysis and tenderness, and their activity depends on various post-mortem factors such as pH, temperature, and intracellular calcium concentration. Calpain-2 is not

normally activated in the early stages of ageing because it requires a high amount of calcium for activation (Laville et al., 2009; Bhat et al., 2018b; Bhat et al., 2019c). PEF application (T1 = 0.38 kV/cm, 5 kV, 90 Hz, 20 μs; T2 = 0.61 kV/cm, 10 kV, 20 Hz, 20 μs) causes premature release of calcium ions from the sarcoplasmic reticulum via electroporation. As a result, it has been determined that calpain-2 causes early post-mortem activation and decreases the shear force by improving calpain activity in bovine muscle (Bhat et al., 2019c). At the same time, cathepsins, which are inactive in lysosomes, are released from lysosomes under the conditions created by PEF in order to be active in myofibril degradation, and take their place as another factor in the proteolysis and tenderness of meat thanks to electric field applications (Bekhit et al., 2014).

In the study conducted by Bekhit et al. (2014) on this subject, the effect of PEF applications of different intensities (0.29-0.56 kV/cm, 5-10 kV, 20-50-90 Hz, 20 μs, 606-2726 pulses) on the tenderness of fresh (raw) beef loin (*Musculus longissimus lumborum*) and topside (*Musculus semimembranosus*) was investigated, and it was determined that in beef loin, PEF-treated samples had a 19.5% reduction in shear force compared to the control group, regardless of processing intensity, that the tenderness increased with the increase in the application density in beef topsides samples, and that there was a decrease of 4.1%, 10.4% and 19.1% in shear force in the applications at 20, 50, and 90 Hz, respectively.

In another study by Suwandy et al. (2015a), the effect of repeated (1×, 2×, or 3×) PEF applications (0.58 kV/cm, 10 kV, 90 Hz, 20 μs) on the tenderness of raw beef (loins and topsides) was investigated. It was determined that the shear force of PEF-treated samples in beef loin meats (*longissimus lumborum*) decreased significantly and that an additional 2.5 N reduction in shear force was achieved with each extra application. However,

unlike beef loin samples, it was also stated that topsides samples (*Musculus semimembranosus*) were not affected by PEF applications and the aforementioned mechanisms (Suwandy et al., 2015a).

In another study conducted by Chian et al (2019), it was found that sarcomere length was significantly higher in raw beef samples treated with PEF (1-1.25 kV/cm, 50 Hz, 20 μs, 500 and 2000 pulses) compared to the control group. It was reported that sarcomere length increased with increasing application density, which indicates that PEF application causes physical fragmentation of muscle fibers. In the aforementioned study, it was observed that the elongation in sarcomeres was caused by the weakening of the Z-disc and I-band junctions, that the effect of endogenous proteolytic enzymes increased during the post-mortem ageing process with the decrease in the tensile strength in myofibrils, and that the physical breakdown of the muscle structure, therefore, had a positive correlation with the tenderness of the meat. It was also reported that the meat ageing process could be accelerated by PEF administration due to the breakdown of muscle structure and the interaction of both cathepsins released from lysosomes and calcium-activated calpains released from the sarcoplasmic reticulum, and that tenderness could, for that reason, be improved (Chian et al., 2019).

3.2. Effect of PEF on Color

Color and color stability is an important quality parameter of meat. During the storage of meat, clearly visible color changes occur on the muscle surface and affect the consumer's preference. While the red-pink color is associated with freshness by consumers, the brown color is perceived as a product whose freshness has decreased and/or spoiled. The color of the muscle surface is mainly determined by the amount of myoglobin and its redox state. In general, myoglobin

exists in three redox forms: deoxymyoglobin (DeoMb), oxymyoglobin (OxyMb), and metmyoglobin (MetMb). The action and penetration of oxygen at the muscle surface causes rapid oxygenation of pinkish-red myoglobin to bright red oxymyoglobin and slow autoxidation to brown metmyoglobin. The depth of oxygen penetration and the relative amount of myoglobin, oxymyoglobin, and metmyoglobin affect the degree of brightness and saturation of muscle color (Feldhusen et al., 1995; Wu et al., 2016).

In a study conducted by Arroyo et al. (2015) on this subject, it was stated that PEF application at different intensities (1.4 kV/cm, 10 Hz, 20 μs, 300-600 pulses) did not cause any negative effect on the L*, a* and b* values of beef compared to other technologies such as high hydrostatic pressure. In another study by Khan et al (2017), it was found that the brightness (L*) value of beef treated with high-intensity PEF (10 kV, 200 Hz, 20 μs) was much higher after 24 hours of aging compared to samples treated with controlled and low-intensity PEF (2.5 kV, 200 Hz, 20 μs). This is explained by the fact that the lower water retention capacity due to more heat production (40,5°C) during the application in the high-density PEF process leads to more moisture on the meat surface, resulting in a lighter color by reflecting more light from the surface. A* value was higher in the control and low-intensity PEF groups compared to the high-intensity PEF group. At the end of the first day, a very rapid loss of color was observed in the high-density PEF group. It was observed that the relatively high heat generated in the process in question adversely affected the antioxidant capacity of samples, and that this was due to a higher rate of oxidation of myoglobin to metmyoglobin. Also, samples treated with high-density PEF exhibited a higher b* value compared to other samples on the first post-treatment day. In general, the time dependent b* value of meat samples decreased, and at the end of the fourteenth day, a delay was detected in reaching the

maximum b* values of samples treated with high-density PEF, as was the case with the a* values. As a result of the research, it was reported that samples treated with low-density PEF had better color stability compared to the control and the other group. In a different study conducted by Khan et al (2018a) on chicken breast meat, it was reported that the L* and b* values of the product were not affected by the application, and that samples treated with low-intensity (2.5 kV, 200 Hz, 20 μs) PEF, however, had a higher redness (a*) value.

3.3. Effect of PEF on Water Retention Properties

Water is the most common component present in the muscle, varying between 70% and 80%, depending on muscle type, slaughter age and animal type. Excessive water loss in meat causes quality losses for several reasons: (I) water seeping around the meat creates an unpleasant appearance, and (II) during cooking it causes loss in both meat size and (III) sensory properties such as tenderness or juiciness. It, for that reason, reduces the appeal of meat (Toldra, 2003). Meat myofibrils are known to be responsible for the water retention capacity of the meat. Denaturation of muscle proteins, particularly myosin, results in a reduction in the water retention capacity of the meat in general (Suwandy et al., 2015b). If the water retention capacity is low, cooking loss and leakage loss (water release) in the meat are also high and have a negative effect on the product. The breakdown of the membrane structure due to the interaction between the cells and the electric field causes the formation of pores that allow the free exchange of components within the cell; therefore, changes in microstructure and texture as a result of permeabilization may affect the water retention capacity of the muscle (Faridnia et al., 2014).

Considering the studies carried out, O'Dowd et al. (2013) reported that PEF applications (1.1-2.8 kV/cm, 5-200 Hz, 20 μs, 152-

300 pulses) did not cause a change in the water release, moisture and water activity values of beef that would adversely affect the quality, and that an increase in mass loss was, however, observed as the processing intensity increased (electric field strength, total energy input, and number of pulses). In the study conducted by Bekhit et al. (2014), it was determined that leakage loss in fresh beef increased with increasing voltage and frequency values of PEF applications (0.29-0.56 kV/cm, 5-10 kV, 20-50-90 Hz, 20 μs, 606-2726 pulses). In another study by Faridnia et al. (2014), it was stated that PEF application (0.2-0.6 kV/cm, 1-50 Hz, 20 μs) reduced moisture content in beef by 0.7-3.6%, that more water loss occurred due to a more porous structure, and that cooking loss was not, however, affected. Suwandy et al. (2015b) reported that increasing voltage and frequency values in PEF application did not affect leakage loss in pre-rigor beef, but caused an increase of 1.2% in cooking loss. In another study by Khan et al. (2017), it was revealed that low-intensity (2.5 kV, 200 Hz, 20 μs) PEF reduced leakage loss in beef compared to high-intensity (10 kV, 200 Hz, 20 μs) PEF application, but did not affect cooking loss and slightly reduced cooking loss. In the study conducted by Bhat et al. (2019a), it was observed that the increase in leakage loss of both control samples and PEF-treated samples was the same during the ageing period, and that PEF treatments (0.36-0.60kV/cm, 5-10 kV, 20-90Hz, 20 μs) had no effect on the cooking loss of beef during the ageing period (days 7 and 14).

3.4. Effect of PEF on Protein Digestibility

Protein digestibility is the main factor affecting the bioavailability of dietary proteins. Digestive kinetics of meat protein are affected by various factors depending on physical, chemical and enzymatic conditions (Kondjoyan et al., 2015; Primozic et al., 2017). It has been stated that the application of PEF can affect the quaternary, tertiary

and secondary structures of proteins by breaking down cell membranes and affecting disulfide or hydrogen bonds with electrostatic or hydrophobic interactions, therefore improving the digestibility of proteins (Giteru et al., 2018). In other words, this technique can destabilize the secondary and tertiary structures of proteins by disrupting the electrostatic interactions of individual polypeptide chains and local electrostatic fields. In addition to this inhomogeneous charge distribution in the protein structure, the heat generated during the process (if the protein is close to the denaturation level) may play a key role in the denaturation and aggregation of heat-sensitive proteins (Bhat et al., 2019b, d). In this context, in the study conducted by Bhat et al. (2019b), it was determined that PEF application (10 kV, 20 Hz, 20 μs) increased in vitro protein digestibility (94%) in cooked beef compared to the control group (92%), and that more and faster enzymatic hydrolysis occurred during digestion in PEF-treated samples. In another study by Bhat et al. (2019e), PEF pretreatment applications (T1 = 2.5 kV, 50 Hz, 20 μs; T2 = 10 kV, 90 Hz, 20 μs) increased the in vitro protein digestibility of venison (T1 = 92.81%, T2 = 93.35%) compared to the control group (91,69%) without any adverse effect on mineral substance content. It was also observed that PEF had a significant effect on the soluble protein and free amino acid content of meat. In another study carried out by Chian et al. (2019), in vitro protein digestibility was measured by the ninhydrin reaction of free amino acids released at different times (0, 60, 180 min), and it was determined that PEF application (1-1.25 kV/cm, 50 Hz, 20 μs, 500 and 2000 pulses) increased the protein digestibility of raw beef samples in the small intestine (180. min, 11.9-12.2%) compared to the control group (180. min, 9-10.4%).

3.5. Effect of PEF on Mineral Content and Release

Minerals in bound form in the meat matrix are released in the stomach environment at acidic pH with the interaction of peristaltic movements and gastric enzymes, and are absorbed in the small intestine by passive and active transport (Alminger et al., 2014; Corte-Real and Bohn, 2018). Since meat is an important source of minerals, such as iron, phosphorus and zinc, it can be stated that a process that may cause a decrease in the amount of these minerals will adversely affect the commercial value of meat. It has been reported that PEF application may have an effect on the mineral content of meat during processing and storage in terms of creating pores in cell membranes and increasing cellular permeability (Bhat et al., 2019b). However, data on the effect of PEF application on the mineral content of meat and meat products are still very limited. In the study by Khan et al (2017), in raw beef samples subjected to high-intensity (10 kV, 200 Hz and 20 μs) PEF treatment due to higher leakage loss, it was determined that phosphorus, potassium and iron contents were lower than those samples in the low-intensity (2.5 kV, 200 Hz and 20 μs) treatment and control groups. In a different study examining the effect of PEF application on the mineral content of chicken breast meat, low- (2.5 kV, 200 Hz, 20 μs) or high-intensity (10 kV, 200 Hz, 20 μs) applications did not cause any negative effects on the mineral profile of the product. (Khan et al., 2018a). In another study of Khan et al (2018b), the effects of low- and high-density PEF treatments (2.5 and 10 kV, 200 Hz, 20 μs, respectively) on a total of 40 macro- and micro-minerals in beef tenderloin and chicken breast were investigated. It was found that both high- and low-density treatments decreased the calcium, sodium and magnesium content in raw beef samples, while high-intensity treatment increased the chromium content in samples (mineral material migration from the electrodes to the samples depending on

the treatment intensity). In raw chicken breast samples, regardless of the processing intensity, PEF applications did not cause any negative effects on macro-minerals (such as sodium, magnesium, and calcium) in chicken breast samples. However, it was reported that especially high-intensity treatment increased the nickel content of samples due to migration, and that both applications increased the copper content in samples. In another study by Bhat et al (2018c), it was stated that PEF application (5-10 kV, 20-90 Hz, 20 μs) had no effect on minerals such as iron, potassium, phosphorus, calcium, sodium, magnesium, chromium and nickel in beef.

3.6. Effect of PEF on Mass Transfer and Diffusion in Processes such as Salting and Curing

In simple terms, the traditional salting process is applied by coating or rubbing the raw material with solid salt. The general purpose of salting in meat and meat products is to provide taste, odor and aroma development in the product along with food preservation. However, cell membranes play an important role in the curing and brining process of meats, as they resist free diffusion of salt in muscle tissue (Albarracin et al., 2011; Bhat et al., 2018a). Other non-thermal technologies, such as high pressure and ultrasound, can improve mass transfer in curing by influencing various factors such as diffusion and release of sodium from the meat matrix, interaction between protein and salt ions, and sensory perceptions (Inguglia et al., 2017). The effect of PEF application on mass transfer depends on parameters, such as field strength and frequency and number of pulses, and the most important parameter is electric field strength. In addition, high energy input can cause crust formation on the meat surface, restricting mass transfer. Hence, it optimizes the application time and the number of pulses to achieve a high degree of electroporation in the muscle cell membrane and to accelerate the

absorption of curing agents, and it is stated that brine absorption can be maximized with an effective electric field application that provides cell membrane permeabilization (McDonnell et al., 2014).

Toepfl and Heinz (2007) reported that salt and nitrate diffusion developed in pork immersed in brine solution after PEF application. In addition, it was determined that mass transfer (moisture removal) from meat occurred faster after low-density PEF treatment. Since the high energy input caused the formation of a crusty structure in the product that restricted mass transfer, it was also pointed out that the PEF application with 3 kV/cm and 5 kJ/kg density gave better results compared to the application with 4 kV/cm and 20 kJ/kg density. In another study by McDonnell et al (2014), the effectiveness of PEF application (22.6-181 kJ/kg, 1.2-2.3 kV/cm, 100-200 Hz, 150-300 pulses) as a pre-treatment for faster and more effective salting of pork was investigated, and it was reported that more electroporation occurred with the application of a large number of pulses at low frequencies, thus increasing the salt diffusion by 10.4-13%. In another study, from a different perspective, the effectiveness of PEF application (0.52 kV/cm, 10 kV, 20 Hz, 20 μs) was investigated as an alternative method for reducing sodium content in dried beef by Bhat et al. (2020). In the study, various quality parameters of the control sample with 2% salt content and the samples with only reduced salt content (T1 = 1.2% salt) and both reduced salt content and treated with PEF (T2 = 1.2% salt + PEF) were examined. As a result of the study, it was determined that PEF improved the sodium release and perception during chewing by affecting the salt diffusion and its distribution in the product matrix, and that most of the panelists preferred the ones that were pretreated with PEF (T2) among the samples with reduced salt content. As a result of the research, it was emphasized that pretreatment with PEF could significantly (40%) reduce the amount of salt (NaCl) without

causing any negative effects on the sensory quality, lipid oxidation and microbial stability of the dried meat product (Bhat et al., 2020).

3.7. Antimicrobial Effect of PEF

PEF, which is considered as one of the most valid alternatives for non-thermal food preservation techniques, has been studied in detail for the non-thermal pasteurization and sterilization of mostly liquid and semi-solid foods such as milk, fruit juices and liquid eggs, and successful results have been obtained (Toepfl et al., 2014b). However, unlike liquid foods, it has been pointed out that PEF technology has limited applicability to ensure microbial safety in meat and meat products due to its low electrical conductivity and high protein/fat content (Bolton et al., 2002). In addition, since they are heterogeneous products with different electrical resistances, it has been stated that while some of the product remains untreated in practice, some parts are exposed to excessive processing intensity (Faridnia et al., 2015). In this context, in the study conducted by Stachelska et al. (2012), after PEF applications at different pulse frequencies (0.3 kV/cm, 28, 280 and 2800 MHz), Y. enterocolitica ATCC 35669 inhibition was investigated in ground beef stored for 3 days at +4°C and 1 month at -20°C. In the study, PEF applications of 28 and 280 MHz were found to be insufficient in terms of inhibiting Y. enterocolitica in ground meat samples, whereas it was observed that the application of 2800 MHz PEF reduced the initial Yersinia enterocolitica population from 6.7 log cfu/g to 6.4 log cfu/g in ground beef stored for 3 days at +4°C and 1 month at -20°C. In a different study, the inhibitory effectiveness of PEF application (3.75 and 15 kV/cm, 5 Hz, 10 μs) on indicator microorganisms and foodborne pathogens contaminated on raw chicken meat was investigated by Haughton et al. (2012). It was reported that PEF application did not have a significant effect on Enterobacteriaceae, C.

jejuni, E. coli and S. enteritidis populations in raw chicken meat under the conditions examined in this study, and that it was not, thus, an effective technology for ensuring the microbial safety of chicken meat. Faridnia et al. (2015) reported that the aerobic microbial population of beef frozen at -20°C for 1 week and then thawed after 7 days of storage at +4°C was 3.10 log cfu/g, and that frozen/thawed and then PEF-treated (1.4 kV/cm, 250 kJ/kg specific energy input, 50 Hz and 20 μs) samples, however, had a higher aerobic microbial population (5.02 log cfu/g) during storage at the same time and temperature. The researchers attributed this significant increase of approximately 2 log units to higher leakage loss (6.67% compared to the control group with 4.84%) observed after 7 days of cold storage of frozen/thawed and subsequently PEF-treated samples. More recently, a study by Clemente et al (2020) first examined the antimicrobial effect of various essential oils and organic acids on Campylobacter jejuni strains; then, the inhibitory effect of PEF treatment (20 kV/cm, 1 Hz, 20 μs, 50 pulses) on suspended C. jejuni strains (Mueller Hinton Broth, 5-6 log cfu/mL) was investigated. In these examinations, thyme oil was found to be the most effective antimicrobial agent, while the most resistant strain to PEF treatment was C. jejuni 1146DF. In the second part of the study, raw chicken samples were immersed in the suspension prepared with the most resistant strain detected. After this process, PEF application (0.25, 0.5, 0.75, 1 kV/cm, 1 Hz, 20 μs, 50 pulses) was applied to raw chicken meat (4.41 log cfu/g) contaminated with C. jejuni 1146DF strain, both alone and together with thyme essential oil at the most effective concentration (15,625 ppm), and the inhibitory effect of these treatments on C. jejuni 1146DF strain was investigated. PEF administration alone was not effective for the inhibition of C. jejuni 1146DF in raw chicken meat, whereas following the treatment of the samples with 50 electrical pulsed PEF at 1 kV/cm, immersing them

in a solution containing 15,625 ppm thyme essential oil for 20 minutes provided significant inhibition (1.5 log cfu/g reduction) in C jejuni 1146 DF strain. The researchers determined the inhibition level achieved by immersion in hot water (75-85°C, 10-30 s, 1.7 log cfu/g reduction) or steam application (90-100°C, 10-12 s, 1.3 log cfu). /g reduction) as equivalent to the methods generally used for decontamination in chickens, and observed that with a low energy input of 2.12 kJ per 1 kg of chicken, the application of PEF combined with thyme essential oil eliminated the possible negative effects of heat treatment in chicken meat (skin shrinkage, discoloration, and damage to outer epidermal skin tissue) without the need for any heating or cooling. They therefore suggested that it was a promising alternative for decontamination of chicken at low temperatures (Clemente et al., 2020). According to the results of the study, it is clearly seen that PEF technology alone is not an alternative and valid method that can be used to ensure microbial safety in meat and meat products. In order to obtain better results in terms of food safety and microbial inactivation in meat and similar foods, it is thought that the use of PEF technology in combination with other applications, such as high hydrostatic pressure, ultraviolet light, high-intensity accent light, ultrasound, and addition of antimicrobial agents, should be investigated.

3.8. Effect of PEF on Lipid Oxidation

Lipid oxidation is another important factor affecting the quality of meat. Processing meat with PEF breaks down the membranes of muscle cells and facilitates the interaction of unsaturated fatty acids and cell membrane phospholipids with pro-oxidants in meat (Faridnia et al., 2015). In this case, unsaturated fatty acids react with molecular oxygen and can form free radicals and hydroperoxides, which decompose into many secondary products such as

hydrocarbons, aldehydes, ketones, alcohols, esters and acids, negatively affecting both nutritional and sensory quality of the product (Dominguez et al., 2019). The degree of lipid oxidation, which adversely affects product quality, varies depending on the composition of the meat, especially the fatty acid and antioxidant content, temperature and other processing parameters (Danowska-Oziewicz, 2009). Apart from these parameters, applications such as pre-/post-process cooling and freezing and storage conditions also have the potential to increase lipid oxidation of PEF-processed meat (Faridnia et al., 2015; Ma et al., 2016).

Faridnia et al (2015) examined the effect of freezing as a pretreatment (1 week at -20°C) on the quality characteristics of bovine muscles prior to PEF application (1.4 kV/cm, 250 kJ/kg specific energy input, 50 Hz and 20 μs), and reported that lipid oxidation significantly increased (TBARS value 0.96 mg MDA/kg meat) when PEF was applied to frozen/thawed samples compared to the control group (TBARS value ~0.70 mg MDA/kg meat). Researchers noted that applying PEF to frozen-thawed meat made it more susceptible to lipid oxidation due to exposure of fatty acids to pro-oxidants such as iron released from muscle cells. However, despite the changes in the fatty acid profile of the muscle, it was determined that the ratios of polyunsaturated fatty acids/saturated fatty acids and omega 6/omega 3 remained at the recommended levels (0.32 and 2.09, respectively) (Faridnia et al., 2015).

In a different study by Ma et al. (2016), the effects of cooling (48 hours at +4°C) and freezing (3 months at -20°C) on mutton prior to PEF application (1-1.4 kV/cm, 88-109 kJ/kg specific energy input, 90 Hz, 20 μs and 964 pulses) were investigated. In the study, the TBARS values of sheep rib and ridge samples, which were cooled after slaughter and then stored in the cold (+4°C) for 7 days by applying PEF, increased from 0.215 mg MDA/kg to 0.407 and 0.304

mg MDA/kg, respectively. These results indicated that meats cooled after slaughter and subsequently treated with PEF were more susceptible to oxidation than the control group (no PEF treated) during cold storage for 7 days. It was stated that the results obtained were below the values (0.6-2 mg MDA/kg) that could cause the development of undesirable taste and odor in meat, and that frozen samples, however, showed higher concentrations of MDA during the storage period (7 days at +4°C) compared to the cooled samples. In the study, it was determined that the highest accumulation of lipid oxidation among frozen/thawed and PEF-treated samples occurred in rib samples (1,047 mg MDA/kg) stored cold for 7 days, which was associated with rancid taste. The researchers stated that these high TBARS values detected in the arm and rib meat were due to the high amount of polyunsaturated fatty acids (30.16 mg/100 g and 37.28 mg/100 g, respectively) of the samples (Ma et al., 2016).

In the study by Khan et al (2017), it was observed that low-intensity PEF application (2.5 kV, 200 Hz and 20 μs) did not affect lipid oxidation in raw beef. However, it was found that the antioxidant capacity of the meat decreased due to high heat (40.5°C) produced during high-intensity treatment (10 kV, 200 Hz, and 20 μs), and that lipid oxidation was at higher levels (1.02±0.12 mg MDA/kg) during storage, which negatively affected the quality of the product. Bhat et al (2020), on the other hand, reported that TBARS values in dried beef were affected only by storage time, and that PEF application (0.52 kV/cm, 10 kV, 20 Hz, 20 μs) did not cause any change in the product. Additional studies examining the effect of the PEF method on the quality characteristics of different animal meats are summarized in Table 1.

Table 1. PEF Studies on Different Animal Meats

Meat Type	Muscle Condition and Application Conditions	Results	Reference
Beef Musculus Semitendinosus	Post-Rigor Field strength; 1.1-2.8 kV/cm, energy input; 12.7-225, kJ/kg, frequency; 5-200 Hz, number of pulses; 152-300 pieces, pulse length; 20 µs	As a result of the application, it was observed that there was a temperature increase in the range of 5-22°C, that the weight loss increased in direct proportion to temperature, that PEF did not affect water release, humidity, water activity and shear force, and that muscle fiber bundles had a smaller diameter in PEF-applied samples.	O'Dowd et al. (2013)
Beef Tenderloin *Musculus Longissimus lumborum*	Post-Rigor Batch mode, meat fiber direction parallel or diagonal to the electrodes, field strength; 0.58-0.73 kV/cm, energy input; 16.2-19.3 kJ/kg, voltage; 10 kV, frequency; 90 Hz, pulse length 20 µs.	It was found that PEF application did not affect leakage loss and water retention capacity, that meat direction parallel to the electrodes decreased the cooking loss in the samples above pH 5.8, that shear force, color and lipid stability were not affected by PEF application, and that proteolysis increased with PEF application, especially in samples with low pH (5.5-5.8).	Suwandy et al. (2015c)
Beef *Longissimus thoracis et lumborum*	Post-Rigor Batch mode, field strength; 1.4 kV/cm, energy input; 25-50 kJ/kg, frequency; 10 Hz, pulse length; 20 µs, number of pulses; 300-600 pieces and pulse type; square wave.	As a result of PEF application, it was found that there was a temperature increase in the range of 7.7-14.5°C, that weight loss, color parameters, cooking loss, storage loss and odor properties were not adversely affected, that shear force decreased, that tenderness increased, and that texture improved.	Arroyo et al. (2015)

Meat Type	Muscle Condition and Application Conditions	Results	Reference
Beef Breast *Biceps femoris*	Post-Rigor Batch mode, meat fiber direction parallel to the electrodes, field strength; 1.7-2.0 kV/cm, energy input; 185 kJ/kg, frequency; 50 Hz, pulse length; 20 µs, and pulse type; square bipolar.	It was found that PEF application did not adversely affect cooking loss and color stability, caused a temperature increase of ~16°C, significantly reduced shear force and thus stiffness, increased leakage loss, caused Z line fragmentation and degraded myofibril structure, and increased tenderness and shortened ageing time by causing changes on meat microstructure and texture.	Faridnia et al. (2016)
Beef Breast Derin Pektoralis Kası	Post-Rigor Batch mode, meat fiber direction parallel to the electrodes, field strength; 1.0-1.5 kV/cm, energy input; 40-100 kJ/kg, voltage; 15-35 kV, frequency; 50 Hz, pulse length; 20 µs, number of pulses; 424-10000 pieces and pulse type; square bipolar.	It was determined that PEF application weakened the connective tissues of tough meat, decreased denaturation temperature, increased the solubility of collagen, and thus was a suitable technology to shorten cooking time and improve tenderness.	Alahakoon et al. (2017)
Venison Tenderloin *Musculus longissimus et lumborum*	Post-Rigor Energy input; 1.93-70.2 kJ/kg, voltage; 2.5-7.5 kV, frequency; 50 Hz, and pulse length; 20 µs.	It was observed that dry-maturated high-density PEF-treated sample was more tender compared to the control group, and that dry curing of venison could be accelerated without any adverse effect on total weight loss (cooking loss, dissolution loss, and water release), conjugated linoleic acid content, and shear force.	Mungure et al. (2017)

Meat Type	Muscle Condition and Application Conditions	Results	Reference
Beef Breast Deep Pectoralis Muscle	Pre-Rigor Batch mode, field strength; 1.5 kV/cm, energy input; 90-100 kJ/kg, frequency; 50 Hz, pulse length; 20 µs and pulse type; square bipolar.	After PEF treatment, an increase in collagen solubility and meat tenderness and a decrease in cooking loss were observed in samples subjected to sous vide treatment, and it was found that PEF application could reduce the effect of biological changes in sous vide-treated meat and soften heterogeneous meat pieces.	Alahakoon et al. (2018a)
Beef Breast Deep Pectoralis Muscle	Post-Rigor Batch mode, field strength; 0.7-1.5 kV/cm, energy input; 90-100 kJ/kg, frequency; 50 Hz pulse length; 20 µs and pulse type; square bipolar.	It was observed that the shear force and toughness of samples, which were subjected to PEF application at 0.7 kV/cm, followed by 24 hours of sous vide treatment at 60°C, decreased significantly, that other textural features were greatly improved, that collagen solubility increased, and that vacuum cooking time could be shortened without adverse effects on lipid oxidation, color stability, cooking loss or protein digestibility.	Alahakoon et al. (2018b)
Beef Breast Biceps femoris	Post-Rigor Batch mode, meat fiber direction parallel to the electrodes, voltage; 5-10 kV, frequency; 20-90 Hz, pulse length; 20 µs and pulse type; square bipolar.	It was determined that protein digestibility, soluble protein and free amino acid content significantly increased as a result of pretreatment of meat with PEF (especially at 10 kV and 90 Hz application) without any negative effect on mineral substance content, and that protein profile improved.	Bhat et al. (2018c)

Meat Type	Muscle Condition and Application Conditions	Results	Reference
Beef Breast Biceps femoris	Post-Rigor Batch mode, meat fiber direction parallel to the electrodes, field strength; 0.38-0.61 kV/cm, energy input; 21.17-74.24 kJ/kg, voltage; 5-10 kV, frequency; 20-90 Hz, number of pulses; 2723-2725 pieces, pulse length; 20 µs and pulse type; square bipolar.	It was found that Calpain 2 activation was found to occur during early post-mortem in PEF-treated samples, that calpain activity and desmin and troponin-T proteolysis increased, that there was a temperature increase of 8.18-11.08°C according to the density, that that the application did not affect leakage loss and firing loss and caused a slight reduction in shear force and myofibrillar fragmentation index, and that since a rapid tenderness was observed in the first week of ageing, total ageing time could be shortened.	Bhat et al. (2019c)
Red Deer Tenderloin Longissimus dorsi	Post-Rigor Batch mode, meat fiber direction parallel to the electrodes, field strength; 0.2-0.5 kV/cm, energy input; 1.93-70.2 kJ/kg, voltage; 2.5-10 kV, frequency; 20-90 Hz, pulse length; 20 µs and pulse type; square bipolar.	It was observed that calpain activity, troponin-T proteolysis, amino acid content and digestible protein ratio of venison increased without any negative effect on mineral release, especially as a result of PEF application at 10 kV and 20 Hz, and that shear force and myofibrillar fragmentation index decreased.	Bhat et al. (2019f)
Beef Breast Deep Pectoralis Muscle	Post-Rigor Batch mode, field strength; 0.7-1.5 kV/cm, energy input; 90-100 kJ/kg, voltage; 15-37 kV, frequency; 50 Hz, number of pulses; 1030-6400 pieces, pulse length; 20 µs and pulse type; square bipolar.	It was observed that there was a temperature increase in the range of 2.4-4.3°C depending on the application intensity, that the application did not affect leakage loss and cooking loss and increased the water loss slightly, that especially the application of 0.7 kV/cm significantly reduced toughness and chewiness, and that the solubility of collagen increased with increasing field strength.	Alahakoon et al. (2019)

Meat Type	Muscle Condition and Application Conditions	Results	Reference
Venison Longissimus dorsi	Post-Rigor Batch mode, voltage; 2.5-10 kV, specific energy input; 1.93-70.2 kJ/kg; frequency; 50 Hz, pulse length; 20 μs and pulse type; square bipolar.	It was observed that myofibrils from samples treated with PEF were seen to be fragmented and torn along the z-lines, that the drying rate increased during the dry curing process, especially after high-intensity application, that leakage loss, dissolution waste and cooking loss were not affected, that low-intensity application had an effect on tenderness, that tenderness improved significantly as a result of high-intensity application, and that the metabolite profiles of the meat did not change as a result of the application.	Mungure et al. (2020)
Bovine Semitendinosus muscle	Post-Rigor Batch mode, field strength; 1.0-2.0 kV/cm, pulse number; 200 pieces, pulse length; 20 μs.	It was reported that an increase in conductivity and muscle tissue deformation occurred depending on the field strength, that shear force, toughness and chewiness decreased significantly, especially as a result of the application of 2.0 kV/cm, that elasticity, cohesiveness, color, weight loss and leakage loss were unaffected by PEF application, that shear forces were significantly reduced after Sous Vide (SV) cooking of pretreated samples with PEF compared to the control group, and that meats cooked with SV retained PEF-induced effects after reheating in the oven.	Jeong et al. (2020)

Meat Type	Muscle Condition and Application Conditions	Results	Reference
Beef Breast	Post-Rigor Batch mode, field strength; 0.7 kV/cm, energy input; 99 kJ/kg, frequency; 50 Hz and pulse length; 20 µs.	It was found that there was an increase of approximately 8.4°C in meat temperature after PEF application, that in vitro protein digestibility increased by approximately 29% with the combination of Sous Vide (SV) cooking (24 hours at 60°C) following PEF application, that proteolysis of PEF-treated and SV-cooked meat proteins increased during digestion simulation, and that more damage to muscle micro- and ultrastructures occurred in PEF-treated and SV-cooked samples at the end of in vitro digestion.	Chian et al. (2021)
Chicken breast	Post-Rigor field strength; 0.60-1.20 kV/cm, energy input; 0.15-2.42 kJ/kg, frequency; 50 Hz, number of pulses; 150-600 pieces, pulse length; 20 µs, application time; 3-12 s and pulse type; square monopolar.	It was determined that PEF treatment did not affect the pH of chicken meat and slightly changed its brightness and yellowness, that low-intensity application significantly increased the water retention capacity of chicken meat without harming protein integrity and functionality, and reduced leakage loss up to 28.5% during 4 days of storage in cold conditions, and that it was more effective to increase the number of pulses rather than increasing the field strength to reduce leakage loss.	Baldi et al. (2021)

4. Conclusion

Today, the usability of PEF, which is one of the non-thermal techniques that finds application in various foods, is intensively studied, since it is an important process in meat and meat products such as extraction, drying, dissolution, improvement of textural properties, development of color, marination, salting, curing, and fermentation. Considering the data of different studies, it can be pointed out that PEF application improves functional properties in meat and meat products, creates very positive results on product processing speed and end product quality, and constitutes a great potential for the sector. However, there are quite a variety of research results, especially depending on the difference in PEF parameters. In this respect, it can be stated that there is a need for optimization studies to investigate the physical, chemical and microbial effects of the PEF process, which is affected by a number of technological and biological factors, in different meat products and to support such studies with sensory analyses.

References

Alahakoon, A.U., Oey, I., Silcock, P., Bremer, P. (2017). Understanding the Effect of Pulsed Electric Fields on Thermostability of Connective Tissue Isolated from Beef Pectoralis Muscle Using A Model System. *Food Research International*, *100*: 261-267.

Alahakoon, A.U., Oey, I., Bremer, P., Silcock, P. (2018a). Optimisation of Sous Vide Processing Parameters for Pulsed Electric Fields Treated Beef Briskets. *Food and Bioprocess Technology*, *11*: 2055-2066.

Alahakoon, A.U., Oey, I., Bremer, P., Silcock, P. (2018b). Process Optimisation of Pulsed Electric Fields Pre-Treatment to Reduce the Sous Vide Processing Time of Beef Briskets.

International Journal of Food Science & Technology, *54*: 823-834.

Alahakoon, A.U., Oey, I., Bremer, P., Silcock, P. (2019). Quality and Safety Considerations of Incorporating Post-PEF Ageing into the Pulsed Electric Fields and Sous Vide Processing Chain. *Food and Bioprocess Technology*, *12*: 852-864.

Albarracin, W., Sanchez, I.C., Garu, R., Barat, J.M. (2011). Salt in Food Processing; Usage and Reduction: A Review. *International Journal of Food Science & Technology*, *46*(7): 1329-1336.

Alminger, M., Aura, A.M., Bohn, T., Dufour, C., El, S.N., Gomes, A., Santos, C.N. (2014). *In vitro* Models for Studying Secondary Plant Metabolite Digestion and Bioaccessibility. *Comprehensive Reviews in Food Science and Food Safety*, *13*: 413-436.

Arroyo, C., Lascorz, D., O'Dowd, L., Noci, F., Arimi, J., Lyng, J.G. (2015). Effect of Pulsed Electric Field Treatments at Various Stages During Conditioning on Quality Attributes of Beef *Longissimus thoracis et lumborum* muscle. *Meat Science*, *99*: 52-59.

Baldi, G., D'Elia, F., Soglia, F., Tappi, S., Petracci, M., Rocculi, P. (2021). Exploring the Effect of Pulsed Electric Fields on the Technological Properties of Chicken Meat. *Foods*, *10*, 1-15.

Barba, F.J., Ahrne, L., Xanthakis, E., Landerslev, M.G., Orlien, V. (2018). Innovative Technologies for Food Preservation. In: Barba FJ, Sant'Ana AS, Orlien V, Koubaa M (editors). Innovative Technologies for Food Preservation. *Inactivation of spoilage and pathogenic microorganisms* (pp. 25-51). Academic press: The UK.

Barbosa-Canovas, G.V., Sepulveda, D.R. (2005). Present Status and the Future of PEF Technology. In: Barbosa-Canovas GV,

Tapia MS, Cano TP (editors). *Novel food processing technologies* (pp. 1-45). CRC press: The USA.

Bhat, Z.F., Morton, J.D., Mason, S.L., Bekhit, A.E.D.A. (2018a). Current and Future Prospects for the Use of Pulsed Electric Field in the Meat Industry. *Critical Reviews in Food Science and Nutrition*, *59*(10): 1660-1674.

Bhat, Z.F., Morton, J.D., Mason, S.L., Bekhit, A.E.D.A. (2018b). Role of Calpain System in Meat Tenderness: A Review. *Food Science and Human Wellness*, *7*: 196-204.

Bhat, Z.F., Morton, J.D., Mason, S.L., Bekhit, A.E.D.A. (2018c). Pulsed Electric Field: Role in Protein Digestion of Beef *Biceps femoris*. *Innovative Food Science & Emerging Technologies*, *50*: 132-138.

Bhat, Z.F., Morton, J.D., Mason, S.L., Bekhit, A.E.D.A. (2019a). Does Pulsed Electric Field Have A Potential to Improve the Quality of Beef from Older Animals and How? *Innovative Food Science & Emerging Technologies*, *56*: 1-8.

Bhat, Z.F., Morton, J.D., Mason, S.L., Jayawardena, S.R., Bekhit, A.E.D.A. (2019b). Pulsed Electric Field: A New Way to Improve Digestibility of Cooked Beef. *Meat Science*, *155*: 79-84.

Bhat, Z.F., Morton, J.D., Mason, S.L., Bekhit, A.E.D.A. (2019c). Pulsed Electric Field Operates Enzymatically by Causing Early Activation of Calpains in Beef During Ageing. *Meat Science*, *153*: 144-151.

Bhat, Z.F., Morton, J.D., Mason, S.L., Bekhit, A.E.D.A (2019d). Pulsed Electric Field Improved Protein Digestion of Beef During In-Vitro Gastrointestinal Simulation. *LWT – Food Science and Technology*, *102*: 45-51.

Bhat, Z.F., Morton, J.D., Mason, S.L., Bekhit, A.E.D.A, Mungure, T.E. (2019e). Pulsed Electric Field: Effect of In-Vitro

Simulated Gastrointestinal Protein Digestion of Deer *Longissimus dorsi*. *Food Research International*, *120*: 793-799.

Bhat, Z.F., Morton, J.D., Mason, S.L., Mungure, T.E.M., Jayawardena, S.R., Bekhit, A.E.D.A. (2019f). Effect of Pulsed Electric Field on Calpain Activity and Proteolysis of Venison. *Innovative Food Science & Emerging Technologies*, *52*: 131-135.

Bhat, Z.F., Morton, J.D., Mason, S.L., Bekhit, A.E.D.A. (2020). The Application of Pulsed Electric Field As a Sodium Reducing Strategy for Meat Products. *Food Chemistry*, *306*: 125622.

Bekhit, A.E.D.A., Ven, R., Suwandy, V., Fahri, F., Hopkins, D.L. (2014). Effect of Pulsed Electric Field Treatment on Cold-Boned Muscles of Different Potential Tenderness. *Food and Bioprocess Technology*, *7*(11): 3136-3146.

Bolado-Rodriguez, S., Gongora-Nieto, M.M., Pothakamury, U., Barbosa-Cánovas, G.V., Swanson, B.G. (2000). A Review of Nonthermal Technologies. In: Lozano JE, Añón C, Parada-Arias E, Barbosa-Cánovas GV (editors). *Trends in food engineering* (pp. 227-256). CRC press: New York.

Bolton, D.J., Catarame, T., Byrne, C., Sheridan, J.J., McDowell, D.A., Blair, I.S. (2002). The Ineffectiveness of Organic Acids, Freezing and Pulsed Electric Fields to Control *Escherichia coli* O157:H7 in Beef Burgers. *Letters in Applied Microbiology*, *34*: 139-143.

Bouzrara, H., Vorobiev, E. (2003). Solid-Liquid Expression of Cellular Materials Enhanced by Pulsed Electric Field. *Chemical Engineering and Processing*, *42*: 249-257.

Buckow, R., Sieh, N.G., Toepfl, S. (2013). Pulsed Electric Field Processing of Orange Juice: A Review on Microbial, Enzymatic, Nutritional, and Sensory Quality and Stability.

Comprehensive Reviews in Food Science and Food Safety, *12*: 455-467.

Chang, D.C. (1992). Structure and dynamics of electric field-induced membrane pores as revealed by rapid-freezing electron microscopy. In: Chang DC, Chassy BM, Saunders JA, Sowers AE (editors). *Electroporation and electrofusion* (pp. 9-28). Academic press, inc.: California.

Chian, F.M., Kaur, L., Oey, I., Astruc, T., Hodgkinson, S., Boland, M. (2019). Effect of Pulsed Electric Fields (PEF) on the Ultrastructure and *in vitro* Protein Digestibility of Bovine *Longissimus thoracis. LWT–Food Science and Technology*, *103*: 253-259.

Chian, F.M., Kaur, L., Oey, I., Astruc, T., Hodgkinson, S., Boland, M. (2021). Effects of Pulsed Electric Field Processing and Sous Vide Cooking on Muscle Structure and In Vitro Protein Digestibility of Beef Brisket. *Foods*, *10*, 1-13.

Choe, J.H., Stuart, A., Kim, Y.H.B. (2016). Effect of Different Aging Temperatures Prior to Freezing on Meat Quality Attributes of Frozen/Thawed Lamb Loins. *Meat Science*, *116*: 158-164.

Clemente, I., Condon-Abanto, S., Pedros-Garrido, S., Whyte, P., Lyng, J.G. (2020). Efficacy of Pulsed Electric Fields and Antimicrobial Compounds Used Alone and in Combination for the Inactivation of *Campylobacter jejuni* in Liquids and Raw Chicken. *Food Control*, *107*: 106-491.

Corte-Real, J., Bohn, T. (2018). Interaction of Divalent Minerals with Liposoluble Nutrients and Phytochemicals During Digestion and Influences on Their Bioavailability–A Review. *Food Chemistry*, *252*: 285-293.

Danowska-Oziewicz, M. (2009). The Influence of Cooking Methods on the Quality of Pork Patties. *Journal of Food Processing and Preservation*, *33*: 473-485.

Doevenspeck, H. (1961). Influencing Cells and Cell Walls by Electrostatic Impulses. *Fleischwirtschaft*, *13*(12): 968-987.

Dominguez, R., Pateiro, M., Gagaoua, M., Francisco, J.B., Zhang, W., Lorenzo, J.M. (2019). A Comprehensive Review on Lipid Oxidation in Meat and Meat Products. *Antioxidants*, *8*(10): 429.

Dziadek, K., Kopeć, A., Dróżdż, T., Kiełbasa, P., Ostafin, M., Bulski, K., Oziembłowski, M. (2019). Effect of Pulsed Electric Field Treatment on Shelf Life and Nutritional Value of Apple Juice. *Journal of Food Science and Technology*, *56*: 1184–1191.

Faridnia, F., Bekhit, A.E.D.A., Niven, B., Oey, I. (2014). Impact of Pulsed Electric Fields and Post-Mortem Vacuum Ageing on Beef *Longissimus thoracis* Muscles. *International Journal of Food Science & Technology*, *49*(11): 2339-2347.

Faridnia, F., Ma, Q.L., Bremer, P.J., Burritt, D.J., Hamid, N., Oey, I. (2015). Effect of Freezing as Pre-Treatment Prior to Pulsed Electric Fields Processing on Quality Traits of Beef Muscles. Innovative Food Science and Emerging Technologies, 29: 31-40.

Faridnia, F., Bremer, P., Burritt, D.J., Oey, I. (2016). Effect of Pulsed Electric Fields on Selected Quality Attributes of Beef Outside Flat (*Biceps femoris*). IFMBE Proceedings, 51-54.

Farouk, M.M., Al-Mazeedi, H.M., Sabow, A.B., Bekhit, A.E.D.A., Adeyemi, K.D., Sazili, A.Q., Ghani, A. (2014). Halal and Kosher Slaughter Methods and Meat Quality: A Review. Meat Science, 98(3): 505-519.

Feldhusen, F., Warnatz, A., Erdmann, R., Wenzel, S. (1995). Influence of Storage Time on Parameters of Colour Stability of Beef. Meat Science, 40(2): 235-243.

Giteru, S.G., Oey, I., Ali, M.A. (2018). Feasibility of Using Pulsed

Electric Fields to Modify Biomacromolecules: A Review. Trends in Food Science & Technology, 72: 913-113.

Gomez, B., Munekata, P.E.S., Gavahian, M., Barba, F.J., Marti-Quijal, F.J., Bolumar, T., Campagnol, P.C.B., Tomasevic, I., Lorenzo, J.M. (2019). Application of Pulsed Electric Fields in Meat and Fish Processing Industries: An Overview. Food Research International, 123: 95-105.

Grahl, T., Markl, H. (1996). Killing of Microorganisms by Pulsed Electric Fields. Applied Microbiology and Biotechnology, 45: 148-157.

Gudmundsson, M., Hafsteinsson, H. (2001). Effect of Electric Field Pulses on Microstructure of Muscle Foods and Roes. Trends in Food Science & Technology, 12: 122-128.

Haughton, P.N., Lyng, J.G., Cronin, D.A., Morgan, D.J., Fanning, S.W. (2012). Efficacy of Pulsed Electric Fields for the Inactivation of Indicatior Microorganisms and Foodborne Pathogens in Liquids and Raw Chicken. Food Control, 25: 131-135.

He, G., Yin, Y., Yan, X., Wang, Y. (2016). Semi-Bionic Extraction of Effective Ingredient from Fishbone by High Intensity Pulsed Electric Fields. Journal of Food Process Engineering, 40(2): 1-9.

Hwang, I.H., Devine, C.E., Hopkins, D.L. (2003). The Biochemical and Physical Effects of Electrical Stimulation on Beef and Sheep Meat Tenderness. Meat Science, 65(2): 677-691.

Inguglia, E.S., Zhang, Z., Tiwari, B.K., Kerry, J.P., Burgess, C.M. (2017). Salt Reduction Strategies in Processed Meat Products – A review. Trends in Food Science & Technology, 59: 70-78.

Jeong, S.H., Kim, E.C., Lee, D.U. (2020). The Impact of A Consecutive Process of Pulsed Electric Field, Sous-Vide

Cooking, and Reheating on the Properties of Beef *Semitendinosus* Muscle. *Foods*, *9*(11), 1674.

Khan, M.I., Jo, C., Tariq, M.R. (2015). Meat Flavor Precursors and Factors Influencing Flavor Precursors–A Systematic Review. *Meat Science*, *110*: 278-284.

Khan, A.A., Randhawa, M.A., Carne, A., Mohamed-Ahmed, I.A., Barr, D., Reid, M., Bekhit, A.E.D.A. (2017). Effect of Low and High Pulsed Electric Field on the Quality and Nutritional Minerals in Cold Boned Beef *M. Longissimus et lumborum*. *Innovative Food Science and Emerging Technologies*, *41*: 135-143.

Khan, A.A., Randhawa, M.A., Carne, A., Mohamed-Ahmed, I.A., Barr, D., Reid, M., Bekhit, A.E.D.A. (2018a). Quality and Nutritional Minerals in Chicken Breast Muscle Treated with Low and High Pulsed Electric Fields. *Food and Bioprocess Technology*, *11*: 122-131.

Khan, A.A., Randhawa, M.A., Carne, A., Mohamed-Ahmed, I.A., Al-Juhaimi, F.Y., Barr, D., Reid, M., Bekhit, A.E.D.A. (2018b). Effect of Low and High Pulsed Electric Field Processing on Macro and Micro Minerals in Beef and Chicken. *Innovative Food Science and Emerging Technology*, *45*: 273-279.

Klonowski, I., Heinz, V., Toepfl, S., Gunnarsson, G., Porkelsson, G. (2006). Application of Pulsed Electric Field Technology for the Food Industry. *R&D report summary* (pp. 1-10). Icelandic Fisheries Laboratories.

Kondjoyan, A., Daudin, J.D., Sante-Lhoutellier, V. (2015). Modelling of Pepsin Digestibility of Myofibrillar Proteins and of Variations due to Heating. *Food Chemistry*, *172*: 265-271.

Koohmaraie, M., Geesink, G.H. (2006). Contribution of Postmortem Muscle Biochemistry to the Delivery of Consistent Meat

Quality with Particular Focus on the Calpain System. *Meat Science*, *74*(1): 34-43.

Korma, S.A., Alahmad, K., Ali, A.H., Shoaib, M., Abed, S.M., Yves, H., Atindana, J.N., Qin, J. (2016). Application of Pulsed Electric Field Technology in Apple Juice Processing. *Austin Journal of Nutrition and Food Sciences*, *4*(2): 1080.

Laville, E., Sayd, T., Morzel, M., Blinet, S., Chambon, C., Lepetit, J., Renand, G., Hocquette, J.F. (2009). Proteome Changes During Meat Aging in Tough and Tender Beef Suggest the Importance of Apoptosis and Protein Solubility for Beef Aging and Tenderization. *Journal of Agricultural and Food Chemistry*, *57*(22): 10755-10764.

Li, M., Lin, J., Chen, J., Fang, T. (2016). Pulsed Electric Field-Assisted Enzymatic Extraction of Protein from Abalone (*Haliotis discus hannailno*) Viscera. *Journal of Food Process Engineering*, *39*(6): 702-710.

Longo, V., Lana, A., Bottero, M.T., Zolla, L. (2015). Apoptosis in Muscle-To-Meat Aging Process: The Omic Witness. *Journal of Proteomics*, *125*: 29-40.

Ma, Q., Hamid, N., Oey, I., Kantono, K., Faridnia, F., Yoo, M., Farouk, M. (2016). Effect of Chilled and Freezing Pre-Treatments Prior to Pulsed Electric Field Processing on Volatile Profile and Sensory Attributes of Cooked Lamb Meats. *Innovative Food Science and Emergin Technologies*, *37*: 359-374.

Martin-Belloso, O., Soliva-Fortuny, R. (2010). Pulsed Electric Fields Processing Basics. In: Zhang HQ, Barbosa-Cánovas GV, Balasubramaniam VM, Dunne CP, Farkas DF, Yuan JTC (editors). *Nonthermal processing technologies for food* (pp157-176). Blackwell publishing ltd.: Oxford, The UK.

McDonnell, C.K., Allen, P., Chardonnereau, F.S., Arimi, J.M., Lyng,

J.G. (2014). The Use of Pulsed Electric Fields for Accelerating the Salting of Pork. *LWT–Food Science and Technology*, *59*(2): 1054-1060.

Mungure, T.E., Bekhit, A.E.D.A, Birch, J., Kanokruangrong, S., Carne, A., Farouk, M.M. (2017). Impact of Aging Method and PEF Treatment on Meat Quality and Stability of Conjugated Linoleic Acid in Venison. *63rd International congress of meat science and technology* (pp: 620-621). 13-18 August, Cork, Ireland.

Mungure, T.E., Farouk, M.M., Birch, E.J., Carne, A., Staincliffe, M., Stewart, I., Bekhit, A.E.D.A. (2020). Effect of PEF Treatment on Meat Quality Attributes, Ultrastructure and Metabolite Profiles of Wet and Dry Aged Venison *Longissimus dorsi* muscle. *Innovative Food Science & Emerging Technologies*, *65*, Article 102457.

Neumann, E., Rosenheck, K. (1972). Permeability Changes Induced by Electric Impulses in Vesicular Membranes. *The Journal of Membrane Biology*, *10*: 279-290.

O'Dowd, L.P., Arimi, J.M., Noci, F., Cronin, D.A., Lyng, J.G. (2013). An Assesment of the Effect of Pulsed Electrical Fields on Tenderness and Selected Quality Attributes of Post-Rigour Beef Muscle. *Meat Science*, *93*: 303-309.

Oliveira, G., Tylewicz, U., Rosa, M.D., Andlid, T., Alminger, M. (2019). Effects of Pulsed Electric Field-Assisted Osmotic Dehydration and Edible Coating on the Recovery of Anthocyanins from *in vitro* Digested Berries. *Foods*, *8*(10): 1-11.

Primozic, M., Duchek, A., Nickerson, M., Ghosh, S. (2017). Formation, Stability and *in vitro* Digestibility of Nanoemulsions Stabilized by High-Pressure Homogenized Lentil Proteins Isolate. *Food Hyrdocolloids*, *77*: 126-141.

Stachelska, M.A., Szymczak, W.S., Jakubczak, A., Swislocka, R., Lewandowski, W. (2012). Influence of Pulsed Electric Field on the Survival of *Yersinia enterocolitica* in Minced Beef Meat. *Aparatura Badawcza i Dydaktyczna*, *17*: 13-17.

Suwandy, V., Carne, A., Ven, R., Bekhit, A.E.D.A., Hopkins, D.L. (2015a). Effect of Repeated Pulsed Electric Field Treatment on the Quality of Cold-Boned Beef Loins and Topsides. *Food and Bioprocess Technology*, *8*(6): 1218-1228.

Suwandy, V., Carne, A., Ven, R., Bekhit, A.E.D.A., Hopkins, D.L. (2015b). Effect of Pulsed Electric Field Treatment on Hot-Boned Muscles of Different Potential Tenderness. *Meat Science*, *105*: 25-31.

Suwandy, V., Carne, A., Ven, R., Bekhit, A.E.D.A., Hopkins, D.L. (2015c). Effect of Pulsed Electric Field Treatment on the Eating and Keeping Qualities of Cold-Boned Beef Loins: Impact of Initial pH and Fibre Orientation. *Food and Bioprocess Technology*, *8*(6): 1355-1365.

Toepfl, S., Heinz, V. (2007). Application of Pulsed Electric Fields to Improve Mass Transfer in Dry Cured Meat Products. *Fleischwirtschaft International: Journal for Meat Production and Meat Processing*, *22*: 62-64.

Toepfl, S., Siemer, C., Heinz, V. (2014a). Effect of High Intensity Elecetric Field Pulses on Solid Foods. In: Sun DW (chief editor). *Emerging technologies for food processing* (pp. 147-154). Academic press: The UK.

Toepfl, S., Siemer, C., Saldana-Navarro, G., Heinz, V. (2014b). Overview of Pulsed Electric Fields Processing for Food. In: Sun DW (chief editor). *Emerging technologies for food processing* (pp. 93-114). Academic press: The UK.

Toldra, F. (2003). Muscle Foods: Water, Structure and Functionality. *Food Science and Technology International*, *9*(3): 173-177.

Weaver, J.C. (2000). Electroporation of Cells and Tissues. *IEEE Transactions on Plasma Scienc*e, *28*(1): 24-33.

Wu, W., Yu, Q.Q., Fu, Y., Tian, X.J., Jia, F., Li, X.M., Dai, R.T. (2016). Towards Muscle-Specific Meat Color Stability of Chinese Luxi Yellow Cattle: A Proteomic Insight into Post-Mortem-Storage. *Journal of Proteomics*, *147*: 108-118.

Zhang, H.Q., Barbosa-Canovas, G.V., Balasubramaniam, V.M., Dunne, C.P., Farkas, D.F., Yuan, J.T.C. (2011). *Nonthermal processing technologies for food* (pp. 626). Blackwell publishing ltd.: Oxford, The UK.

Zhao, W., Yang, R. (2019). Pulsed Electric Field Processing of Protein-Based Foods. In: Jia J, Liu D, Ma H (editors). *Advances in food processing technology* (pp. 137-147). Zheijang university press: Hangzhou, China.

Zhao, Y.M., de Alba, M., Sun, D.W., Tiwari, B. (2019). Principles and Recent Applications of Novel Non-Thermal Processing Technologies for the Fish Industry–A Review. *Critical Reviews in Food Science and Nutrition*, *59*(5): 728-742.

Zhou, Y., He, Q., Zhou, D. (2016). Optimization Extraction of Protein from Mussel by High-Intensity Pulsed Electric Fields. *Journal of Food Processing and Preservation*, *41*(3): 1-8.

Zimmermann, U., Pilwat, G., Riemann, F. (1974). Dielectric Breakdown of Cell Membranes. *Biophysical Journal*, *14*(11): 881-899.

CHAPTER III

SHOOTING CONTROL OF FOUR-LEGGED ROBOT WITH ARTIFICIAL NEURAL NETWORKS TECHNIQUE

Ahmet Burak Tatar[1] & Beyda Taşar[2*] & Oğuz Yakut[3]

[1]Department of Mechatronics Engineering,
Firat University, Turkey
atatar@firat.edu.tr [1], Orcid: 0000-0001-5848-443X

[2]Department of Mechatronics Engineering,
Firat University, Turkey
btasar@firat.edu.tr[2], Orcid: 0000-0002-4689-8579

[3]Department of Mechatronics Engineering,
Firat University, Turkey
oyakut@firat.edu.tr[3], Orcid: 0000-0002-0986-1435

1. Introduction

The rapid development of military technologies makes gun systems more complex. Therefore, research methods, which are used in the selection of gun systems, are increasing day by day (Lee et al., 2001). The main purpose of the gun control system is to maximize the possibility of hitting a fixed or moving target from a fixed or moving vehicle as soon as possible (Purdy, 2001). The most basic way to solve this problem is the stabilization of the gun barrel. If the gun systems, which are used in vehicles, are subjected to disruptive

effects on the move, other precautions must be taken to keep the gun or aiming unit stationary at the target. These measures are called stabilization (Germershausen et. al.,1982). With the gun barrel stabilization, a successful target tracking is ensured despite under all disruptive effects.

Today, many organizations in the field of defense industry get help from military robots (Simon,2015). Legged robots are the best option for moving on rough terrain. Legged robots have 5 potential advantages according to wheeled or tracked vehicles over this type of terrain: higher speed, better fuel performance, greater mobility, better walking in ground irregularities and less environmental damage (Song et. al, 1989). Four-legged robots provide more balanced movement than two-legged robots. However, increasing the number of legs of the robot not only increases the balance of the robot, but also increases the complexity of control and walking required for movement. However, the weight of the robot increases and the robot's productivity is reduced. Therefore, four-legged robots are preferred in legged robots applications (Brewer, 2011). In this study, the gun turret system, which was placed on a four-legged robot, was modeled on a planar basis. Dynamic expressions of the model were obtained and walking simulations of the robot were made. Artificial Neural Network (ANN) is a mathematical model that tries to simulate the structure and functionality of biological neural networks. The basic building block of each artificial neural network is an artificial neuron, which is a simple mathematical function (Krenker et al, 2011). When the robot is walking, the walking movement causes disruptive effects on the gun systems.

Under these external effects, shootings directed at fixed targets during the walking of the robot were performed by using the artificial neural network based control method.

While the robot was walking, the shooting simulations were

made for randomly determined fixed targets. These targets, which were determined randomly, were selected between 5-15 meters. Under disruptive effects the success of the gun barrel stabilization, was evaluated with graphics and tables. Also in the system simulation, the internal ballistics and the planar mathematical model of the bullet core are also discussed.

Figure. 1. shows the simulation of the shooting to the fixed target over the four-legged robot. To fix the barrel to the target coordinate, the barrel reference angle (β_{target}) was updated simultaneously and used in the control system.

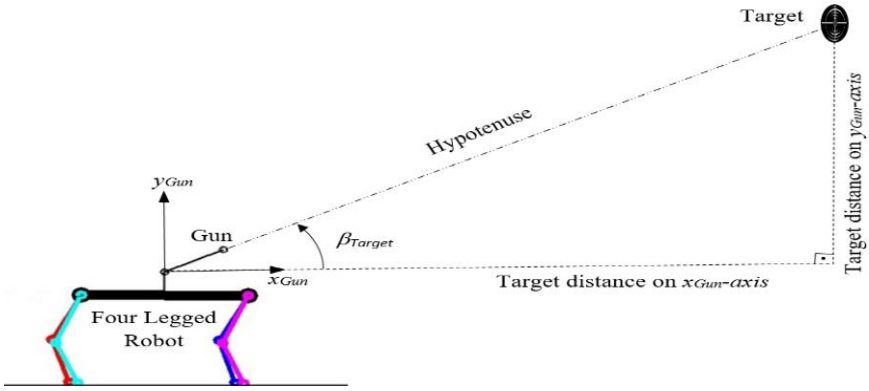

Figure. 1 Image of the shooting simulation
from over the robot to fixed target

Because of the fact that position of the target on the horizontal and vertical axes is known, the distance of the barrel to the target is calculated and the barrel reference angle is determined by the geometric approach. In the simulations, Runge-Kutta numerical approach method was used. Runge-Kutta method is widely used in numerical solutions of differential equations (Dontchey et al.,2001; Kaya, 2010).

2. Material and Method

2.1. Kinematic Analysis

Kinematic analysis is used to calculate the position and orientations of the manipulator without considering the external forces and moments in robotic systems (Fernandes et al., 2018). Forward and inverse kinematic analysis are examined separately. Forward kinematic analysis is used to calculate the angular orientation of the known robot's end-function. Inverse kinematic analysis refers to the calculation of joint angles in a kinematic chain. Thus, the end-effector reaches the set target (Erleben et al, 2019).

Figure. 2. shows the axial placement of the four-legged robot's single-leg. According to Denavit-Hartenberg method, D-H table was created with this axis placement and given in Table 1.

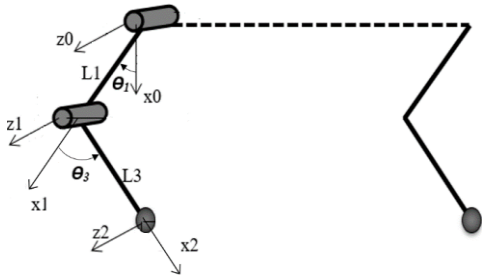

Figure. 2 Axial placement of a single leg

Table 1 D-H Table

Link	$\boldsymbol{\theta}$	**d**	$\boldsymbol{\alpha}$	**a**
1	θ_1	0	0	l_1
2	θ_3	0	0	l_3

The transformation matrices (A_i) of each joint in a leg of the robot were calculated and basic transformation matrices obtained as in Eqs. (1) and (2). The last column of the matrix in (2) gives the position expressions of the robot's end effector. Therefore, the position equations in the x, y and z axes are obtained as in (3).

$$^{2}_{0}T = A_1 A_2 \tag{1}$$

$$^{2}_{0}T = \begin{bmatrix} \cos(\theta_1+\theta_3) & -\sin(\theta_1+\theta_3) & 0 & l_1\cos\theta_1 + l_3\cos(\theta_1+\theta_3) \\ \sin(\theta_1+\theta_3) & \cos(\theta_1+\theta_3) & 0 & l_1\sin\theta_1 + l_3\sin(\theta_1+\theta_3) \\ 0 & 0 & 1 & 0 \\ 0 & 0 & 0 & 1 \end{bmatrix} \tag{2}$$

$$p_x = l_1\cos\theta_1 + l_3\cos(\theta_1+\theta_3),$$

$$p_y = l_1\sin\theta_1 + l_3\sin(\theta_1+\theta_3),$$

$$p_z = 0 \tag{3}$$

In inverse kinematic analysis, the angular equations of the leg joints were obtained as in (4) and (5) by using these calculated position expressions.

$$\cos\theta_3 = \sqrt{\frac{p_x^2+p_y^2-l_1^2-l_3^2}{2l_1l_3}},\ \sin\theta_3 = \pm\sqrt{1-\cos\theta_3{}^2},\ \theta_3 = \arctan\left(\frac{\sin\theta_3}{\cos\theta_3}\right) \tag{4}$$

$$\cos\theta_1 = \frac{p_x l_3\cos\theta_3 + p_x l_3 + p_y l_3\sin\theta_3}{p_x^2+p_y^2},\ \sin\theta_1 = \pm\sqrt{1-\cos\theta_1{}^2},$$

$$\theta_1 = \arctan\left(\frac{\sin\theta_1}{\cos\theta_1}\right) \tag{5}$$

2.2. Dynamic Model of the System

Four legged robot with a gun turret placed on it, is modeled planarly to create the dynamic model. In accordance with this model, equations of motion are obtained. The physical model of the system is given in Figure. 3. When the physical model given in Figure 3 is examined, it can be seen that the body can perform angular motion in one axis and linear motion in two axes. Therefore, the system has a total of 12 degrees of freedom (DOF). Due to the modeling is carried out planarly, the movement of the gun barrel is made by an angular joint with a single degree of freedom. There are two revolute joints on each leg of the four-legged robot. However, the body of the robot

can make angular and translatory motion relative to the ground in horizontal and vertical axes. According to this physical model, dynamic motion equations of robot have been obtained by using parametric expressions. Lagrange-Euler method was used to calculate these mathematical expressions. The Lagrange-Euler method is used to systematically derive equations of motion taking into account the kinetic and potential energies of a given system (Dhaouadi et al., 2013). The basic equation of the method is as given in (6).

$$\frac{d}{dt}\frac{\partial}{\partial \dot{q}_i} L(q,\dot{q}_i) - \frac{\partial}{\partial q_i} L(q,\dot{q}_i) = \tau_i \; 1 \le i \le n \qquad (6)$$

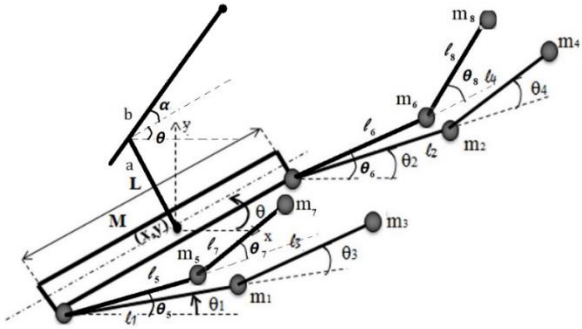

Figure. 3 Physical model of the system

In this equation, $\boldsymbol{n}$ represents the degree of freedom, $\boldsymbol{q_i}$ is the position of the moving element, and $\boldsymbol{i}$ is the moving element index. According to the Lagrange-Euler method, the basic Lagrange equation is calculated as (7) by taking the difference of the total kinetic energy (8) and the total potential energy (9) of the system.

$$L = T - V \qquad (7)$$

$$T = \frac{1}{2}M(\dot{x}^2 + \dot{y}^2) + \frac{1}{2}I\dot{\theta}^2 + \frac{1}{2}m_1(\dot{x}_1^2 + \dot{y}_1^2) + \frac{1}{2}m_2(\dot{x}_2^2 + \dot{y}_2^2) + \frac{1}{2}m_3(\dot{x}_3^2 + \dot{y}_3^2) + \frac{1}{2}m_4(\dot{x}_4^2 + \dot{y}_4^2) + \frac{1}{2}m_5(\dot{x}_5^2 + \dot{y}_5^2)$$

$$+\frac{1}{2}m_6(\dot{x}_6^2+\dot{y}_6^2)+\frac{1}{2}m_7(\dot{x}_7^2+\dot{y}_7^2)+\frac{1}{2}m_8(\dot{x}_8^2+\dot{y}_8^2)$$

$$+\frac{1}{2}m_n(\dot{x}_n^2+\dot{y}_n^2) \quad (8)$$

$$V = Mgy + m_1gy_1 + m_2gy_2 + m_3gy_3 + m_4gy_4 + m_5gy_5 + m_6gy_6 + m_7gy_7 + m_8gy_8 + m_ngy_n \quad (9)$$

In order to calculate the kinetic and potential energy equations in (8) and (9), the position expressions of all system elements must be determined. Position equations of the gun barrel and legs are given in (10) - (27).

$$x_1 = x - \frac{l_g}{2}\cos\theta + l_1\cos\theta_1 \quad (10)$$

$$y_1 = y - \frac{l_g}{2}\sin\theta + l_1\sin\theta_1 \quad (11)$$

$$x_2 = x + \frac{l_g}{2}\cos\theta + l_2\cos\theta_2 \quad (12)$$

$$y_2 = y + \frac{l_g}{2}\sin\theta + l_2\sin\theta_2 \quad (13)$$

$$x_3 = x - \frac{l_g}{2}\cos\theta + l_1\cos\theta_1 + l_3\cos(\theta_1+\theta_3) \quad (14)$$

$$y_3 = y - \frac{l_g}{2}\sin\theta + l_1\sin\theta_1 + l_3\sin(\theta_1+\theta_3) \quad (15)$$

$$x_4 = x + \frac{l_g}{2}\cos\theta + l_2\cos\theta_2 + l_4\cos(\theta_2+\theta_4) \quad (16)$$

$$y_4 = y + \frac{l_g}{2}\sin\theta + l_2\sin\theta_2 + l_4\sin(\theta_2+\theta_4) \quad (17)$$

$$x_5 = x - \frac{l_g}{2}\cos\theta + l_5\cos\theta_5 \quad (18)$$

$$y_5 = y - \frac{l_g}{2}\sin\theta + l_5\sin\theta_5 \quad (19)$$

$$x_6 = x + \frac{l_g}{2}\cos\theta + l_6\cos\theta_6 \quad (20)$$

$$y_6 = y + \frac{l_g}{2}\sin\theta + l_6\sin\theta_6 \quad (21)$$

$$x_7 = x - \frac{l_g}{2}\cos\theta + l_5\cos\theta_5 + l_7\cos(\theta_5 + \theta_7) \quad (22)$$

$$y_7 = y - \frac{l_g}{2}\sin\theta + l_5\sin\theta_5 + l_7\sin(\theta_5 + \theta_7) \quad (23)$$

$$x_8 = x + \frac{l_g}{2}\cos\theta + l_6\cos\theta_6 + l_8\cos(\theta_6 + \theta_8) \quad (24)$$

$$y_8 = y + \frac{l_g}{2}\sin\theta + l_6\sin\theta_6 + l_8\sin(\theta_6 + \theta_8) \quad (25)$$

$$x_n = x - \mathrm{a}\sin\theta + b\cos(\alpha + \theta) \quad (26)$$

$$y_n = y + \mathrm{a}\cos\theta + b\sin(\alpha + \theta) \quad (27)$$

The positions of the vertical axis are used to calculate the potential energy of the system. The expression of kinetic energy is calculated by deriving the position of the legs and barrel on the horizontal and vertical axes by time. As a result of all these middle tiers, Lagrange expression was obtained and given in Appendix-1. Moreover, since the system has 12 degrees of freedom, the dynamic equations of the moving joints are presented in Appendix-2. During the movement of the robot, the Jacobian matrix form (28) was used to transmit the reaction force of the ground to the robot body and to determine the effects of this force.

$$[J] = \begin{bmatrix} \frac{\partial x_i}{\partial x} & \frac{\partial x_i}{\partial y}\frac{\partial x_i}{\partial \theta} & \frac{\partial x_i}{\partial \theta_1} & \frac{\partial x_i}{\partial \theta_2}\frac{\partial x_i}{\partial \theta_3} & \frac{\partial x_i}{\partial \theta_4} & \frac{\partial x_i}{\partial \theta_5}\frac{\partial x_i}{\partial \theta_6} & \frac{\partial x_i}{\partial \theta_7} & \frac{\partial x_i}{\partial \theta_8} \\ \frac{\partial y_i}{\partial x} & \frac{\partial y_i}{\partial y}\frac{\partial y_i}{\partial \theta} & \frac{\partial y_i}{\partial \theta_1} & \frac{\partial y_i}{\partial \theta_2}\frac{\partial y_i}{\partial \theta_3} & \frac{\partial y_i}{\partial \theta_4} & \frac{\partial y_i}{\partial \theta_5}\frac{\partial y_i}{\partial \theta_6} & \frac{\partial y_i}{\partial \theta_7} & \frac{\partial y_i}{\partial \theta_8} \end{bmatrix} \quad (28)$$

When the appropriate parameters are adapted to this Jacobian matrix form, the expressions showing the effect of the movements on the horizontal and vertical axes to the body and legs are shown in Appendix-3. The Jakobien matrix form (29), which calculates the effect of single degree of freedom gun barrel movements on the body, has been given and the gun barrel Jacobian matrix is included in Appendix-4. Table 2. shows the numerical values of the system parameters.

Table 2 Parametric values in the system

Parameter	Value
M	12 kg
l_g	0.8 m
l_1, l_2, l_5, l_6	0.24 m
l_3, l_4, l_7, l_8	0.2 m
m_n	1 kg
m_1, m_2, m_5, m_6	1.5 kg
m_3, m_4, m_7, m_8	0.5 kg
a	0.1 m
b	0.3 m

2.3. Quadruped Walking with PID Control Method

The PID controller is the most common form of feedback control. PID controllers are available in all areas where control systems are available today (Aström, 2002). The control signal of the ideal PID controller is calculated by the formula given in (30).

$$u(t) = K_p e(t) + K_d \frac{d_{e(t)}}{d_t} + K_i \int_0^t e(t)\, d_t \quad (30)$$

In this study, proportional, derivative and integral coefficients of the controller were determined as K_p = 500, K_d = 50, K_i = 0.1 by trial and error technique. The basis of the robot's walking motion is that the leg joints track the appropriate angular positions. PID controller is used to keep leg joints in the reference angular position. Therefore, the trajectory planning was carried out for this purpose. Walking patterns for four-legged robots are divided into 3 groups:

- ✓ Gait transition at which the three legs support the main body at any time during the walking motion
- ✓ Gait transition at which two legs support the body at any time during walking motion such as trot, pace, bounce

✓ Gait transition at which least one leg support the body at any time during walking motion such as gallop

The trot walking sequence, which is used for the simulations, is shown in Figure. 4 (Tsujita et al.,2001). As can be seen, the robot performs a symmetrical walking in each case, since both legs are in contact with the ground.

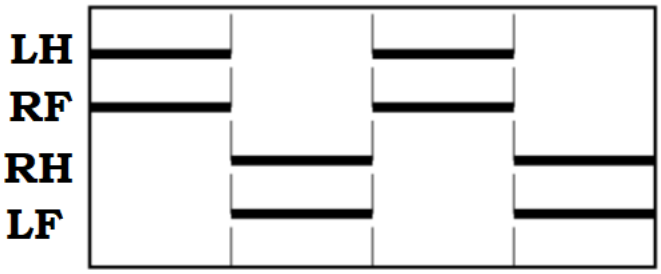

Figure. 4 Trot gait sequence

In the first half of the walking period, the left hind and right front leg contact the ground. in the second half, the right hind and left front leg contact the ground. So, robot can realize its trot walking. The movement of the legs during the walking will affect the body and the body will be under movement. Therefore, this body ovement acts as a disruptive effect on the gun barrel stabilization. When the performing its trot gait, the trajectory, which is tracked by the leg steps, is given in Figure. 4. There are two different phases in each step of the leg; flight andstance. When the leg is in contact with the ground, it is seen that the flight phase is over. At the same time, as soon as the leg interrupts its contact with the ground, it is seen that the stance phase is over.

It is considered that, while the robot taking a step, it tracks a sinusoidal trajectory. Thus, the defined sinusoidal function is indicated in the expression in (31).

$$h_s = h_{step} Sin(2\pi\omega t) \quad (31)$$

L_S indicates the amount of displacement of the leg in the horizontal axis while the leg taking a step in Figure. 5. h_{step} refers to the height of the leg from the ground during the stepping. The mathematical expression used to calculate the displacement of the robot is given in (32).

$$V_r = \frac{L_S}{T_G} \quad (32)$$

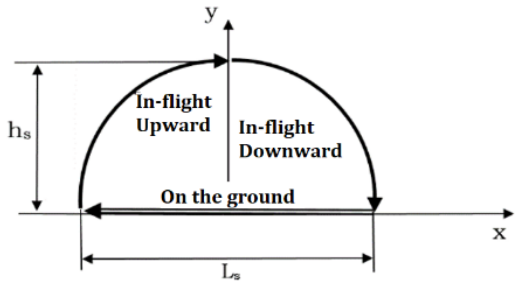

Figure. 5 The trajectory of the robot leg in one step

2.4. Control of Gun Barrel Stabilization with Artificial Neural Network

Artificial neural networks are used as an indispensable method for many modeling and control applications in non-linear systems due to their generalization and learning abilities (Duda et al., 2012). In this study, the numerical value of the control for gun barrel stabilization was calculated with an ANN model. As seen in Figure. 6., the ANN model is composed of two layers and two cells in the first layer and one cell in the last layer. The "Tansig" function was used as the activation function in the cells of the first layer and the "Purelin" function was used for the cell in the last layer. The error and the derivative of the error were applied as input to ANN, and the control signal was obtained at the output.

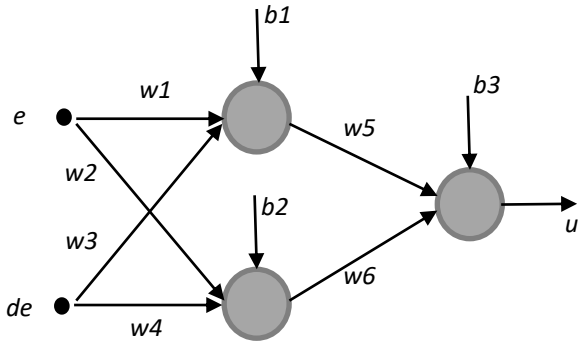

Figure. 6 ANN model for gun barrel control signal

The weighting coefficients are determined by using the appropriate training method in the learning process of an ANN. In the method to be used, the weight values of a network to be trained must be changed dynamically within a certain measurement (Ripley, 1996). Learning methods in literature are divided into three groups; controlled, uncontrolled and reinforced (Bishop, 1995)

In this study, the weight and bias coefficients required for ANN were optimized using genetic algorithm (GA) technique. This optimization process has been done by using the genetic algorithms toolbox of the Matlab package program. As a performance index, a objective function such as (33) is defined.

$$F_J = \sum e^2 \tag{33}$$

Initially, weight coefficients were selected randomly and their optimum values were calculated based on the performance index. The block diagram representing the optimization of ANN weights with the genetic algorithm technique is shown in Figure. 7.

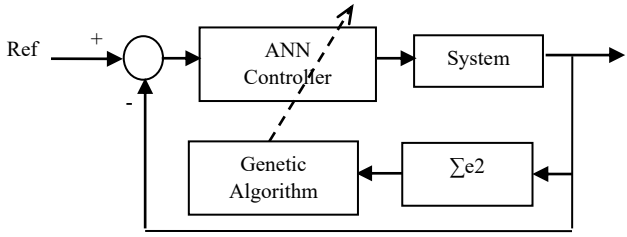

Figure. 7 Block diagram of optimization of ANN weight coefficients with GA

2.5. Mathematical model of bullet and shooting

In this study, hits were made from the four-legged robot to fixed target coordinates, which is determined randomly, by using the dynamics of the bullet core in the gun barrel.

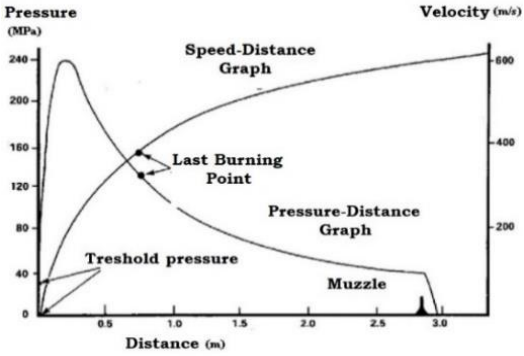

Figure. 8 Graph of gas pressure and velocity in the gun barrel

The parameters such as bullet core, thrust force and bullet velocity were taken into account when leaving the gun barrel. Graphical values in Figure. 8. were used while examining the dynamic motion of the bullet (Yıldırım, 2013).

In this study, technical specifications of 9 mm parabellum bullet core are discussed. These specifications are given in Table 3 (Milli Savunma, 2017). Bullet core other than shell m_{bullet}=8 grams weight.

Table 3 Parabellum pistol 9 mm bullet features

Technical Characteristics	
Specification	Stanag 4090, AEP-97 Edition A (Multi Calibre MOPI)
Cartridge Length	29,69 – 0,3 mm
Cartridge Weight	~12,15 g
Velocity	370 $\pm$ 10 m/s (in 16 m)
Velocity Standard Deviation	max. 9 m/s
Average shell mouth pressure	max. 2850 bar
Distribution	7,6 cm (in 46 m)
Bullet Contact Force	min. 20,4 kgf
Shell Model Number	9 mmx19 parabellum shell
Bullet Type	FMJ, bullet liner thimble brass (CuZn36), cartridge bullet – Antimony alloys
Bullet Weight	8 $\pm$0,075 g
Shell Material	Brass (CuZn30)
Capsule	9 mm capsule, boxer

In Figure. 9., the physical model of the dynamic behavior of the projectile is given. It is seen that the bullet moves linearly in horizontal and vertical axes. The bullet, which is throwed with F_{thrust} force from the gun barrel, leaves the barrel with V_b velocity. From this moment on, the motion of the bullet core is affected only by the gravity and the F_{Aero} surface friction force caused by the atmosphere.

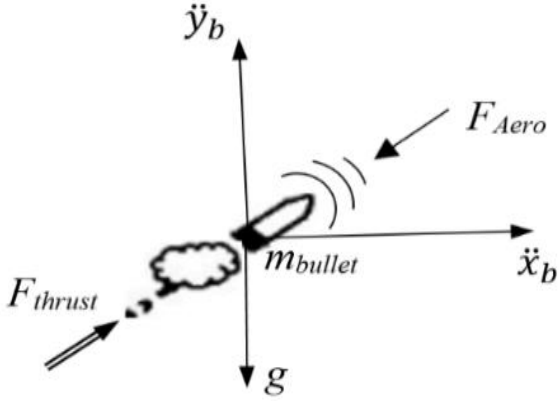

Figure. 9. The physical model of the bullet moving in the plane

In this study, the thrust pressure P_b (34), which the bullet core is exposed to until it leaves the barrel, is modeled with a mathematical function as in the expression. The parameters in the model are defined as P=1500, λ=500, ω_b=50. In the simulations, it was assumed that the bullet had a t (0-10) millisecond time interval to leave the gun barrel. From the moment the bullet leaves the barrel, the value of this pressure will be zero.

$$P_b = Pe^{-\lambda t} Sin(2\pi\omega_b t) \tag{34}$$

The bullet with a diameter of 9 mm can be calculated by the expression of the F_{thrust} thrust force (35), which is proportional to the pressurized surface area A_b.

$$F_{thrust} = A_b P_b \tag{35}$$

The planar dynamic behavior of the bullet was obtained mathematically by using the physical model in Figure 9 and according to Newton's laws of motion. The equation of motion in the horizontal x_b -axis (36) and the equation of motion in the vertical y_b -axis were obtained as (37). Here g is the acceleration of gravity.

$$\ddot{x}_b = \frac{F^x_{thrust} - F^x_{Aero}}{m_{bullet}} \tag{36}$$

$$\ddot{y}_b = \frac{F^y_{thrust} - F^y_{Aero} - g}{m_{bullet}} \tag{37}$$

The $\boldsymbol{F_{Aero}}$ friction force (38), which occurs when moving with $\boldsymbol{V_b}$ velocity in the atmosphere, is calculated by the expression.

$$F_{Aero} = \frac{1}{2}\rho S C_d {V_b}^2 \qquad (38)$$

Here, $\boldsymbol{\rho}$ is density of the air and **S** is the surface area, which is perpendicular to the progression direction of bullet.

3. Experimental Results

3.1. Simulation results of trot pattern

The trot gait of the four-legged robot with a dynamic model was realized by simulating it in Matlab. The image obtained from different stages of the walking simulation is given in Figure 10. The robot moved from a stationary state to a distance of about 4 meters at the end of a 7-second simulation.

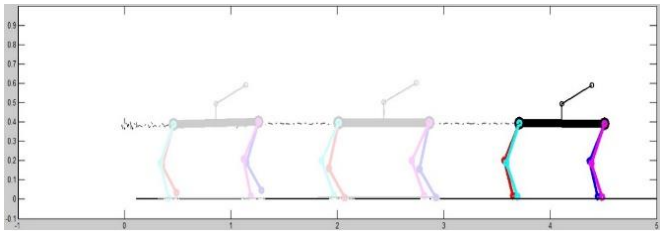

Figure 10. Trot gait simulation of quadruped robot

According to this formulation, the feed rate is calculated by the ratio of the the distance taken in one step to a period of time. When we look at the graphical results obtained in Figure 11, the position and velocity values of the robot body on the horizontal axis can be seen. After the 4th second of the simulation, a linear velocity of 1 m / s moved towards up to 4 meters. However, the swing amplitude of the robot body on the vertical axis is approximately 3 cm to 4 cm. In addition, when looking at the angular position graph of the body, it is seen that the rolling amplitude is in the range of 2 ° -3 °.

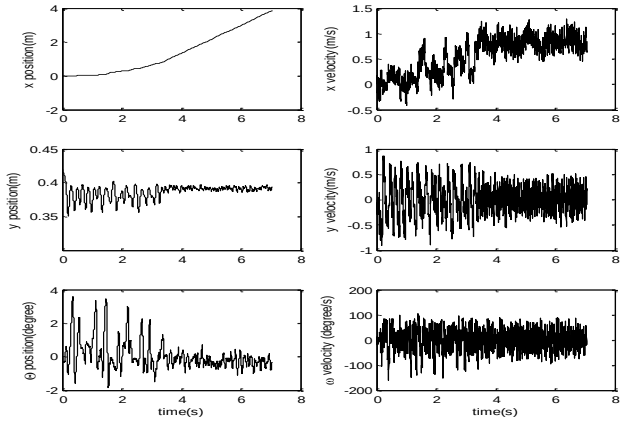

Figure. 11 Graphical results of walking simulation

3.2. Simulation results of gun barrel control

The coefficient of friction between bullet and air was taken as $\mathbf{C_d}$ = 0.12. By using these expressions, the velocity curve of the bullet is shown in Figure 12, together with the change of the thrust force, which effects to the bullet core, in the time from the moment of triggering to the leaving of the gun barrel.

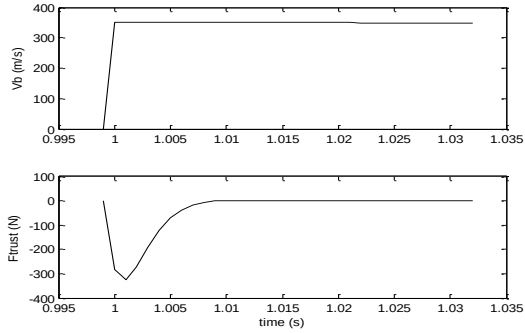

Figure. 12 Ballistics of bullet core

Table 4 Optimum values of weight and bias coefficients of ANN

w_1	w_2	w_3	w_4	w_5	w_6	b_1	b_2	b_3
48.47	0.33	11.89	23.08	33.90	8.13	0.17	29.70	0.77

The optimum values of the weights and bias coefficients of ANN are given in Table 4. In the optimization process realized by the genetic algorithm method, the population number was selected as 20 and the weight coefficients were obtained as a result of 100 iterations. Within this study, controls were performed in order to orient the gun barrel to the designated reference points while the robot walking movement was performing in Figure 13. In the simulations, 3 different target angles were determined and the barrel starting angle was accepted as 0 °.

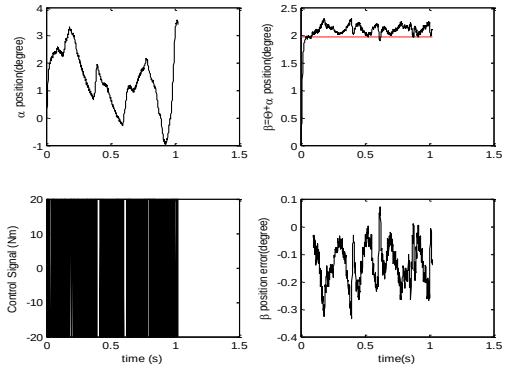

Figure 13. System responses of the gun barrel in simulation for 2°

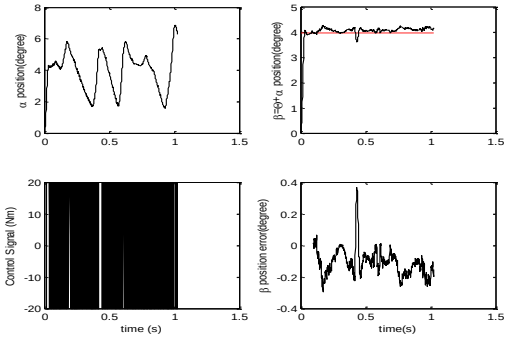

Figure. 14 System responses of the gun barrel in simulation for 4°

The second reference angle value was set to $\beta_{target}(\alpha+\theta) = \mathbf{4^o}$ and the barrel was intended to be kept in this reference. Figure 14 shows the system responses of the simulation. The angular error value of the barrel around the reference position was at most 0.36 °.

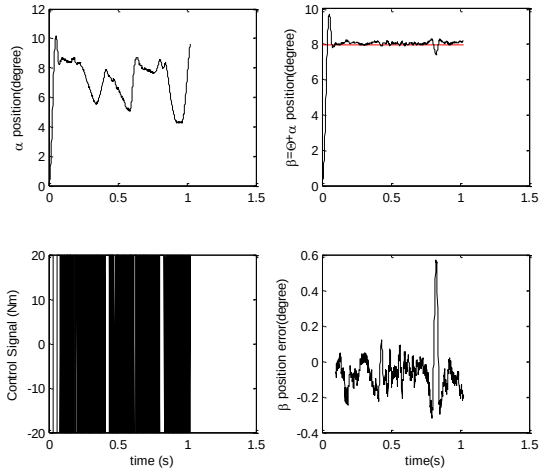

Figure 15. System responses of the gun barrel in simulation for 8°

Finally, the reference angle value was determined as $\beta_{target}(\alpha+\theta) = \mathbf{8^o}$ and the barrel was intended to be kept in this reference. Figure 15 shows the system responses of the simulation. Angular error value of the barrel angular position, β_{target} angle was observed to be at most 0.57 °.

3.3. Simulation results of of shooting fixed target

According to these results, it is seen that the bullet core has reached a maximum velocity value of about 350 m / s in a very short time. The coordinates of the fixed targets for the shooting simulations were determined randomly between 5-15 meters in the horizontal axis and 0.5-2 meters in the vertical axis. During the simulation, the barrel reference angle was updated and calculated instantly, taking into account the position of the robot, which changed according to the fixed target during walking. The reference angle was calculated as β_{target} (39), depending on the e_x-position error of the gun on the horizontal axis and the e_y-position error to the target on the vertical axis.

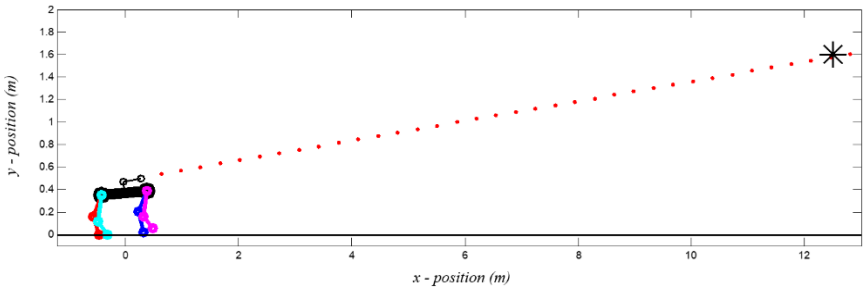

Figure 16 Simulation image at the time of target hitting

$$\beta_{target} = atan2\left(\frac{e_y}{e_x}\right) = atan2\left(\frac{y_{target}-y_{gun}}{x_{target}-x_{gun}}\right) \qquad (39)$$

Simulations were performed using Runge-Kutta numerical approach developed in Matlab program. Figure. 16. shows the simulation image of a hit on target from the four-legged robot while its walking.

As a result of the simulations, the errors of the hits made with the positions of the randomly determined targets are given in Table 5. According to this, it is seen that the maximum hit error is 0.16 meters. The lowest hit error value is 0.02 meters. The mean value of these errors was 0.076 m and the standard deviation was 0.047 m.

Table 5 Randomly set fixed target coordinates and hit errors

Target Number	x_{target} (m)	y_{target} (m)	Error (m)
1	13,90	1,63	0,05
2	7,94	1,46	0,04
3	10,61	2,04	0,12
4	6,29	1,17	0,04
5	10,61	1,09	0,16
6	12,79	0,63	0,13
7	14,35	1,18	0,04
8	6,85	1,46	0,10
9	13,34	0,61	0,02
10	6,06	0,60	0,06

If the target distance is increased, it is thought that the bullet core will reach the target with a greater deviation from the gravitational effect. In order to demonstrate the success of the barrel stabilization, it was approved to perform the simulation with short distance hits. Accordingly, the success of the hits directed to 10 different targets were examined and the numerical values were presented as a Table 5. As a result of the hits made from these distances, it was revealed that a fixed target with a diameter of 14 cm could be hit with a very high success rate. With these successful results, it is clear that the gun system placed on the four-legged robot can be used in practice for the defense industry. It is thought that this study contributes to the literature, in the field of defense industry.

4. Conclusions

In this study, a gun system was placed on a four-legged robot and it was modeled in planar. With this model, it is aimed to realize the shooting simulations to randomly determined fixed targets. The mathematical motion equations of the system required for the realization of the simulations were also obtained and the walk of the robot was simulated using the commonly used trot walking sequence for four-legged robots. Therefore, this walking motion of the robot will cause rolling and oscillation movements in the gun system. Despite these disruptive effects, the gun barrel stabilization was performed in order to keep the barrel in the desired reference angular position. Artificial neural network based control method was applied to stabilize the gun system. The weight coefficients of ANN were determined by an optimization technique. System responses of applied control simulations are presented graphically. According to these results, it has been seen that it can be achieved successful hits to the fixed targets on four-legged robot. It is recommended that such systems should not be used for any reason other than the deterrence

purpose. In the future, other control methods with different characteristics will be applied to this system and the results will be compared. Some methods can be developed to increase the success of the hit.

Nomenclature

M	Mass of robot body	β	Barrel reference angle
x	Position of robot body in horizontal axis	g	Gravity
y	Position of robot body in vertical axis	h_{ste}	The height of the leg up from the ground
m_{1-8}	Masses of robot leg limbs	w	The frequency of the step motion
θ	Angular position of robot body to floor by vertical axis	L_s	Step length
θ_{1-8}	Angular positions of leg limbs	F_{th}	Bullet force
l_g	Length of robot body	F_{aero}	Surface frictional force of gravity and atmosphere
l_{1-8}	Length of leg limbs	V_b	Bullet velocity
a	Gun turret length	P_b	Repulsion pressure
b	Gun barrel length	A_b	Pressure surface area
x_{1-8}	Positions of robot leg limbs in horizontal axis	C_d	Coefficient of friction between bullet and air
y_{1-8}	Positions of robot leg limbs in vertical axis	x_{tar}	Position of the target on the horizontal axis
I	Moment of inertia of robot body	y_{tar}	Position of the target on the vertical axis
α	Relative angular position of gun barrel to body	x_{gun}	Position of the gun barrel on the horizontal axis
x_n	Position of the gun barrel on the horizontal axis	y_{gun}	Position of the gun barrel on the vertical axis
y_n	Position of the gun barrel on the vertical axis	e_x	Position error on the horizontal axis
m_n	The mass of the gun barrel	e_y	Position error on the vertical axis

Acknowledgment

This study was performed as part of the doctoral thesis titled "Four-Legged Hunter Robot" carried out under the supervision of Assoc. Prof. Dr. Oğuz YAKUT in the Department of Mechatronics Engineering, Faculty of Engineering at Firat University.

Declaration

Funding: There isn't any funding source for this research.

Conflicts of Interest/Competing Interests: Ahmet Burak TATAR, Beyda TAŞAR and Oğuz YAKUT declare that they have no conflict of interest.

Availability of data and material: All data used to support the findings of this study are included within the article.

Code Availability: Not applicable

Ethics Approval: Not Applicable

Consent to participate: We accept to participate

Consent for publication: We accept to send this manuscript for publication. Not open access.

Authors' contributions: Ahmet Burak Tatar took part in all phases of kinematic and dynamic calculations, design, modeling, simulation and control. Beyda Taşar contributed to simulation and control studies. Oğuz Yakut contributed to the design and simulation studies. All authors contribute to the article writing.

References

Aström, K.J.: Control system design. Department of Mechanical & Environmental Engineering. University of California, Santa Barbara, pp. 216-217 (2002)

Bishop, C.M.: Neural networks for pattern recognition: Oxford

university press (1995)

Brewer, T.K.: Development of a quadruped robot and parameterized stair-climbing behavior. Master Thesis, Department of Mechanical Engineering Institute for Systems Research, pp. 3-4 (2011)

Dhaouadi, R., Hatab, A.A.: Dynamic Modelling of Differential-Drive Mobile Robots using Lagrange and Newton-Euler Methodologies: A Unified Framework. Advanced in Robotics and Automation, **2**(3) (2013)

Dontchey, A.L., Hager, W.W., Veliov, V.M.: Second order Runge-Kutta approximations in control constrained optimal control. SIAM J. Numer. Anal. **38**(1), 202-226 (2001)

Duda, R.O., Hart P.E., Stork, D.G.: Pattern classification: John Wiley & Sons, 2nd Edition (2012)

Erleben, K., Andrews, S.: Solving inverse kinematics using exat Hessian matrices. Computers & Graphics, **78**, 1-11 (2019)

Fernandes, J.J., Selvanukar, A.A.: Kinematic and Dynamic analysis of 3PPPU parallel manipülatör for medical applications. Procedia Computer Science, **133**, 604-611 (2018)

Germershausen, R., et. al,: Handbook on weaponary. Rheinmetall GmbH, Düsseldorf, pp. 257 (1982)

Kaya, C.Y.: Inexact restoration for Runge-Kutta discretization of optimal control problems. SIAM J. Numer. Anal. **48**(4), 1492-1517 (2010)

Krenker, A., Bešter, J., Kos, A.: Introduction to the artificial neural networks. Artificial Neural Networks-Methodological Advances and Biomedical Applications, InTech (2011)

Lee, J., Kang, S.H., Rosenberger, J., Kim, S.B.: A hybrid approach of goal programming for weapon systems selection. Computers & Industrial Engineering, **58**, 521-527 (2010)

Milli Savunma, http://www.millisavunma.com/mkek-hafif-ve-agir-

muhimmat-ailesi/, (last update) 21.01.2017, 18:48

Purdy, D.J.: Comparison of balance and out of balance main battle tank armaments. Shock and Vibration, **8**, 167-174 (2001)

Ripley, B.D.: Pattern recognition and neural networks. Cambridge university press (1996)

Simon, P.: Military Robotics: Latest trends and spatial grasp solutions. International Journal of Advanced Research in Artificial Intelligence (IJARAI), **4**, 9-18 (2015) https://doi.org/10.14569/IJARAI.2015.040402

Song, S.M., Waldron, K.J.: Machines that walk: The adaptive suspension vehicle. The MIT PRESS, Cambridge, MA., pp. 1-18 (1989)

Tsujita, K., Tsuchiya, K., Onat, A.: Adaptive gait pattern control of a quadruped locomotion robot. IEEE/RSJ International Conference on Intelligent Robots and Systems, pp. 3 (2001)

Yıldırım, F.: The effect of geometric changes of propellants which used in large caliber weapons on barrel pressure and muzzle velocity. Master Thesis – Ankara University, Ankara, Turkey, 5-6 (2013)

CHAPTER IV

APPROACH DISINTEGRATION OF SEWAGE SLUDGE WITH ROTOR TYPE HYDRODYNAMIC CAVITATION REACTORS

Ekrem Güllüce

(Ph.D. Candidate), Atatürk University, Erzurum, Turkey,

e-mail: gulluceekrem@hotmail.com

Orcid: 0000-0003-2290-3799

1. Introduction

Due to the increase in population, rapid growth of industrialization and prolonged drought, pollutants have spread in water resources. Wastewater treatment processes were designed using various technologies to remove these pollutants from water resources (Xu et al., 2012).

Activated sludge process is a widely used system in wastewater treatment plants where biological treatment is done. The reason for choosing this system is its high efficiency, low operating cost and small space requirement (Y. Zhang, Lu, Zhang, Li, & Li, 2020).

Excess sludge is produced in activated sludge processes. The cost of treatment and disposal of excess sludge accounts for approximately 50-60% of the operating cost of the wastewater treatment plant. It has been revealed that the disposal of this excess sludge released by the wastewater treatment plant requires high economic costs. If the excess sludge released in the facilities is disposed of, it minimizes the cost, energy and land use of the facility (Chanda, 2008).

Excess sludge produced in the activated sludge process; It is disposed of by methods such as landfilling, use in agricultural areas and incineration. These disposal methods are not very popular due to the reduction of land used and high costs (Chanda, 2008). Due to these problems, scientists have sought new methods in recent years. It has been observed that the disintegration process is beneficial in the researches (Zhen, Lu, Kato, Zhao, & Li, 2017).

2. Disintegration Process

Disintegration process is destroying the organic substances in the cell the process of partially or completely by breaking down the bacterial cells, and then releasing them into the liquid phase (Grübel & Machnicka, 2010). Particulate or colloidal compounds that cannot be separated from the liquid phase exist in solution in the liquid, while the components are readily biodegradable. Carbonaceous compounds released after the disintegration process can be accessed and can be broken down much faster than sludge in the particle stage in later biological processes (Erden, 2010). Disintegration mechanism is given in Figure 1.

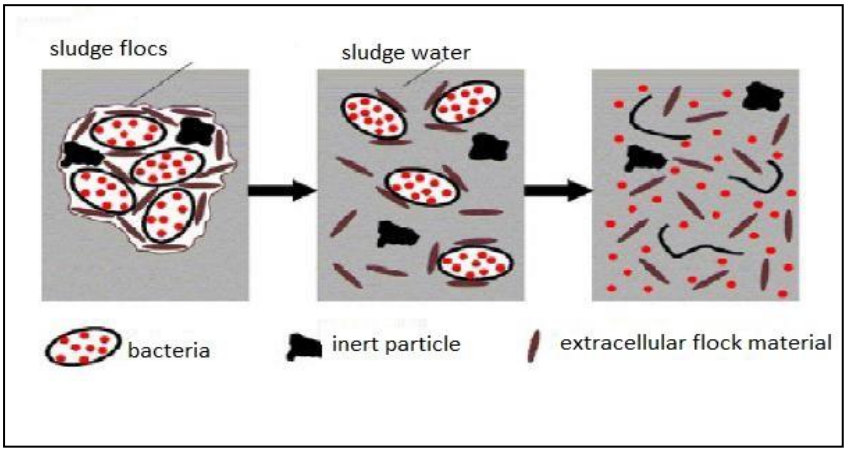

Figure 1: Disintegration mechanism (Yeşil, 2011)

2.1 Disintegration Degree

Disintegration degree is a parameter developed by (Müller, 1996) to determine the disintegration performance of sludge in sludge treatment. Disintegration degree is calculated using Eq. (1).

$$Disintegration\ Degree\ (DD) = \frac{SCOD - SCOD_0}{SCOD_1 - SCOD_0} X100 \qquad (1)$$

DD (%) = Disintegration degree
SCOD = concentration of soluble COD in the sludge after disintegration (mg/L)
$SCOD_0$ = concentration of soluble COD in the raw sludge before disintegration (mg/L)
$SCOD_1$ = concentration of soluble COD in the after chemical disintegration (mg/L)

2.2 Disintegration Methods

Sewage sludge disintegration has attracted great interest in recent years (Walczak, Zubrowska-Sudol, & Piechna, 2017). Various disintegration technologies have emerged to minimize the excess sludge produced in treatment plants. These technologies are; physical disintegration (Hogan, Mormede, Clark, & Crane, 2004; Wood, Tran, & Master, 2009), chemical disintegration (Chiu, Chang, Lin, & Huang, 1997; Filibeli & Erden, 2010; Ramteke & Gogate, 2015), biological disintegration (Ai, Liu, Wu, Zeng, & Yang, 2018; You et al., 2013) and thermal disintegration (Cano, Pérez-Elvira, & Fdz-Polanco, 2015; Dereix, Parker, & Kennedy, 2006) methods. These disintegration technologies are gathered into 3 basics groups as physical, chemical and biological methods (Fig. 2).

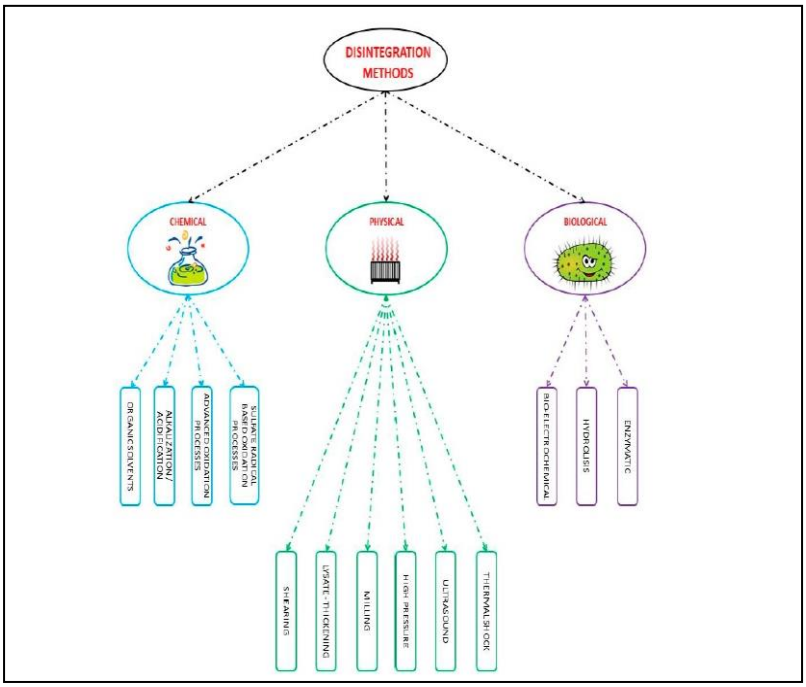

Figure 2: Disintegration methods (Walclawek et al., 2018)

2.2.1 Biological Disintegration

Biological disintegration process can effectively reduce volatile solids by destroying pathogens and positively affects biogas production (Wacławek et al., 2018). Process basically requires bio enzymes to be able to decompose the sludge. Enzymes reduce the viscosity of long-chain proteins, carbohydrates and lipids by catalytic decomposition of organic matter. Then, macromolecular organic substances are decomposed into small molecules (You et al., 2013).

2.2.2 Thermal Disintegration

Thermal disintegration is an effective process disintegration organic matters at high temperatures of sludge decomposition, biogas production and removal of pathogens (Anjum, Al-Makishah, & Barakat, 2016; Souza, Ferreira, Sapkaite, Pérez-Elvira, & Fdz-Polanco, 2013; Tyagi & Lo, 2012). The most important parameter of

the thermal disintegration process is temperature. The average temperature in this process is 185^{o}C. If it rises above 200^{o}C, biodegradation does not occur (Etyam, 2017).

2.2.3 Chemical Disintegration

Chemical disintegration is a chemical oxidation process using different reagents. It oxidizes the sludge by using conventional and advanced oxidation reagents to reduce the sewage sludge. In this way, treatment reduces sludge disposal and biomass yield. While some of the sludge is mineralized by chemical oxidation, the other part is dissolved with biodegradable organic compounds (Collivignarelli, Abbà, Carnevale Miino, & Torretta, 2019).

2.2.3.1 Ozone

Ozone is widely used in water and wastewater treatment processes because it is a strong oxidant (Gao et al., 2019). Activated sludge degradation in ozonation process is a result of cell lysis-cryptic growth. The amount of new biomass produced during the process is very small compared to the amount of biomass that is disintegrated (Ren et al., 2016).

2.2.3.2 Fenton

Fenton process is advanced oxidation processes. Fenton process is based on the formation of hydroxyl radical (OH·) by reacting with hydrogen peroxide (H_2O_2) and ferrous iron (Fe^{+2}) under acidic conditions (Olabi & Yildiz, 2021; Parsons, 2005). Formed hydroxyl radical (OH·) is a very strong oxidant reagent (Gogate & Pandit, 2004). Fenton reagent is used in the sludge disintegration process due to the release of water and organic matter from the sludge by breaking down the extracellular polymers and cell walls (X. Zhang, Miao, Li, & Li, 2019).

2.2.4 Physical Disintegration

Physical or mechanical processes of the sewage sludge destroy the cell walls and break up the flocs with the principle of force-external energy. Disintegration of the sewage sludge effectively breaks down the flocs and bacterial cells under the influence of its mechanical forces, resulting in the release of organic substances, which in turn causes an increase in biogas production (Wacławek et al., 2018).

2.2.4.1 Cavitation

Various techniques have been used since recent years to reduce the amount of excess sludge formed in the wastewater treatment plant. Cavitation, which are among these new methods, have shown a significant improvement (Kim, Sun, Koo, & Yoon, 2019). As the pressure decreases, bubbles form in the liquid. Cavitation is a process that causes these bubbles to grow and then collapse. The bubbles formed in the cavitation grow by performing the heat transfer process with the liquid near it. When the bubbles reach a certain size, the bubbles collapse with the release of a large amount of energy thanks to the physical, chemical and thermal effects (Kim et al., 2019; Rayleigh, 1917; Suslick, 1990). After the bubbles collapse, an energy is formed. After this energy, water molecules decompose into H· and OH· radicals, which is a strong oxidant. Thanks to these effects in cavitation, it makes a great contribution to the treatment of sludge (Kim et al., 2019).

If cavitation and conventional biological sludge treatment systems combine, treatment performances can have a positive effect. Since there are high pressure oscillations in hydrodynamic cavitation, it causes the small bubbles in the liquid to grow and then these bubbles to collapse (Brennen, 2013; Şağban, Dindar, Cirakoglu, & Keskinler, 2017). With the collapse of the bubbles, it reaches both high temperatures and pressures from the inner regions. Under these

conditions, water molecules split into OH· and H· radicals. Formed OH· radicals oxidize them by reacting with organic pollutants and diffuse into the liquid (Padoley, Saharan, Mudliar, Pandey, & Pandit, 2012; Şağban et al., 2017).

2.2.4.2 Hydrodynamic Cavitation

Hydrodynamic cavitation (HC) occurs due to pressure distribution due to sudden contraction and expansion of cross-sectional area. Flow velocity is calculated as the product of cross-sectional area and velocity in an incompressible fluid. With the narrowing of the cross-sectional area at a constant flow rate, the velocity of the fluid increases and the pressure drops. A hydrodynamic cavitation reactor (HCR) is used for to occur cavitation. The liquid passes through the cavitation production zone is uniformly dispersed and treatment takes place (Badve, Gogate, Pandit, & Csoka, 2013; Gągol, Przyjazny, & Boczkaj, 2018; Kim et al., 2019).

Hydrodynamic cavitation performs cell fragmentation of extracellular polymeric substances and bacteria in sewage sludge. After disintegration with hydrodynamic cavitation, the dissolved organic matter concentration increases with the decomposition of organic matter. Hydrodynamic cavitation breaks down the biomass and provides bacterial decomposition and high efficiency biogas yield is obtained in the anaerobic digester process (Şağban et al., 2017).

With the development of new effective HC, activated sludge decomposition has become a key to large-scale commercial applications. Various conventional HCR processes such as venturi, orifice, high pressure jet, Ecowirl and high-pressure homogenizer have been investigated (Kim, Koo, Sun, & Yoon, 2020)

2.2.4.3 Rotor Type Hydrodynamic Cavitation Reactors (Rotor Type HCRs)

Rotor type HCRs increases the cavitation density depending on the rotation speed provided by the rotating discs (Kim et al., 2020). Turbulent flow occurs in the liquid as the rotor type HCRs create cavitation. In this case, thermal energy is significant produced (Kim et al., 2020; Kwon & Yoon, 2012; Sun et al., 2018). Several studies have been carried out in the literature on the disintegration of sewage sludge using rotor type HCRs. (Kim et al., 2020) studied the effect of rotor speed for sewage sludge disintegration in rotor type HCRs. In their study, it was stated that the particle size of the treatment sludge decreased by 77% with the increase of rotor speed.

(Kim et al., 2019) presented on the disintegration of sludge collected from the wastewater treatment plant using rotor type HCRs and ultrasonic processes. In this study, it was determined that the particle fragmentation of the rotor type HCRs system was higher than the ultrasonic system. Another study, (Petkovsek et al., 2015) examined using rotor type HCRs for sludge disintegration. In this study, it was observed that the soluble chemical oxygen demand (SCOD) value increased from 45 mg/L to 602 mg/L by using rotor type HCRs. It was observed that biogas production increased by 12.7% with the use of rotor type HCRs. Comparing the analysis of hydrodynamic and biological results, it was concluded that cavitation interference has a more important role in sludge disintegration than the amount of cavitation.

As a result, because the use of rotor type HCRs in the disintegration process of sewage sludge is new, very few studies come into prominence in the literature. It is thought that these reactors will have a very important share in the disintegration of sewage sludge in the future due to a more economical and effective sludge fragmentation.

References

Ai, S., Liu, H., Wu, M., Zeng, G., & Yang, C. (2018). Roles of acid-producing bacteria in anaerobic digestion of waste activated sludge. Frontiers of Environmental Science & Engineering, 12(6), 3. doi:10.1007/s11783-018-1050-y

Anjum, M., Al-Makishah, N. H., & Barakat, M. A. (2016). Wastewater sludge stabilization using pre-treatment methods. Process Safety and Environmental Protection, 102, 615-632. doi:10.1016/j.psep.2016.05.022

Badve, M., Gogate, P., Pandit, A., & Csoka, L. (2013). Hydrodynamic cavitation as a novel approach for wastewater treatment in wood finishing industry. Separation and Purification Technology, 106, 15-21. doi:https://doi.org/10.1016/j.seppur.2012.12.029

Brennen, C. E. (2013). Cavitation and Bubble Dynamics. New York, USA: Cambridge University Press.

Cano, R., Pérez-Elvira, S. I., & Fdz-Polanco, F. (2015). Energy feasibility study of sludge pretreatments: A review. Applied Energy, 149, 176-185. doi:https://doi.org/10.1016/j.apenergy.2015.03.132

Chanda, S. K. (2008). Distengration of Sludge Using Ozone-Hydrodynamic Cavitation. Bangladesh, Bangladesh University of Engineering and Technology,.

Chiu, Y.-C., Chang, C.-N., Lin, J.-G., & Huang, S.-J. (1997). Alkaline and ultrasonic pretreatment of sludge before anaerobic digestion. Water Science and Technology, 36(11), 155-162. doi:https://doi.org/10.1016/S0273-1223(97)00681-1

Collivignarelli, M. C., Abbà, A., Carnevale Miino, M., & Torretta, V. (2019). What Advanced Treatments Can Be Used to Minimize the Production of Sewage Sludge in WWTPs? Applied Sciences, 9(13). doi:10.3390/app9132650

Dereix, M., Parker, W., & Kennedy, K. (2006). Steam-explosion pretreatment for enhancing anaerobic digestion of municipal wastewater sludge. Water Environ Res, 78(5), 474-485. doi:10.2175/106143006x95456

Erden, G. (2010). The Investigation of Sludge Disintegration Using Oxidation Process. Dokuz Eylül University Graduate School of Natural and Applied Sciences, İzmir.

Etyam, C. (2017). Atık Aktif Çamurun Hidrodinamik Kavitasyon Destekli Yöntemlerle Dezentegrasyonu. Bursa, Uludağ Üniversitesi Fen Bilimleri Enstitüsü.

Filibeli, A. e., & Erden, G. (2010). Anaerobik yöntemle stabilize edilen kentsel nitelikli aritma çamurlarin nihai bertaraf açisindan df erlendirilmesi.

Gągol, M., Przyjazny, A., & Boczkaj, G. (2018). Highly effective degradation of selected groups of organic compounds by cavitation based AOPs under basic pH conditions. Ultrasonics Sonochemistry, 45, 257-266. doi:https://doi.org/10.1016/j.ultsonch.2018.03.013

Gao, Y., Duan, Y., Fan, W., Guo, T., Huo, M., Yang, W., . . . An, W. (2019). Intensifying ozonation treatment of municipal secondary effluent using a combination of microbubbles and ultraviolet irradiation. Environ Sci Pollut Res Int, 26(21), 21915-21924. doi:10.1007/s11356-019-05554-8

Gogate, P. R., & Pandit, A. B. (2004). A review of imperative technologies for wastewater treatment I: oxidation technologies at ambient conditions. Advances in Environmental Research, 8(3), 501-551. doi:https://doi.org/10.1016/S1093-0191(03)00032-7

Grübel, K., & Machnicka, A. (2010). Hydrodynamic disintegration of foam biomass to upgrade of wastewater. Ecological Chemistry and Engineering S-chemia I Inzynieria

Ekologiczna S, 17, 137-148.

Hogan, F., Mormede, S., Clark, P., & Crane, M. (2004). Ultrasonic sludge treatment for enhanced anaerobic digestion. Water Sci Technol, 50(9), 25-32.

Kim, H., Koo, B., Sun, X., & Yoon, J. Y. (2020). Investigation of sludge disintegration using rotor-stator type hydrodynamic cavitation reactor. Separation and Purification Technology, 240. doi:10.1016/j.seppur.2020.116636

Kim, H., Sun, X., Koo, B., & Yoon, J. Y. (2019). Experimental Investigation of Sludge Treatment Using a Rotor-Stator Type Hydrodynamic Cavitation Reactor and an Ultrasonic Bath. Processes, 7(11). doi:10.3390/pr7110790

Kwon, W. C., & Yoon, J. Y. (2012). Experimental study of a cavitation heat generator. Proceedings of the Institution of Mechanical Engineers, Part E: Journal of Process Mechanical Engineering, 227(1), 67-73. doi:10.1177/0954408912451535

Müller, J. (1996). Mechanischer Klärschlamm aufschluß. Institut für Mechanische Verfahrenstechnik, Technical University of Braunschweig, Aachen, Germany.

Olabi, A., & Yildiz, S. (2021). Sludge disintegration using UV assisted Sono-Fenton process. Environ Sci Pollut Res Int. doi:10.1007/s11356-021-14505-1

Padoley, K. V., Saharan, V. K., Mudliar, S. N., Pandey, R. A., & Pandit, A. B. (2012). Cavitationally induced biodegradability enhancement of a distillery wastewater. Journal of Hazardous Materials, 219-220, 69-74. doi: https://doi.org/10.1016/j.jhazmat.2012.03.054

Parsons, S. (2005). Advanced Oxidation Processes for Water and Wastewater Treatment: IWA Publishing.

Petkovsek, M., Mlakar, M., Levstek, M., Strazar, M., Sirok, B., & Dular, M. (2015). A novel rotation generator of

hydrodynamic cavitation for waste-activated sludge disintegration. Ultrason Sonochem, 26, 408-414. doi:10.1016/j.ultsonch.2015.01.006

Ramteke, L. P., & Gogate, P. R. (2015). Treatment of toluene, benzene, naphthalene and xylene (BTNXs) containing wastewater using improved biological oxidation with pretreatment using Fenton/ultrasound based processes. Journal of Industrial and Engineering Chemistry, 28, 247-260. doi:https://doi.org/10.1016/j.jiec.2015.02.022

Rayleigh, L. (1917). VIII. On the pressure developed in a liquid during the collapse of a spherical cavity. The London, Edinburgh, and Dublin Philosophical Magazine and Journal of Science, 34(200), 94-98. doi:10.1080/14786440808635681

Ren, H., Ma, L., Wang, B., Gong, H., Yuan, Z., & Li, Z. (2016). Systematic Analysis of the Biochemical Characteristics of Activated Sludge During Ozonation for Lowering of Biomass Production. Ozone: Science & Engineering, 39(2), 80-90. doi:10.1080/01919512.2016.1268948

Souza, T. S. O., Ferreira, L. C., Sapkaite, I., Pérez-Elvira, S. I., & Fdz-Polanco, F. (2013). Thermal pretreatment and hydraulic retention time in continuous digesters fed with sewage sludge: Assessment using the ADM1. Bioresource Technology, 148, 317-324. doi:https://doi.org/10.1016/j.biortech.2013.08.161

Sun, X., Kang, C. H., Park, J. J., Kim, H. S., Om, A. S., & Yoon, J. Y. (2018). An experimental study on the thermal performance of a novel hydrodynamic cavitation reactor. Experimental Thermal and Fluid Science, 99, 200-210. doi:https://doi.org/10.1016/j.expthermflusci.2018.02.034

Suslick, K. S. (1990). Sonochemistry. Science, 247(4949), 1439-

1445. doi:10.1126/science.247.4949.1439

Şağban, F. O. T., Dindar, E., Cirakoglu, C., & Keskinler, B. (2017). Hydrodynamic Cavitation of Waste-Activated Sludge. Environmental Engineering Science, 35(8), 775-784. doi:10.1089/ees.2016.0408

Tyagi, V. K., & Lo, S. L. (2012). Enhancement in mesophilic aerobic digestion of waste activated sludge by chemically assisted thermal pretreatment method. Bioresour Technol, 119, 105-113. doi:10.1016/j.biortech.2012.05.134

Wacławek, S., Grübel, K., Silvestri, D., Padil, V. V. T., Wacławek, M., Černík, M., & Varma, R. S. (2018). Disintegration of Wastewater Activated Sludge (WAS) for Improved Biogas Production. Energies, 12(1). doi:10.3390/en12010021

Walczak, J., Zubrowska-Sudol, M., & Piechna, P. (2017). Influence of Hydrodynamic Disintegration on the Release of Organic and Nutrient Compounds From Activated Sludge. CLEAN - Soil, Air, Water, 45(11). doi:10.1002/clen.201700487

Wood, N., Tran, H., & Master, E. (2009). Pretreatment of pulp mill secondary sludge for high-rate anaerobic conversion to biogas. Bioresource Technology, 100(23), 5729-5735. doi:https://doi.org/10.1016/j.biortech.2009.06.062

Xu, P., Zeng, G. M., Huang, D. L., Feng, C. L., Hu, S., Zhao, M. H., . . . Liu, Z. F. (2012). Use of iron oxide nanomaterials in wastewater treatment: a review. Sci Total Environ, 424, 1-10. doi:10.1016/j.scitotenv.2012.02.023

Yeşil, E. (2011). Atık Çamur Dezentegrasyonu Yöntemlerinin Çamur Minimisazyonu Açısından Değerlendirilmesi. İstanbul, İstanbul Teknik Üniversitesi Fen Bilimleri Enstitüsü.

You, M. Y., Chai, T. Y., Pan, Y., Zhu, Y. N., Cao, Y. H., Li, X. J., . . . Zhu, T. (2013). Review of Excess Sludge Disintegration Research. Advanced Materials Research, 726-731, 2949-

2955. doi:10.4028/www.scientific.net/AMR.726-731.2949

Zhang, X., Miao, X., Li, J., & Li, Z. (2019). Evaluation of electricity production from Fenton oxidation pretreated sludge using a two-chamber microbial fuel cell. Chemical Engineering Journal, 361, 599-608. doi:10.1016/j.cej.2018.12.117

Zhang, Y., Lu, G., Zhang, H., Li, F., & Li, L. (2020). Enhancement of nitrogen and phosphorus removal, sludge reduction and microbial community structure in an anaerobic/anoxic/oxic process coupled with composite ferrate solution disintegration. Environmental Research, 190, 110006. doi:https://doi.org/10.1016/j.envres.2020.110006

Zhen, G., Lu, X., Kato, H., Zhao, Y., & Li, Y.-Y. (2017). Overview of pretreatment strategies for enhancing sewage sludge disintegration and subsequent anaerobic digestion: Current advances, full-scale application and future perspectives. Renewable and Sustainable Energy Reviews, 69, 559-577. doi:10.1016/j.rser.2016.11.187

CHAPTER V

STATISTICAL PROCESS CONTROL FOR CUTTING AND TIGHTENING PROCESSES OF ALUMINUM PIPES

Ezgi Aktar Demirtas

(Prof. PhD) Department of Industrial Engineering, Eskisehir Osmangazi University, email: eaktar@ogu.edu.tr

Orcid: 0000-0002-3762-6256

1. Introduction

Statistical process control (SPC) studies were carried out for critically important cutting and tightening processes in a company that manufactures precision aluminum pipes used in the household appliances, automotive and aviation industries.

After cutting and tightening processes, outer diameters (mm.) of the aluminum pipes, an important quality characteristic, are monitoring whether the process was out of control. With the help of traditional Shewart charts and process capability analysis (PCA) the processes were monitored and the sigma level of the production were evaluated.

In addition, unlike other studies of SPC literature related to household appliances, the sensitivity of the process to possible variability and deviations was analyzed. For this purpose, β values and Average Run Lengths (ARL) were calculated. β, the probability of not detecting a deviation of $\pm k\sigma$ is also called the second type error, false alarm or consumer risk. The number of samples expected to be taken before the deviation is noticed is called ARL (Montgomery, 2011). After computations, Operating Characteristic

Curves (OCC) that give beta probabilities depending on the shifts were drawn.

In the literature, there is a considerable amount of paper conducted SPC, Six Sigma and Lean Six Sigma in the household appliances industry. You can see the most used SPC and Six Sigma tools from the different literature review studies. According to the review by Uluskan (2016) and Jenicke et al. (2008) flow charts, run charts, scatter diagrams, fishbone diagram, Pareto charts, control charts, process mapping are among the most commonly used Six Sigma tools. Mahanti and Antony (2009) stated that control charts, cause-effect diagram, gap analysis, regression, process mapping, QFD, FMEA, process capability analysis (PCA) are among the most used SPC tools in the software industry. On the other hand, Walter and Paladini (2019) reported that Six Sigma techniques such as ANOVA, hypothesis testing and confidence intervals, GageR&R analysis were not frequent. Additionally, different quality management techniques were also used in specific case studies, e.g. SERVQUAL analysis and poka-yoke (Kumar et al., 2008); lean six sigma tools such as value stream map and 5 why analysis (Cheng, 2018); two samples Poisson's rate analysis (Gijo and Sarkar, 2013) SIPOCCE diagram (Antony and Sunder, 2019). hypothesis tests (Improta et al., 2019).

2. SPC for Cutting Process

The company produces cooling system elements, heat pump elements, defrost heaters and precision aluminum pipes used in the automotive/aviation sectors.

The company, which produces 1000, 3000 and 6000 series aluminum pipe extrusions, develops and tests special alloys suitable for the intended use and high corrosion resistance in its own laboratories. The flow chart of the aluminum pipe production is given in Appendix.

After the cutting and tightening processes, the outer diameters of the aluminum pipes are measured and the pipes that do not meet the specifications are scrapped. Lower and Upper Specification Limits (USL and LSL) have been determined by the manufacturer as 17.9 and 18.1. The nominal value is 18 mm.

After the cutting process, samples consisting of 5 units were taken randomly in different time periods for 20 days. The histogram and descriptive statistics of the data was given in Figure 1.

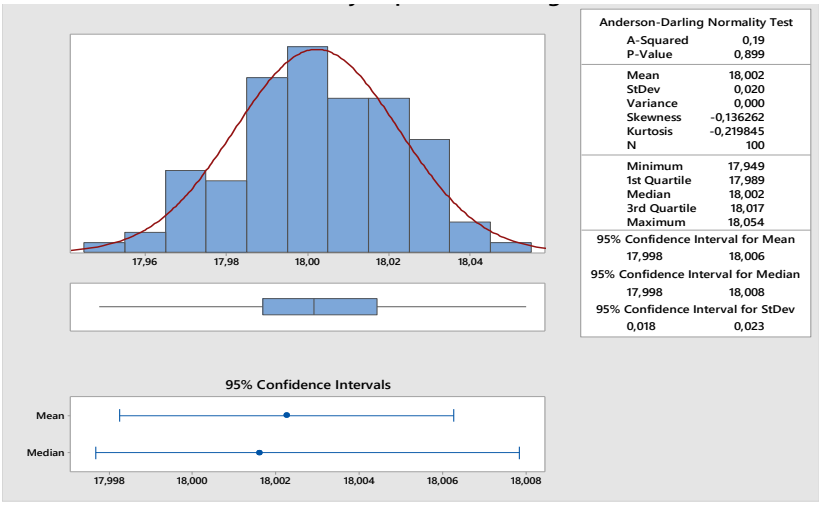

Figure 1. Histogram of the outer diameters after cutting

It is seen that the mean, mode and median are close to each other, and the skewness and kurtosis values are in the range of ±0.5. The results of the normality test ($p>0.05$) also show that the data are normally distributed at the 5% significance level.

Control chart of subgroup means and range were used to monitor variability and deviation from the mean if the cutting process was under control.

Lower and upper control limits (LCL and UCL), for the chart of subgroup means and range chart are calculated as seen in equation 1-4.

$$LCL_{\bar{X}} = \bar{\bar{X}} - A_2\bar{R} = 18.002 - 0.577 * 0.0468 = 17.9805 \quad (1)$$

$$UCL_{\bar{X}} = \bar{\bar{X}} + A_2\bar{R} = 18.002 + 0.577 * 0.0468 = 18.024 \quad (2)$$

$$LCL_R = D_3\bar{R} = 0 * 0.0468 = 0 \quad (3)$$

$$UCL_R = D_4\bar{R} = 2.114 * 0.0468 = 0{,}099 \quad (4)$$

When the control charts in Figure 2 (left side) are examined, it is seen that the cutting process is under control.

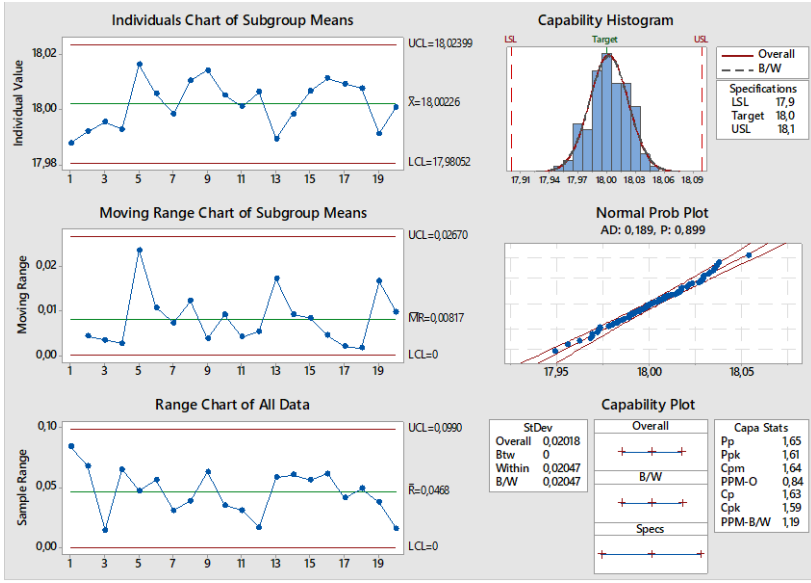

Figure 2. PCA for cutting process

In order for companies to reach the desired quality level, the products must be within the specification values that show the consumer expectations.

The capability of the process to produce products that meet specifications is expressed in ratios called Cp, Cpk and Cpm (Eq. 5-8).

$$C_p = \frac{USL - LSL}{6\hat{\sigma}} \quad (5)$$

$$C_{pk} = enk\left\{\frac{USL-\mu}{3\hat{\sigma}}; \frac{\mu-LSL}{3\hat{\sigma}}\right\} \quad (6)$$

$$C_{pm} = \frac{USL-LSL}{6\sqrt{\hat{\sigma}^2+(\mu-T)^2}} \quad (7)$$

$$\hat{\sigma} = \frac{\bar{R}}{d_2} = \frac{0.0468}{1.128} = 0.02040 \quad (8)$$

$USL = 18.1\ ASL = 17.9\ T = 18\ \mu = 18.002$

When Figure 2 is examined, it is seen that the Cp and Cpk values are 1.63 and 1.59. Both values are above 1.33. The mean of production is consistent with the target value. It can be said that the process is capable.

The sigma level corresponding to the Cp is 4.79. If desired, studies can be carried out to reach the 6 sigma perfection level.

3. SPC for tightening process

After tightening, samples consisting of 5 units were taken randomly in different time periods during 20 days. Statistics of 100 data are summarized in Figure 3. Similar to the cutting process, when the statistics in Figure 3 are examined, it is seen that the data are normally distributed.

LCL and UCL for the chart of subgroup means and range chart are calculated as seen in equation 9-12.

$$LCL_{\bar{X}} = \bar{X} - A_2\bar{R} = 17.999 - 0.577 * 0.0382 = 17.9785 \quad (9)$$

$$UCL_{\bar{X}} = \bar{X} + A_2\bar{R} = 18.002 + 0.577 * 0.0382 = 18.0198 \quad (10)$$

$$LCL_R = D_3\bar{R} = 0 * 0.0382 = 0 \quad (11)$$

$$UCL_R = D_4\bar{R} = 2.114 * 0.0382 = 0.0808 \quad (12)$$

The graphs in Figure 4 show that the tightening process is under control.

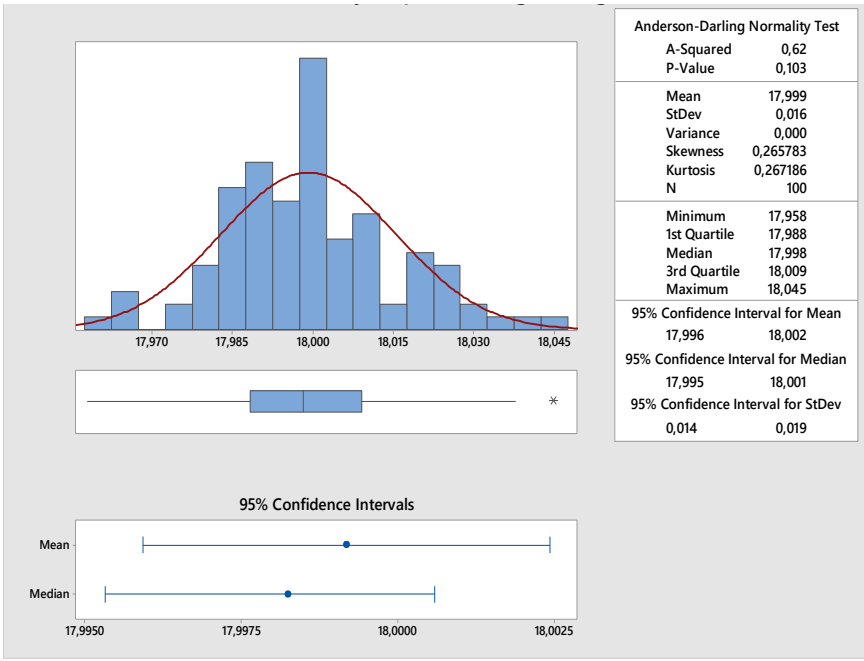

Figure 3. Outer diameters after tightening

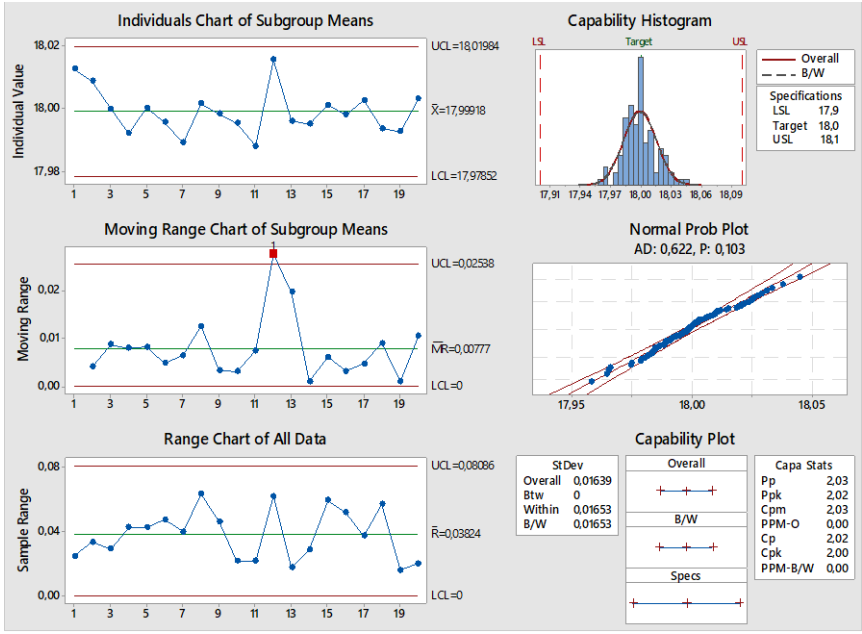

Figure 4. PCA for tightening process

According to Figure 4, it is seen that the Cp and Cpk values are 2.02 and 2. The fact that both values are around two indicates that the 5.98 sigma level has been reached. Defective ppm (part per milion) is too low for the tightening process. The current situation must be maintained.

4. OCC and ARL for cutting and tightening processes

After it was observed that the cutting and tightening processes were under control and capable, β probabilities and ARL values were approximately calculated with Eq.13-14. For cutting and tightening processes with the parameters, μ≅18 and σ≅0.02, β probabilities and ARL values are placed in Table 1.

$$\beta = P\left(\frac{LCL_{\bar{X}}-\mu^*}{\frac{\sigma}{\sqrt{n}}} \leq \frac{\bar{X}-\mu^*}{\frac{\sigma}{\sqrt{n}}} \leq \frac{UCL_{\bar{X}}}{\frac{\sigma}{\sqrt{n}}}\right) \quad (13)$$

$$\mu^* = \mu \mp k\sigma \; ARL = \frac{1}{1-\beta} \quad (14)$$

Table 1: β and ARL values for cutting and tightening processes

	Cutting		**Tightening**	
Deviation (k)	**β**	**ARL**	**β**	**ARL**
-3	0.000032	1.000	0.000004	1.000
-2.5	0.001933	1.002	0.000396	1.000
-2	0.037720	1.039	0.012402	1.013
-1.5	0.252493	1.338	0.128537	1.147
-1	0.671634	3.045	0.491133	1.965
-0.5	0.939570	16.548	0.861666	7.229
0	0.981039	52.741	0.977647	44.736
0.5	0.854335	6.865	0.898871	9.888
1	0.477847	1.915	0.566179	2.305
1.5	0.121673	1.139	0.172471	1.208
2	0.011370	1.012	0.019913	1.020
2.5	0.000351	1.000	0.000771	1.001
3	0.000003	1.000	0.000009	1.000

Using the beta values in Table 1, OCCs were created. OCC is a curve with probabilities of deviation on the horizontal axis and β probabilities on the vertical axis. Figure 5 illustrates the OCC created for the tightening process.

When Table 1 and Figure 5 are examined, as the deviation increases, it is seen that the probability of detection increases (β decreases) and fewer samples are needed to detect shift (ARL decreases)

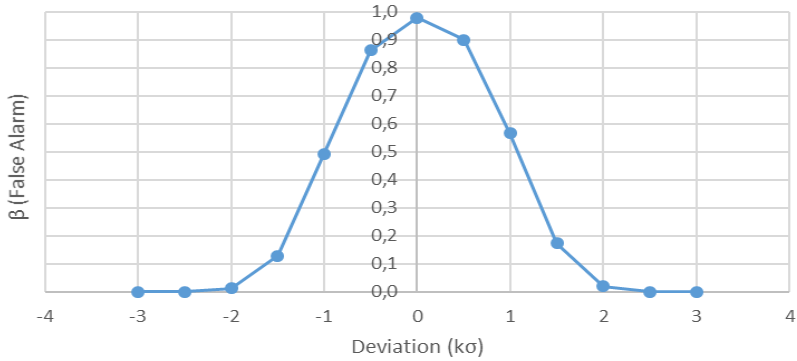

Figure 5. OCC for tightening process

5. Conclusions

As a result of SPC studies for cutting and tightening processes in aluminum pipe production, it is seen that both processes are under control and capable. Assuming that the tolerance band corresponds to ±4σ, the expected σ value is 0.0275, and the estimated σ value for both processes is below this value. It can be said that the process variability is at a reasonable level. In addition, both process means are very close to the target value. The six sigma level has been achieved in the tightening process. For the other process, the sigma level is quite high. The firm is expected to maintain the current situation with continuous monitoring. Since there is no need for intervention in the processes for now, false alarm probabilities and ARL values are calculated to make the sensitivity analysis in case of

possible deviation. For this purpose, OCC is illustrated for the tightening process.

Similar studies should be carried out for other processes that may cause problems in the future, and projects that can increase sigma level of processes should be supported, with a Six Sigma and Lean Six Sigma perspective.

Acknowledgements

I would like to thank Damla Güngör and Bora Berkan Yalçın for their contributions during the data collection and preparation phase.

References

Antony, J. & Sunder, M.V. (2019). Application of Lean Six Sigma in IT support services – a case study. *The TQM Journal*, 31, 3, 417-435.

Cheng, L.J. (2018). Implementing Six Sigma within Kaizen events, the experience of AIDC in Taiwan. *The TQM Journal*, 30, 1, 43-53.

Gijo, E.V. & Sarkar, A. (2013). Application of Six Sigma to improve the quality of the road for wind turbine installation. *The TQM Journal*, 25, 3, 244-258.

Improta, G., Balato, G., Ricciardi, C., Russo, M.A., Santalucia, I., Triassi, M. & Cesarelli, M. (2019). Lean Six Sigma in healthcare: fast track surgery for patients undergoing prosthetic hip replacement surgery. *The TQM Journal*, 31, 4, 526-540.

Jenicke, L.O., Kumar, A. & Holmes, M.C. (2008). A framework for applying Six Sigma improvement methodology in an academic environment. *The TQM Journal*, 20, 5, 453-462.

Kumar, S., Strandlund, E. & Thomas, D. (2008). Improved service system design using Six SigmaDMAIC for a major US

consumer electronics and appliance retailer. *International Journal of Retail and Distribution Management*, 36, 12, 970-994.

Montgomery,D.C. *Introduction to Statistical Quality Control*, 7th Edition, John Wiley & Sons, New York; 2013.

Uluskan, M. (2016). A comprehensive insight into the Six Sigma DMAIC toolbox. *International Journal of Lean Six Sigma*, 7, 4, 406-429.

Walter, O.M.F.C. & Paladini, E.P. (2019). Lean six sigma in Brazil: a literature review. *International Journal of Lean Six Sigma*, 10, 1, 435-472.

Appendix. Flowchart of aluminum pipe production

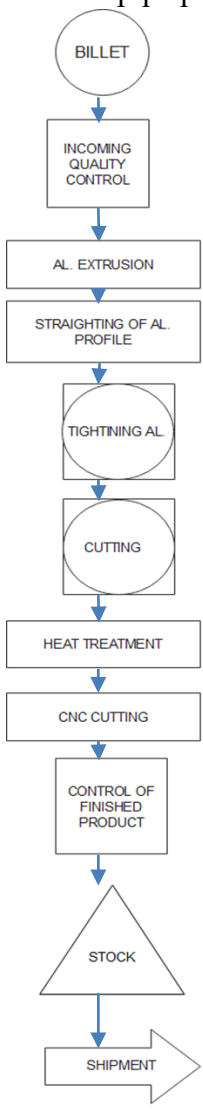

CHAPTER VI

GAME THEORY FOR SPECTRUM ALLOCATION IN COGNITIVE RADIO NETWORKS

Fatih Yavuz Ilgın

(Asst. Prof. Dr.) Erzincan Binali Yildirim University., e-mail:fyilgin@erzincan.edu.tr

Orcid: 0000-0002-7449-4811

1. Introduction to Game Theory

Game theory is a mathematical theory that deals with decision situations where mutual interactions exist and it helps people make decisions by considering the strategy(s) preferred by the other party in situations where two or more people are faced with a decision-making situation (Myerson, 2013). These situations benefit from both cooperative and non-cooperative models (Vorob'Ev, 2012). These two groups of game theory differ in formalizing dependency between players. In non-cooperative Game theory, the game is a model that informs the players the details of all possible movements (Rosenthal, 1989). On the other hand, cooperative game theory normally removes this level of detail and only explains the outcome when players come together in different coalitions (McCain,2008). In practice, game theory is used with different algorithms according to different specific situations. These algorithms can be listed as cooperative/non-cooperative games, zero-sum games, dynamic/differential games, Bayesian games (Guseinov, et al., 2010).

Game Theory was first introduced by the mathematician John Von Neumann in the 1920s to win at card games (Neumann, 1988).

In such games, which are called zero-sum games, the total win is zero because some players gains are others losses. Military operations can also be thought of as these games (Neumann, 2007). Especially during the war years of the 1940s, these games became extremely important. In 1913, the most important work in terms of game theory was made by E.Zermelo (Zermelo, 2010). Examining the game of chess with this work, Zermelo is one of his players. He has found that one always has a winning strategy, no matter where the pieces are on the chessboard. Therefore, he mathematically proved that the game of chess always has a solution (Walker, 1995). With this study, he created the method called backwards induction, which is used in the solution of sequential games in game theory today, which is in the form of a game tree. Another important work in game theory was carried out by John Nash in 1950, and he created the Nash equilibrium theory, which is also known as the solution and equilibrium point and is the most widely used today.

As it is known, studies in the field of communication have focused on these topics in order to solve the spectrum shortage problem experienced in recent years. On the other hand, can be examined in two main parts as spectrum detection and dynamic spectrum access. Dynamic spectrum access, besides deals with spectrum assignment policies. The studies carried out in the field of game theory and BR mostly concentrate on the spectrum assignment title. Some of these studies are carried out in order to increase the transmission quality and some of them are carried out in order to increase the efficiency of the system.

In this study, general information about Game theory and its types is given and a Game theory-based spectrum assignment method for CR systems is explained. To elaborate; it has been examined that two mobile CR users determine the base stations with which they will communicate through the signals they perceive. In this way, CR

users both get rid of bandwidth restrictions and find strategies to maximize their payoffs. This described method is supported by simulation studies.

2. Game theory and its types

In this section, the features of some game types found in the literature will be introduced. Game theory is a sub-groups of mathematics used to analyze situations in which parties, called players, make cohesive or unconnected decisions. This interdependence may cause each player to consider the other player's possible decisions or strategies when strategizing. The solution of a game describes the optimal decisions of players who may have similar, opposing, or mixed interests, and the consequences that may result from those decisions. In game theory, the decisions that players will make are called strategy. If the player's decision does not include any strategy, this strategy is called pure strategy. In addition, if the number of strategies in any game is finite, such games are defined as finite games. each player has to finish the game by applying his own strategy during the game process. The player who finishes the game calls himself a win and this is called a payoff.

2.1. Non-cooperative games

Non-cooperative games are often analyzed within the framework of non-cooperative game theory, which attempts to predict players' individual strategies and payoffs and find the Nash Equilibrium. It is opposed to cooperative game theory, which focuses on predicting which groups of players (coalitions) will form, the joint actions the groups will take, and the resulting collective outcomes. Cooperative game theory does not analyze the strategic bargaining that takes place within each coalition and affects the overall distribution of earnings among members (Nash, 1951).

Non-cooperative game theory provides a low-level approach as it models all the procedural details of the game, while cooperative game theory only describes the structure, strategies and payoffs of coalitions. Non-cooperative game theory is more inclusive than cooperative game theory in this sense (Mertens, 1987).

Cooperative games are more general, as they can be analyzed using non-cooperative game theory terms. Where arbitration exists to enforce an agreement, that agreement is beyond the scope of non-cooperative theory: however, it may be possible to state sufficient assumptions to cover all possible strategies players may adopt in relation to arbitration (Thomas, 2012). This would bring the agreement under the Non-Cooperative theory. Alternatively, it may be possible to identify the arbitrator as a party to the settlement and model the relevant processes and payments accordingly. Besides it is desirable that all games be expressed under a non-cooperative framework (Montola, et al., 2009). In many cases, however, insufficient information is available to accurately model the formal procedures available to players during the strategic bargaining process; or the resulting model will be too complex to offer a practical tool in the real world. In such cases, Cooperative game theory provides a simplified approach that allows general analysis of the game without making any assumptions about their bargaining power (Dutta, et al.,1999).

A good example of a non-cooperative game is Prisoner's Dilemma (Lacey, 2008). The game involves two players or defendants kept in separate rooms and therefore unable to communicate. Players must decide whether to cooperate among themselves or betray the other player and confess to law enforcement. As the diagram shows, if both remain silent, both players will receive less rewards (in the form of higher prison sentences). If they both confess, they get a higher pay in the form of

less jail time. If one player confesses and the other remains silent and cooperates, the confessor will receive a higher payoff, while the silent player will receive a lower payoff if both players cooperate with each other (Hardin, 1971).

Table 1: Prisoner's Dilemma (prisoner 1, prisoner 2)

	Confess	Not Confess
Confess	5, 5	10, 0
Not Confess	0,10	1,1

- If one of the suspects confesses and the other remains silent, the confessor will be released and the party who chooses to remain silent will be sentenced to year in prison.
- If both remain silent, they will both be sentenced to 1 year in prison.
- If both confess, both suspects will each be sentenced to 5 year in prison.

In this case, the two suspects in different rooms have no means of communicating with each other. Both suspects must choose between testifying or remaining silent. The best decision for the players is to have both remain silent. In this case, the total period of imprisonment is $1 + 1 = 2$ year. The prisoners know that they will not gain any benefit by shortening the sentence of the other. Since he does not know the other person's decision, he has to make a rational decision in distrust. According to game theory, the more rational decision is to confess. Because in this case, he will either go to bed for 5 year or be released. Its risk is $5 - 0 = 5$ year. Otherwise, if he had chosen to remain silent, he would have gone to bed for 1 year or 10 year. Its risk is $10 - 1 = 9$ year. The player must make the decision with less risk.

2.2. Bayesian Games

Bayesian games are a set of games, the only difference being the payoff values (i.e. the players and the actions that the players can choose are the same) and the players beliefs/prejudices (knowledge sets) about which game they are playing (Dekel, et al.,v2004). This definition is the classical one we have used so far. The function defined as information sets in this definition is only a function that contains information about how much probability each player plays which game (Böge and Eisele, 1979). In other words, Bayesian games are a set that includes a set of types and a prejudices (beliefs) function, as well as players, actions sets, and payoff function, which are used to describe games in normal form. Where, the prejudices set refers to the prejudices or beliefs that a player has for every possible type of every player other than himself (about which player has which type), and the types set refers to the types each player can take. There is actually no difference between these two definitions. They simply express two different points of view, and it may make more sense to use a different one in different Bayesian games (Mansour, et al., 2016). For example, the first definition, which goes through information sets and more than one game, is "Are you there or not?" It will be meaningful in games of chance, such as games of chance, or in similar situations where uncertainty arises from the structure of the game.

The example we will give now will be sufficient to explain Bayesian games. Suppose you are in a wild west town. Our town has a sheriff. The sheriff comes across a gunman on his patrol. These two men have to decide whether to shoot each other at the same time. However, the sheriff does not know whether this gunman is a criminal or an innocent; "p" probably thinks he is innocent. (p is a variable representing the sheriff's faith). The earnings are as follows:

The sheriff prefers to shoot if the suspect is going to shoot

himself, and not to shoot if the suspect does not try to shoot himself. As a matter of fact, our sheriff is a lawman, and he doesn't want to kill someone who doesn't take his life no matter what. If the gunman is guilty, he always prefers to shoot, because even if the sheriff does not shoot himself, he will go to jail as soon as he realizes that he is guilty. If the gunman is innocent, he will not want to shoot the sheriff himself, whether or not the sheriff shoots him. This may be because the man adhered to high moral virtues, or because he did not want to be remembered as the one who killed a sheriff. Of course, the game gets angry as the moves will be made at the same time. From the sheriff's point of view, there are two possibilities that completely change the earnings: Is the gunman innocent or guilty? If we express this situation as a Bayesian Game:

Table 2: Payoff matrix for Bayesian Games (Tip is Guilty)

		Sheriff	
		Shoot	Don’t shoot
Tip is guilty	Shoot	-3,-1	-1,-2
	Don’t shoot	-2,-1	0,0

Table 3: Payoff matrix for Bayesian Games (Tip is not Guilty)

		Sheriff	
		Shoot	Don’t shoot
Tip is not guilty	Shoot	0,0	2,-2
	Don’t shoot	-2,-1	-1,1

Where, the sheriff's game can vary depending on what type of Player 1 (the gunman) is. The sheriff has a certain belief in the other players’ type. Now, let's analyze the sheriff's should move, depending on what the sheriff's beliefs are (i.e., the value of p). As we mentioned above, the criminal always chooses to hit, and the innocent always choose not to hit. We can see this from the gain

values: Whether the sheriff hits or not, if the criminal hits, he will be able to earn more if the innocent does not. In other words, hitting is the dominant strategy of the criminal, while not hitting is the dominant strategy of the innocent. So we can simplify the game like this:

Table 4: Simplified Payoff matrix for Bayesian Games (Tip is Guilty)

		Sheriff	
		Shoot	Don't shoot
Tip is guilty	Don't shoot	-2,-1	0,0

Table 5: Simplified Payoff matrix for Bayesian Games (Tip is not Guilty)

		Sheriff	
		Shoot	Don't shoot
Tip is not guilty	Shoot	0,0	2,-2

Now we can easily look at the sheriff's expectations of the hit and the non-hit. i.e. if the Sheriff hits, he will win -1 with probability p and 0 with probability $1-p$. Then;

If the sheriff doesn't hit, he will win with probability p, and with probability $1-p$ he will win -2 .

2.3. Differential Games

Differential games are a type of static non-cooperative game by adopting the tools, methods and models of optimal control theory

(Friedman, 2013); Friedman, 1972). Optimal control theory, on the other hand, has been developed to obtain optimal solutions for planning problems involving dynamic systems. In differential games, an objective function is determined and this objective function is maximized in order to maximize the players' returns. The two main approaches to solving optimal control problems are dynamic programming (Bellman, 1956) and the maximum principle (Kopp, 1962). The former leads to an optimal control (closed-loop feedback control) that is a function of state and time, while the latter leads to a control that is only a function of time and the first state (open-loop control). It is also adopted in differential games where the common solution concepts of a differential game are again Nash equilibrium and Stackelberg equilibrium for non-hierarchical and hierarchical structures, respectively.

In a differential game, all players can interact with a dynamic system that affects players' earnings. The Fig 1. below gives a figure for frequency allocation in a differential game. In a differential game, players can interact with a dynamic system that affects their payoff. For example, Figure 1 shows a different differential game formulation of bandwidth allocation among service providers (base stations) to a group of users in a coverage area. The underlying dynamic system has a ratio of users choosing different providers to maximize the players' earnings, and this affects returns for all providers.

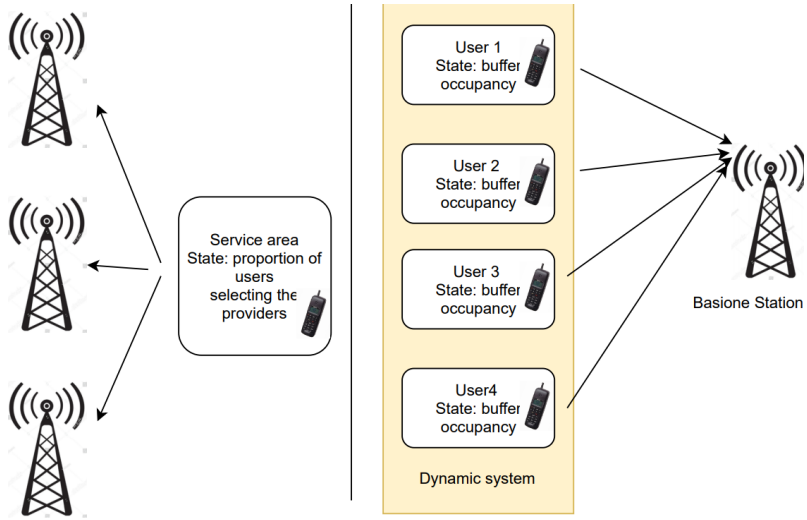

Figure 1. Dynamic system in a differential game of bandwidth allocation among service providers

Optimum control theory can actually be seen as a special form of differential game (Kirk, 2004 ; Sethi and Thompson, 2000). Mathematical tools of optimal control can be useful for differential games where players may adopt the concept of an optimal control Nash equilibrium or Stackelberg equilibrium. In a game involving optimal control theory, there are players who are faced with an optimization problem with a single objective for a certain period of time. On the other hand, in a differential game, even if there is more than one player, if all but one player has fixed strategies, it should be defined as an optimal control problem for the player whose action or strategy is to be determined. Different methods are suggested in the literature to solve the optimization problem.

2.4. Non Zero-Sum Games

A zero-sum game is a form in which the wins or losses of a game are equal to the sum of the wins and losses of the other participants. In

other words, in game and economic theory, the mathematical model of the situation in which each participant's gain or loss is balanced by the other participants' gains or losses is called a zero-sum game. Games in which these explanations do not apply are defined as non-zero-sum games. It is not very convenient to model CR systems (Mitola, 2000). with zero-sum games. For this reason, non zero-sum streams will be explained (Rath, et al., 2014).

Suppose it is a finite nxm game with two player. Let I_1, I_2, I_n be the pure strategy of the first player and II_1, II_2, II_m be the pure strategy of the second player. If the first player plays with the strategy I_i and the second player I_j, the payoff of the first player is $p_{ij}^1 = p^1(I_i, II_j)$ and the payoff of the second player is $p_{ij}^2 = p^2(I_i, II_j)$. If the game is not zero-sum, we cannot talk about the existence of an $p_{ij}^1 + p_{ij}^2 = R$ value such that R for arbitrarily chosen i and j. Thus, the payoff bimatrix in such games is expressed as follows (Guseinov, et al., 2010).

Table 6: Payoff matrix for nonzero-sum games

	II_1	II_2	⋯	II_m
I_1	g_{11}^1, g_{11}^2	g_{12}^1, g_{12}^2	⋯	g_{1m}^1, g_{1m}^2
I_2	g_{21}^1, g_{21}^2	g_{22}^1, g_{22}^2	⋯	g_{2m}^1, g_{2m}^2
⋮	⋮	⋮	⋱	⋮
I_n	g_{n1}^1, g_{n1}^2	g_{n2}^1, g_{n2}^2	⋯	g_{nm}^1, g_{nm}^2

In addition, the mixed strategy set of the first player is expressed as follows.

$$X_n = \{x = (x_1, x_2, \dots., x_n,): \forall\, i = 1,2, \dots \dots, n\ for\ x_i \geq 0\ \}$$

Likewise, the set of mixed strategies for second player's is expressed as follows.

$$Y_m = \{y = (y_1, y_2, \dots\dots, y_m,): \forall\, j = 1,2, \dots\dots, m\ for\ y_j \geq 0\} \quad (1)$$

According to game theory, when the players in the game play according to the mixed strategies given above, the payoff for both players will be as follows, respectively.

$$p_1(x, y) = \sum_{j=1}^{m} \sum_{i=1}^{n} x_i\, p_{ij}^1\, y_j \quad (2)$$

$$p_2(x, y) = \sum_{j=1}^{m} \sum_{i=1}^{n} x_i\, p_{ij}^2\, y_j \quad (3)$$

In any game, player 1's goal will be to maximize her payoff by choosing mixed strategies, and player 2's goal will be to maximize her payoff by choosing mixed strategies. Using the game's payoff bimatrix (Table 6), only player 1's payoffs can be expressed as follows.

Table 7: Payoff bimatrix for players 1

	II_1	II_2	$\cdots$	II_m
I_1	g_{11}^1	g_{12}^1	$\cdots$	g_{1m}^1
I_2	g_{21}^1	g_{22}^1	$\cdots$	g_{2m}^1
$\vdots$	$\vdots$	$\vdots$	$\ddots$	$\vdots$
I_n	g_{n1}^1	g_{n2}^1	$\cdots$	g_{nm}^1

Similarly, the payoffs of the 2nd player can be expressed as follows.

Table 8: Payoff bimatrix for players 2

	II_1	II_2	$\cdots$	II_m
I_1	g_{11}^2	g_{12}^2	$\cdots$	g_{1m}^2
I_2	g_{21}^2	g_{22}^2	$\cdots$	g_{2m}^2
$\vdots$	$\vdots$	$\vdots$	$\ddots$	$\vdots$
I_n	g_{n1}^2	g_{n2}^2	$\cdots$	g_{nm}^2

Where, for simplicity, let's assume that the game is zero-sum. Then player 1 is trying to maximize the payoff $g_1(x, y)$ if he plays with the mixed strategy ($\boldsymbol{x} \in X_n$), and if player 2 plays with the mixed strategy ($\boldsymbol{y} \in Y_m$),, he is trying to maximize the payoff $g_2(x, y)$.

3. Game theory in Cognitive Radio systems

The latest developments in communication technologies and the ever-increasing need for spectrum have led to the development of CR systems, but have still led to studies on these systems (Wang, et al., 2010). Although CR systems reduce the demand for spectrum, it is necessary to reduce this demand further with different methods. Game theory-based dynamic spectrum assignment policies contribute to reducing this demand. As a result, in recent years game theory has emerged as a central tool for the design of future wireless and communication networks (Liu, et al., 2015). The main reason for this is to enable the next generation of wireless and communication nodes of decision-making rules and techniques to work efficiently, and the ubiquitous Internet access in terms of communication services (for example, video streaming over mobile networks, etc.), the simultaneous use of multiple technologies.

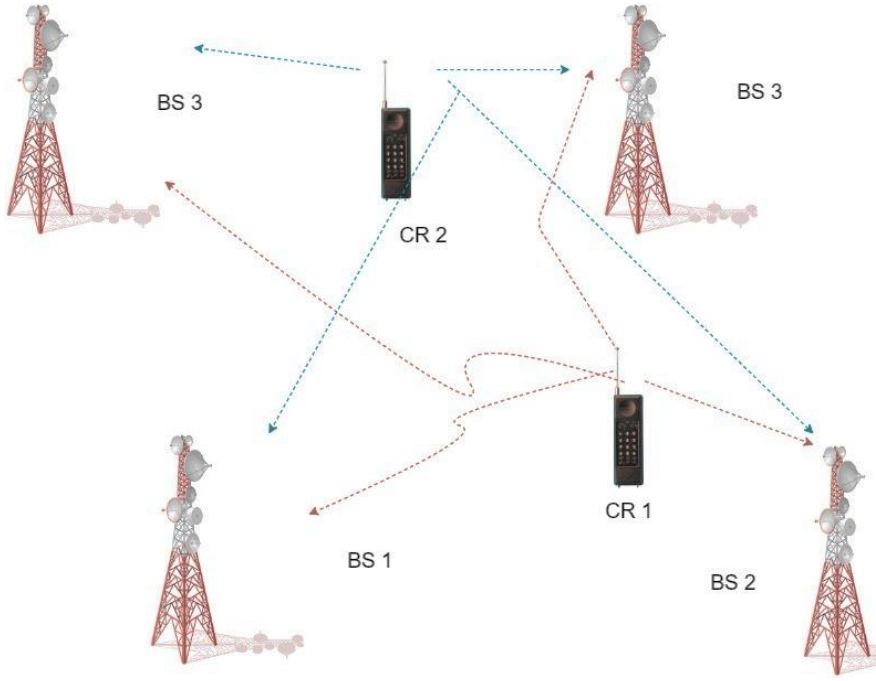

Figure 2. Spectrum allocation schema and Game theory

One of the most popular examples of game theory in wireless networks relates to modeling the power control problem in cellular networks using non-cooperative games. For example, two CR users within range of a base station may want to connect to the same base station at the same time. This may cause a problem in terms of bandwidth in the base station. In order to prevent this, CR users can connect to different base stations that will provide the highest gain by inferring from the signal they detect.

An uncooperative game involves several players whose interests are wholly or partially conflicting as a result of a decision process. For example, consider a CR network with N cognitive users and M primary transmitters. Suppose that BR users should always use the nearest transmitter, but not two CR users from one transmitter at the same time. In such a network, all CR users will want to connect to the closest user. however, doing so increases the overall interference in the system, which negatively affects the performance of all associated wireless nodes.

In this study, firstly, the covariance matrix properties of the signals received by each CR user are used for Game theory based spectrum assignment methods. But it is necessary to make some assumptions here. First, let's assume that each CR user has multiple antennas. Let's assume that CR users know which base station belongs to each beacon that they detect from base stations through their multiple antennas. Because the covariance matrices of the signal received by the CR users also give us information about the power of the base stations. Let's assume that the signal R_x is detected by any CR user through its multiple antennas, then this event can be mathematically expressed as follows (Zeng and Liang, 2008).

$$R_x = R_s + \sigma_\eta^2 I_L \tag{4}$$

where R_s, σ_η^2 and I_L denote base station signal, Gaussian noise and unit matrix with LxL dimensional, respectively. Then the covariance

matrix of the signal received by the CR users is expressed as follows.

$$C_x = E[R_x R_x{}'] \quad (5)$$

According to the Random Matrix Theory (Edelman and Rao, 2005), the covariance matrix also gives information about the signal strength of the base stations. This information will also form the payoff matrices that we will use in Game theory. Thus, CR users will make their base station preferences according to these matrices.

Table 9: Covariance matrices of received signals received by CR users (0dB, 0dB, 0dB, 0dB,)

	BS1 (0dB)	BS2 (0dB)	BS3 (0dB)	BS4 (0dB)
Cov (n,n)	1,25	1,36	1,09	1,14

Table 10: Covariance matrices of received signals received by CR users (10dB, 20dB, -10dB, -20dB,)

	BS1 (10dB)	BS2 (20dB)	BS3 (-10dB)	BS4 (-20dB)
Cov (n,n)	0,042	0,019	0,105	1,05

Table 11: Covariance matrices of received signals received by CR users (-30dB, 0dB, 20dB, 20dB,)

	BS1 (-30dB)	BS2 (0dB)	BS3 (20dB)	BS4 (20dB)
Cov (n,n)	9,98	1,06	0,13	0,04

Accompanied by this information, the gain matrices necessary for Game theory can be created. These matrices also form the payoff matrices for non-zero-sum finite games and two CR users. The goal of each player is to maximize their winnings/payoff. In fact, the concept of gain in this study is connecting the player to the nearest base station. Of course, it is not desirable for both CR users to connect to the same base station with bandwidth restrictions. In fact, the purpose of game theory is to establish a strategy of balance

between two players. The equilibrium strategy for any dimensional game is expressed mathematically as follows.

$$g_1(x, y^*) \leq g_1(x^*, y^*) \quad for\ any\ x \in X_n \tag{6}$$

$$g_2(x, y^*) \leq g_2(x^*, y^*) \quad for\ any\ x \in Y_m \tag{7}$$

where (x^*, y^*) denotes the balance strategies pair for the given game. Balance strategies if the second CR user implements the y^* strategy in a game given by $(x^*, y^*) \in X_n\ x\ Y_m$,the first CR user must play the x^* strategy to maximize his winnings. The table below shows the 7 gain bimatrix. The diagonal elements of the bimatrix are halved while these matrices are being created. because it is not desirable for two CR users to connect to the same base station at the same time due to bandwidth limitation. Thus, their earnings are halved when two CR users want to connect to the same base station. Looking at Table 12, the strategy that will maximize the gains of CR1 and CR2 is marked with a green box. Of course, it should not be forgotten that this gain bimatrix is created by the distance of the CR users to the base stations and the power of the base stations. However, throughout this study, it is assumed that the base stations are equal in power.

Table 12: Payoff bimatrix for 2 CR users and 4 base stations

		CR 1			
		BS 1	BS 2	BS 3	BS 4
CR 2	BS 1	(0,84) (0,92)	(1,69) (1,45)	(1,69) (0,79)	(1,69) (1,91)
	BS 2	(1,45) (1,85)	(0,84) (0,72)	(1,45) (0,79)	(1,45) (1,91)
	BS 3	(0,42) (1,85)	(0,42) (1,45)	(0,21) (0,39)	(0,42) (1,91)
	BS 4	(0.97) (0.97)	(1,85) (1,45)	(1,85) (0,79)	(0,97) (0,95)

Table 13 is an example of a different payoff bimatrix. Where the area marked with the blue box might actually be the Nash equilibrium. However, this box shows that both CR users are connected to BS 2, which is undesirable. Therefore, the Nash equilibrium for Table 11 is marked with a green box.

Table 13: Payoff bimatrix for 2 CR users and 4 base stations

		CR 1			
		BS 1	BS 2	BS 3	BS 4
CR 2	BS 1	(0,31) (0,49)	(0,63) (1,88)	(0,63) (1,19)	(0,63) (1,22)
	BS 2	(1,78) (0,98)	(0,89) (0,94)	(1,78) (1,19)	(1,78) (1,22)
	BS 3	(0,81) (0,98)	(0,81) (1,88)	(0,40) (0,59)	(0,81) (1,22)
	BS 4	(0,87) (0,98)	(0,87) (1,88)	(0,87) (1,19)	(0,43) (0,61)

For the model proposed in this study, assume that there are randomly selected BS stations and two CR users. Let's assume CR users are moving in an orbit.

4. Numerical results

The scenario given in Figure 3 is used for the simulation studies in this study. In order to see the spectrum allocation and which CR user will choose which base station, the CR users are orbited in a trajectory given in Figure 3. Thus, they will create a payoff bimatrix according to the power of the base stations by means of the signals they receive. In Figure 3, the trajectories of the CR users are determined beforehand, and the locations of the base stations are chosen randomly.

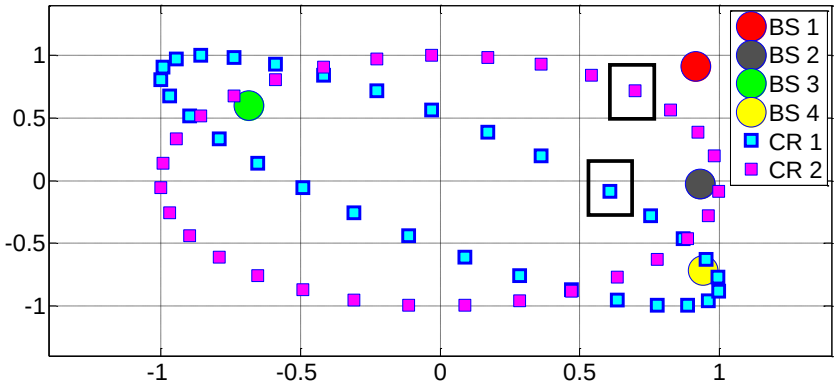

Figure 3. Random CR orbits and base station positions

In addition, where the powers of the base stations are chosen equally. For this reason, the strength of the signals perceived by CR users is inversely proportional to the distance. For example, in Table 9, the payoff bimatrix created at any location of CR users is given below. That is, in order to maximize the gains/payoff of R users, both need to be connected to the base station number 2. However, as mentioned before, it is not desirable for both CR users to connect to the same base station at the same time due to bandwidth constraints. Therefore, when CR1 is connected to base station 4 and CR2 to base station 2, both users maximize their gain.

The payoff bimatrix for the positions (marked with the black square) in Figure 3 is given in Table 14. As mentioned before, the green box here shows the Nash equilibrium, but at the same time, it is the base stations for CR users to gain maximum gain when connected.

Table 14: The payoff bimatrix for the positions given in Figure 3

		CR 1			
		BS 1	BS 2	BS 3	BS 4
CR 2	BS 1	(0,31) (0,49)	(0,63) (1,88)	(0,63) (1,19)	(0,63) (1,22)
	BS 2	(1,78) (0,98)	(1,78) (1,88)	(1,78) (1,19)	(1,78) (1,22)
	BS 3	(0,81) (0,98)	(0,81) (1,88)	(0,40) (0,59)	(0,81) (1,22)
	BS 4	(0,87) (0,98)	(0,87) (1,88)	(0,87) (1,19)	(0,43) (0,61)

Fig. 4 shows which base station CR users use by maximizing their earnings at different positions of any given trajectory.

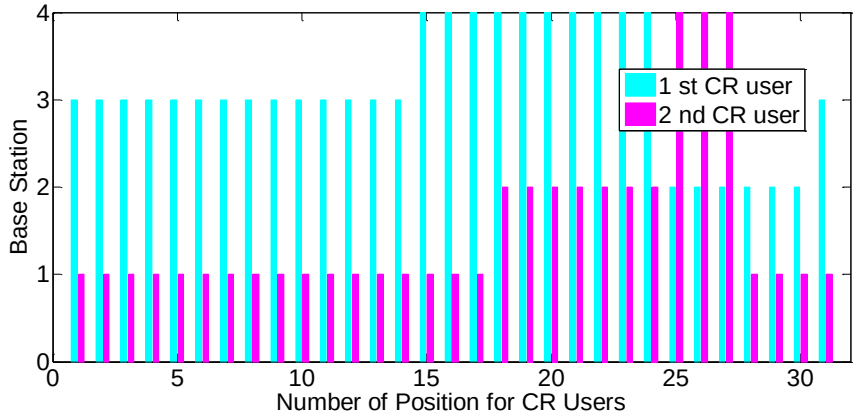

Figure 4. Spectrum assignment table for four base stations

The simulation for 2 CR users and 8 randomly located base stations is given in Figure 5. As expected in this model, the gain bimatrix is an 8X8 matrix. Since this matrix is large, we will not include it here. The results of the spectrum assignment scenario given in Figure 5 are given in Figure 6. Figure 6 shows that two of the 2 CR users can never be assigned to the same base station at the same time. In addition, the base stations to which CR users are assigned are those that will maximize the gains of both.

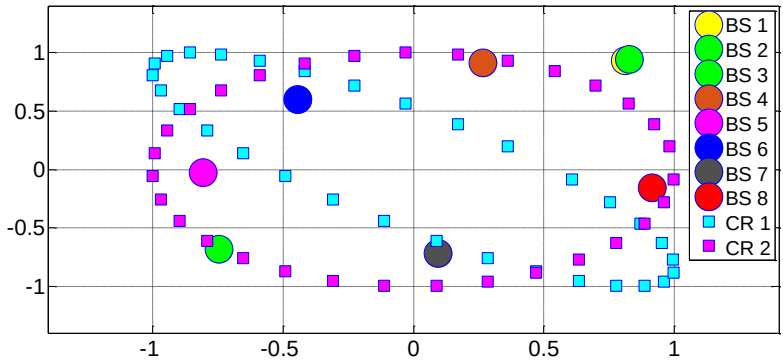

Figure 5. Random CR orbits and base station positions

Today, the internet of things, cloud computing and mobility bring a lot of data transmission for users. It is difficult to ensure Quality of Service (QoS) in the transmission of such a large amount of data. Although the quality of service consists of several important sub-headings in CR systems, bandwidth limitations are one of them. In Fig. 5 (that is, when there are 8 base stations), two CR users will want to transmit with the same base station when they are close to each other.

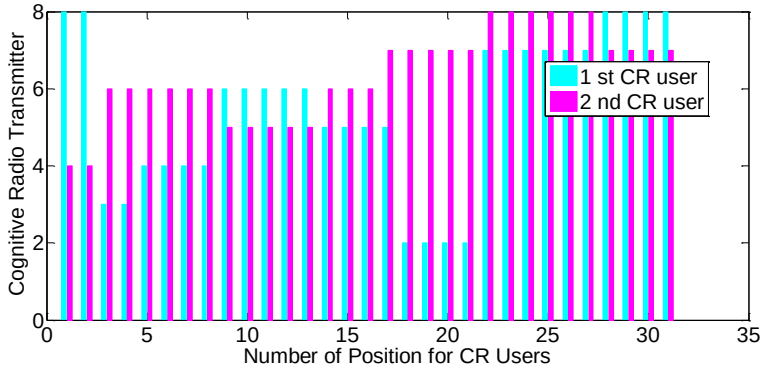

Figure 6. Spectrum assignment table for four base stations

However, as can be seen, when spectrum assignments are made on a Game-based basis, both this negativity is prevented and the gains of 2 CR users are maximized.

Figure 6 clearly shows that 2 CR users do not communicate with the same base station at the same time. for example, at location 1, the first CR is connected to base station 8 and CR 2 is connected to base station 4.

5. Conclusion

In this study, game theory and some of its varieties were examined and a study was carried out on the use of game theory in Cognitive Radios. In the study, a game-based spectrum assignment method was applied with the signals received by CR users. Thanks to Game theory, CR users choose the closest base station to them by maximizing their returns. This study is explained in detail with the simulation results.

References

Bellman, R. (1956). Dynamic programming and Lagrange multipliers. *Proceedings of the National Academy of Sciences of the United States of America*, *42*(10), 767.

Böge, W., & Eisele, T. (1979). On solutions of Bayesian games. *International Journal of Game Theory*, *8*(4), 193-215.

Dekel, E., Fudenberg, D., & Levine, D. K. (2004). Learning to play Bayesian games. *Games and Economic Behavior*, 46(2), 282-303.

Dutta, P. K., & Dutta, P. K. (1999). *Strategies and games: theory and practice*, MIT press.

Friedman, A. (2013). *Differential games*. Courier Corporation.

Friedman, A. (1972). *Stochastic differential games*, Journal of differential equations, 11(1), 79-108.

Edelman, A., & Rao, N. R. (2005). *Random matrix theory*. Acta numerica, 14, 233-297.

Guseinov, K. G., Akyar, E., & Düzce, S. A. (2010). *Oyun Teorisi:*

Çatışma ve anlaşmanın matematiksel modelleri. Seçkin yayınevi.

Hardin, R. (1971). Collective action as an agreeable n-prisoners' dilemma. *Behavioral science*, 16(5), 472-481.

Kirk, D. E. (2004). *Optimal control theory: an introduction*. Courier Corporation.

Kopp, R. E. (1962). Pontryagin maximum principle. *In Mathematics in Science and Engineering* (Vol. 5, pp. 255-279). Elsevier.

Lacey, N. (2008). THE PRISONERS'DILEMMA. *Cambridge UK*.

Liu, X., Zhu, R., Jalaian, B., & Sun, Y. (2015). Dynamic spectrum access algorithm based on game theory in cognitive radio networks. *Mobile Networks and Applications*, 20(6), 817-827.

Mansour, Y., Slivkins, A., Syrgkanis, V., & Wu, Z. S. (2016). Bayesian exploration: Incentivizing exploration in bayesian games. *arXiv preprint arXiv:1602.07570.*

Mertens, J. F. (1987). *Ordinality in non cooperative games* (No. 1987028). Université catholique de Louvain, Center for Operations Research and Econometrics (CORE).

McCain, R. A. (2008). Cooperative games and cooperative organizations. *The Journal of Socio-Economics*, 37(6), 2155-2167.

Mitola, J. (2000). *Cognitive radio* (Doctoral dissertation, Institutionen för teleinformatik).

Montola, M., Stenros, J., & Waern, A. (2009). *Pervasive games: theory and design.* CRC Press.

Myerson, R. B. (2013). *Game theory*. Harvard university press.

Nash, J. (1951). Non-cooperative games. *Annals of mathematics*, 286-295.

Rosenthal, R. W. (1989). A bounded-rationality approach to the study of noncooperative games. *International Journal of Game Theory*, 18(3), 273-292.

Rath, H. K., Revoori, V., Nadaf, S. M., & Simha, A. (2014, June). Optimal controller placement in Software Defined Networks (SDN) using a non-zero-sum game. *In Proceeding of IEEE International Symposium on a World of Wireless, Mobile and Multimedia Networks 2014* (pp. 1-6). IEEE.

Sethi, S. P., & Thompson, G. L. (2000). *What is optimal control theory?* (pp. 1-22). Springer US.

Thomas, L. C. (2012). *Games, theory and applications*. Courier Corporation.

Ordeshook, P. C. (1986). *Game theory and political theory: An introduction*. Cambridge University Press.

Vorob'Ev, N. N. (2012). *Foundations of game theory: noncooperative games*. Birkhäuser.

Von Neumann, J. (1988). John von neumann. *American Mathematical Soc.*

Von Neumann, J., & Morgenstern, O. (2007). *Theory of games and economic behavior*. Princeton university press.

Zermelo, E. (2010). *Ernst Zermelo-Collected Works/Gesammelte Werke: Volume I/Band I-Set Theory, Miscellanea/Mengenlehre, Varia* (Vol. 21). Springer Science & Business Media.

Zeng, Y., & Liang, Y. C. (2008). Spectrum-sensing algorithms for cognitive radio based on statistical covariances. *IEEE transactions on Vehicular Technology*, 58(4), 1804-1815.

Wang, B., Wu, Y., & Liu, K. R. (2010). Game theory for cognitive radio networks: *An overview. Computer networks*, 54(14), 2537-2561.

CHAPTER VII

THE EFFECT OF pH ON THE REMOVAL OF TETRACYCLINE ANTIBIOTIC FROM AQUEOUS SOLUTIONS BY ULTRASOUND/ H_2O_2 AND SONO-FENTON METHODS

Yeliz Aşçı

(Prof.PhD) Department of Chemical Engineering, Eskisehir Osmangazi University, email: yelizbal26@gmail.com/yelizbal@ogu.edu.tr

Orcid: 0000-0001-5618-058X

1. Introduction

With the developing technology and increasing population, the use of drugs is increasing day by day (Odabaşı et al., 2017). Antibiotics, as it is known, are one of the drugs that are widely used all over the world, especially in the treatment of bacterial infections. (Kordestani et al., 2020). The main sources of antibiotics are; homes, hospitals, health centers, poultry and livestock feed operations (growth enhancers) and pharmaceutical manufacturers. Antibiotics enter the environment in various ways. These compounds are not completely metabolized in the body and are generally transferred to the environment through urine and eventually reach wastewater, soil, underground waters and our drinking water if adequate treatment is not done, endangering human and animal health (Topal et al., 2012; Malakootian and

Asadzadeh, 2020). As a result, it is important to treat wastewater in order to eliminate this danger.

Tetracycline (TC) is one of the most widely used antibiotics. Different methods have been studied for TC removal from waste waters in the literature. These are methods such as adsorption (Xia, et al., 2021) electrochemical treatments (Wu et al., 2012), biological treatments (Liu et al., 2018) and membrane treatments (Lu et al., 2017). However, these methods have low yields and/or high costs limit their use (Malakootian and Asadzadeh, 2020). Therefore, both economical and efficient advanced treatment methods are needed for the removal of these antibiotics.

Advanced oxidation processes (AOPs) are one of the advanced treatment methods used for this purpose to oxidize organic compounds that are resistant to conventional treatment methods (Ranjit et al., 2008). Fenton processes, ultrasound, ozonation, photocatalysis and various combinations of these are the most common advanced oxidation methods (Hekimoğlu, 2021; Odabaşı et al., 2017). Fenton oxidation, which is one of these processes, is a frequently used method for the removal of drugs due to its rapidity, low cost and simple technology (Odabaşı et al., 2017). Fenton process, it is a method based on the production of various reactive species, especially hydroxyl radical ($OH^{\cdot}$), which allows the decomposition of non-biodegradable and toxic compounds into H_2O and CO_2. Hydroxyl radical in the presence of Fe^{2+} it is produced by the breakdown of H_2O_2 (Eq.1). Reactive species produced it can decompose and mineralize various organic pollutants (Ammar, 2016).

$$Fe^{+2} + H_2O_2 \rightarrow Fe^{+3} + \cdot OH + OH^- \qquad (1)$$

Another method, which is one of the advanced oxidation processes and has been widely used in the removal of organic chemical compounds in recent years, is the ultrasound process (Zhang et al.,

2009; Malakootian and Asadzadeh, 2020; Yakut, 2019). Ultrasound can be used in various combinations. Ultrasound only (US), combined with the Fenton process (sono-Fenton) or US/H_2O_2 etc.

The application of ultrasound technology is more effective in liquid systems and its effect is mainly dependent on the phenomenon of cavitation (Yüksel, 2013). Ultrasound waves include expansion and compression cycles. The expansion loop creates acoustic cavitation. As the cavitation bubbles burst, the temperature and pressure inside the bubbles can reach several thousand Kelvin and several hundred atmospheres, respectively. When this happens, organic compounds in the bubbles are broken down by pyrolysis. The pyrolysis of polluting organic wastes in wastewater and the production of reactive radicals such as hydroxyl radicals from water or oxygen molecules are the important destructive abilities of this process. The radicals formed cause the decomposition of organic pollutants (Yakut, 2019; Şahinkaya, 2017). The reactions of the process are as seen below (Hekimoğlu, 2021).

$$H_2O +))) \rightarrow \bullet OH + \bullet H \text{ (pyrolysis)} \quad (2)$$

$$\bullet OH + \bullet H \rightarrow H_2O \quad (3)$$

$$2\bullet OH \rightarrow H_2 + O_2 \quad (4)$$

$$2\bullet OH \rightarrow H_2O_2 \quad (5)$$

$$2\bullet H \rightarrow H_2 \quad (6)$$

The application of Fenton and ultrasound method together is called as Sono-Fenton method. In the Sono-Fenton process, both the use of iron and ultrasound waves generate more hydroxyl radicals (Ammar, 2016; Ranjit et al., 2008).

Therefore, the aim of this study was to compare the removal of TCA with Sono-Fenton and ultrasound/H_2O_2. Also, the effect of pH on TCA removal is discussed.

2. Materials and Methods

2.1. Materials

Antibiotic removal efficiencies were compared by performing sono-fenton and ultrasound experiments on antibiotic solutions**.** Tetra antibiotic belonging to the tetracycline group was used in the experiments. Each capsule of this antibiotic contains between 250 mg and 500 mg tetracycline HCl equivalent to tetracycline.

Iron(II) sulfate heptahydrate ($FeSO_4.7H_2O$) used in sono-fenton experiments was obtained from Merck. Hydrogen peroxide (30% w/w) was purchased by Sigma-Aldrich. Additionally, sulfuric acid (H_2SO_4) (98% w/w) and sodium hydroxide (>99%), used to adjust pH, was supplied by Merck. All experiments were carried out at room temperature.

2.2. Experimental procedure

2.2.1. Ultrasound/H_2O_2 process

In both sono-fenton and ultrasound processes, the total solution volume was studied to be 200 ml. 10 ml of the antibiotic-containing aqueous solution is withdrawn and made up to 100 ml with distilled water in the flask. The sample is adjusted to the desired pH value with the help of 2M NaOH and acid solution. The prepared H_2O_2 solution is added to the sample and placed in the device. Sonics VCX 750 brand ultrasonic homogenizer (750 W, 20 kHz) was used in the both sono-fenton and ultrases experiments. The probe 13 mm of device is immersed 4 cm in to the solution and the device is started. The device is set to 60 minutes. After 60 minutes, the sample solution is placed in the sample container with the help of a dropper and placed in the centrifuge. It is centrifuged at 4000 rpm for 15 minutes in the centrifuge device. After centrifugation, the results are read in the UV spectroscopy device (Figure 2).

Figure 1: Ultrasonic homogenizer

2.2.2. Sono-Fenton Process

First, 10 ml of the aqueous solution containing the antibiotic is withdrawn and made up to 100 ml with distilled water in the flask. This sample is adjusted to the desired pH value with the help of 2M NaOH and acid solution. Then, 20 ml of Fe(II) and H_2O_2 stock solution are withdrawn from each stock solution to 50 ml with distilled water and added to the sample. The sample is placed in the ultrases device and the device is set for 60 minutes. After 60 minutes, 3-4 drops of 2M NaOH are added to the sample to stop the reaction and form a precipitate. After waiting for 30 minutes, the solution is placed in the sample container with the help of a dropper and placed in the refrigerator. The results are read on the UV–vis spectrophotometer after one day.

2.3. Analytical methods

Samples of 2, 4, 6, 10, 20, 30 and 40 ppm were prepared from the antibiotic stock solution. The maximum wavelength of the antibiotic

solution was determined by scanning the absorbance in the UV spectroscopy device (Hach Lange LCK 514) (Figure 2). A concentration-absorbance calibration curve was created with the absorbance values read at a wavelength of 357 nm. % removal efficiency of antibiotic is defined as follows:

$$\frac{initial\ concentration - remainig\ concentration\ in\ solution}{initial\ concentration} x100$$

Figure 2: UV spectroscopy device

3. Results and Discussions

3.1. *Effect of the pH in sono-fenton and ultrasound/H_2O_2 process*

In order to investigate the pH effect, samples were taken from the antibiotic stock solution and adjusted to the desired pH values (2, 3, 4, 5, 6). Concentration values of samples and % removal amounts were calculated with the help of the equation y = 0.0273x + 0.0133 found with the drawn calibration curve. As seen in Figure 3.1, the highest removal was obtained at pH=3.0. The optimum pH value for the sonofenton process is 3.0.

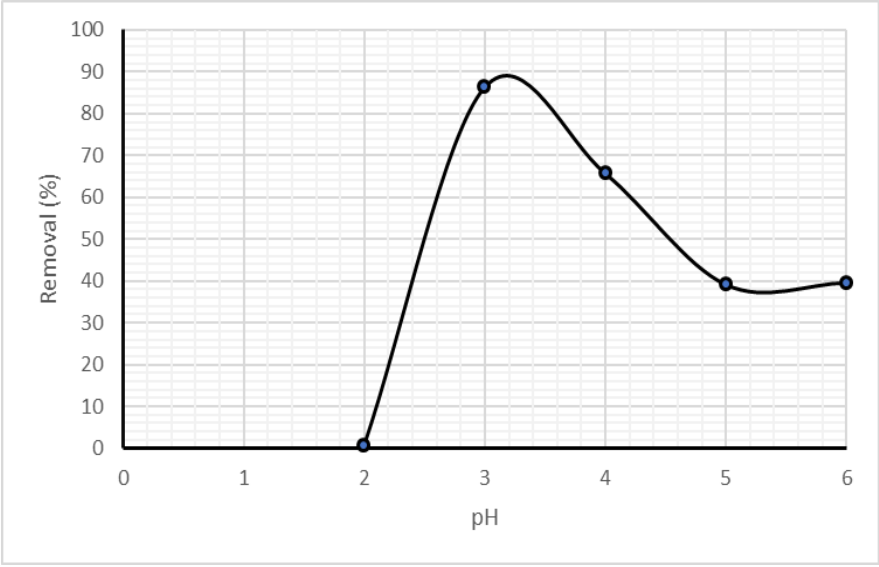

Figure 3.1. pH - % TCA removal graph in sono-fenton process

The effect of pH in ultrasound/H_2O_2 process was investigated by varying the pH from 2.0 to 6.0 and is shown in Fig. 3. 2. The results indicated that the removal of antibiotic was significantly influenced by the pH of the solution. The optimum pH value for the removal of antibiotic was pH 2.0 within 60 min of reaction in ultrasound process.

As it is known, pH is the most important parameter in Fenton processes. As seen in Figure 3.1 almost no removal was achieved in the sono-Fenton process at pH=2.0, i.e. 0.6%. Removal was 86.32% at pH=3.0 and approximately 40% at pH=6.0. In the ultrasound /H_2O_2 process, as seen in Figure 3.2, while it was 91.4% at pH=2.0, the efficiency decreased to 19% at pH=6.0. In other words, only ultrasound/H_2O_2 provided lower removal in basic conditions compared to the sono-Fenton process.

As it is known, Fenton processes work better in acidic conditions (pH=2-4). Because, as seen in Eq. 1, iron ions dissolve better and more $OH^{\cdot}$ radicals are produced at low pH, that is, in an

acidic environment (Kordestani et al., 2020; Odabaşı et al., 2017). The Sono-Fenton process, on the other hand, is slightly different from the Fenton process and gives good results in basic conditions (Ranjit et al., 2008). This result shows that even at pH=6, the sono-fenton process can be used and thus eliminates the danger posed by acidic waters.

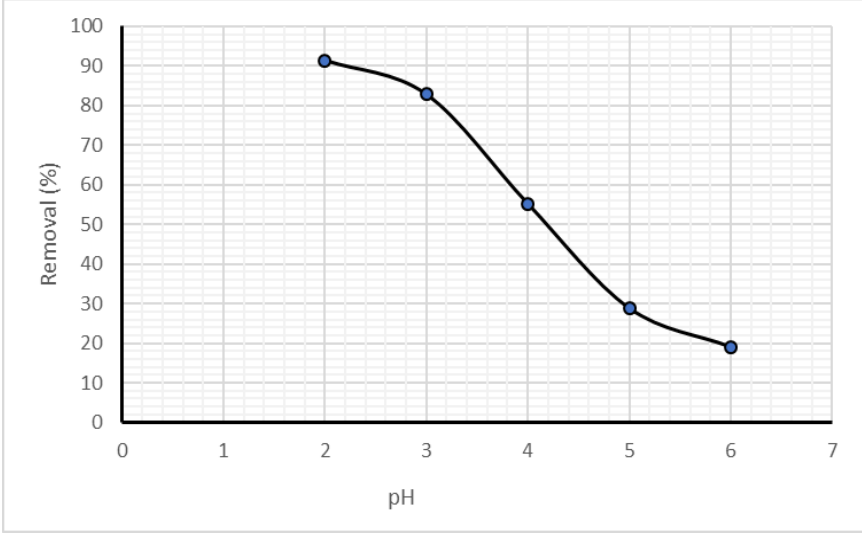

Figure 3.2. pH - % TCA removal graph in ultrasound/H_2O_2 process

4. Conclusion

In this study, the effect of pH on TCA removal from aqueous solution was investigated using sono-Fenton and ultrasound/H_2O_2 processes.

In conclusion, in this experimental study, it can be said that the sono-Fenton process is more advantageous than only ultrasound/H_2O_2. Only one disadvantage here is that it also creates a pollution due to the use of iron. However, this can be prevented by using the required amount of iron powder in accordance with the water pollution discharge standards.

5. Acknowledgments

The author thanks the Eskişehir Osmangazi University Scientific Research Commission (project number: 201615059) for the financial support of this study.

References

Ammar, H. B. (2016). Sono-Fenton process for metronidazole degradation in aqueous solution: effect of acoustic cavitation and peroxydisulfate anion. *Ultrasonics Sonochemistry*, 33, 164-169.

Kordestani, B., Takdastan, A., Yengejeh, R. J. & Neisi, A. K. (2020). Photo-Fenton oxidative of pharmaceutical wastewater containing meropenem and ceftriaxone antibiotics: influential factors, feasibility, and biodegradability studies, *Toxin Reviews*, 2020, 39(3), 292–302.

Liu, H., Yang, Y., Sun, H., Zhao, L. & Liu, Y. (2018). Fate of tetracycline in enhanced biological nutrient removal process. *Chemosphere*, 193, 998-1003.

Lu, T., Xu X., Liu, X. & Sun, T. (2017). Super hydrophilic PVDF based composite membrane for efficient separation of tetracycline. *Chemical Engineering Journal*, 308, 151-159.

Malakootian, M. & Asadzadeh,, S. N. (2020). Oxidative removal of tetracycline by sono Fenton-like oxidation process in aqueous media. *Desalination and water treatment*, 193, 392–401.

Odabaşı, S. Ü., Maryam, B. & Büyükgüngör, H. (2017). Fenton ve Fotofenton Prosesleri ile Atıksudaki Aspirinin Giderim Verimliliğinin Karşılaştırılması. *Nevşehir Bilim ve Teknoloji Dergisi*, 6, 326-332.

Ranjit, P. J. D. Palanivelu, K. & Lee, C.S. (2008). Degradation of 2,4-dichlorophenol in aqueous solution by sono-Fenton

method. *Korean Journal of Chemical Engineering*, 25(1), 112-117.

Şahinkaya, S. (2017). Decolorization of reactive orange 16 via ferrate(VI) oxidation assisted by sonication. *Turkish Journal of Chemistry*, 41(4), 577-586.

Topal, M., Uslu, G., Arslan Topal, E.I. & Öbek, E. (2012). Antibiyotiklerin Kaynakları ve Çevresel Etkileri. *BEÜ Fen Bilimleri Dergisi*, 1(2), 137-152.

Yakut, Ş.M. (2019). Çevre Mühendisliğinde Su Arıtımında Ultrases Uygulamaları. *Nevşehir Bilim ve Teknoloji Dergisi*, 8(1), 73-81.

Yüksel, F. (2013). Gıda Teknolojisinde Ultrases Uygulamaları. *Gıda Teknolojileri Elektronik Dergisi*, 8(2), 29-38.

Wu, J., Zhang, H., Oturan, N., Wang, Y, Chen, L. & Oturan, M. A. (2012). Application of response surface methodology to the removal of
theantibiotic tetracycline by electrochemical process using carbon-felt cathode and DSA (Ti/RuO2–IrO2) anode, *Chemosphere*, 87, 614-620.

Xia, J., Gao Y. & Yu, G. (2021). Tetracycline removal from aqueous solution using zirconium-based metal-organic frameworks (Zr-MOFs) with different pore size and topology: Adsorption isotherm, kinetic and mechanism studies. *Journal of Colloid and Interface Science*, 590, 495-505.

Zhang, H., Zhang, J., Zhang, C., Liu, F. & Zhang, D. (2009). Degradation of C.I. Acid Orange 7 by the advanced Fenton process in combination with ultrasonic irradiation. *Ultrasonics Sonochemistry*, 16, 325–330.

CHAPTER VIII

CEREAL GRAIN-FERMENTED PRODUCTS: HEALTH, NUTRITION AND MICROBIOLOGY

Gözde Özdemir[1] & Dilek Dülger Altıner[2]

[1](PhD Student), Kocaeli University,

e-mail: gozdeozdemr@gmail.com

Orcid: 0000-0001-6258-6260

[2](Asst. Prof. Dr.), Kocaeli University,

e-mail: dilek.dulger@kocaeli.edu.tr

Orcid: 0000-0002-7043-2883

1. Introduction

Cereal grains and processed foods form the basis of the human diet, especially in developing countries (Menis-Henrique et al., 2020; Saleh et al., 2019). The main cereal products produced worldwide are wheat, rice, maize (Ali et al., 2020; Bahgaat & Ghani, 2017), millet, sorghum, rye and oats (Ali et al., 2020). Scientific studies reveal that there are components such as dietary fiber, minerals, vitamins, phenolic compounds (Kumral, 2015; Menis-Henrique et al., 2020), lignans, antioxidants, fat and starch (Kumral, 2015), and polyphenols and phytosterols (Menis-Henrique et al., 2020) in the content of cereal products, and that these components are beneficial in the prevention of chronic diseases such as cancer, obesity, coronary heart disease, diabetes (Kumral, 2015), type II diabetes and gastrointestinal disorders (Saleh et al., 2019). In

addition, it is known that phytochemicals in the content of cereal grains prevent oxidative damage and reduce cell death rate and the effects of aging-related diseases (Saleh et al., 2019). In order to increase the nutritional content of cereals, various methods such as genetic modification methods, and enrichment with some essential amino acids, protein concentrates and isolates have been tried (Karademir et al., 2018).

Fermentation is one of the oldest and most economical food production methods (Iskakowa et al., 2019). Fermented foods have an important place in nutrition in many countries due to the protective, nutritional value-enriching and sensory-enhancing properties of fermentation (Ali et al., 2020; Azam et al., 2017). In addition, fermented foods are known to have antimicrobial, antioxidant, probiotic and cholesterol-lowering effects. Some studies show that fermented milk products have a positive effect on colon and breast cancer and blood cholesterol, that fermented red beet prevents proliferation of tumor cells, that fermented cabbage contains S-methylmethionine, which reduces tumor formation in the stomach, and that soy-based fermented foods, such as soybean sauce, natto and kinema, have antithrombotic and anticancer effects (Karaçıl & Acar Tek, 2013). It is known that the fermentation process in grain-based foods contributes to nutritional value and bioaccessibility, removes endogenous toxins and cyanogenic compounds, and reduces the energy required for cooking (Achi & Ukwuru, 2015).

Bacteria constitute the largest group of organisms with a single-celled prokaryotic cellular organization and are found in almost all ecological habitats. Yeasts, on the other hand, are eukaryotic unicellular microorganisms, and are commonly found in soil, plant surfaces, and especially in habitats with high sugar content such as fruits and flowers (Akçelik & Akçelik, 2019).

Various fermentative bacteria, such as Lactic acid bacteria (LAB) (*Aerococcus, Enterococcus, Lactobacillus, Lactococcus, Pediococcus, Streptococcus,* etc.), acetic acid bacteria (AAB) (*Acetobacter, Gluconobacter,* etc.), and propionic acid bacteria (*Propionibacterium freudenreichii*, etc.), fermentative yeasts (*Saccharomyces cerevisiae, Candida utilis, Kluyveromyces marxianum, Pichia pastoris,* etc.), and mainly fermentative molds (*Penicillium roqueforti, Penicillium camemberti, Penicillium caseicolum,* etc.) (Karahan Çakmakçı et al., 2020) are involved during fermentation. These microorganisms used during fermentation transform the chemical compounds in the raw material into new products and provide the formation of different aroma and flavor components. Lactic acid bacteria are effective on criteria such as nutritional quality, taste, aroma, structure, fluidity, gas formation, color, and shelf life in food during fermentation, and yeasts are effective on nutritional quality, aroma, structure, fluidity, gas formation and shelf life, whereas molds are effective on aroma, structure, fluidity, and gas formation (Akçelik & Akçelik, 2019).

Grain-based fermented foods attract a lot of attention since they reflect different cultures around the world. These products are more common especially in Central Asia, the Middle East, and Africa (Blandino et al., 2003). Fermented foods, which have different characteristics according to different regions, have been developed especially with raw materials specific to the region, and their production has continued for generations. Some grain types and grain-based fermented foods produced from them are presented in Figure 1, whereas the names of grain-based fermented foods common in different countries of the world are presented in Table 1. In this chapter, some grain-based fermented products, which are prominent in human nutrition, were defined, their effects on health were discussed, and the microbiological composition responsible for

fermentation was examined. In this context, some fermented foods such as Bread, Boza, Tarhana, Idli, Dosa, Dhokla, Kishk, Ogi, Kenkey, Mahewu, Pozol, and Chicha, where grain-based products are used, were analyzed.

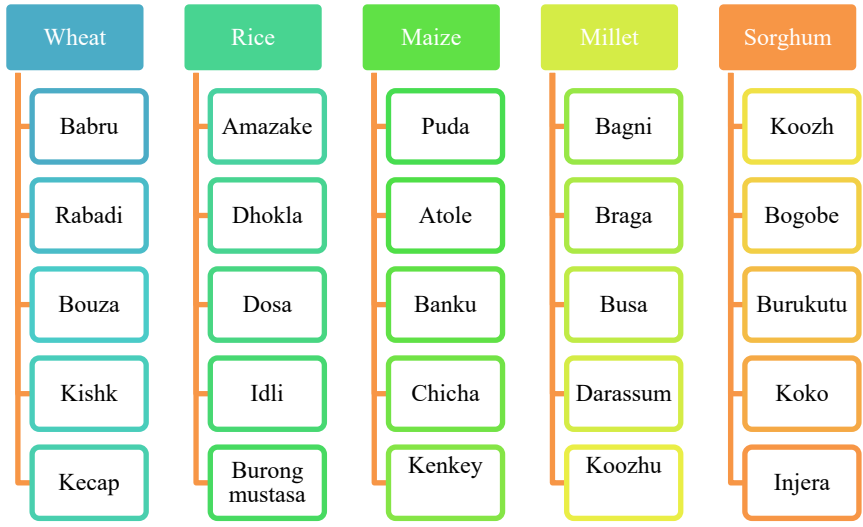

Figure 1 Some Grain Types and Fermented Foods Produced From These Grains

Source: (Bhalla & Savitri, 2017; Tamang, 2016)

Table 1 Traditional Cereal-Based Fermented Foods

Country	Traditional Cereal-Based Fermented Foods
Africa	Munkoyo, Ogi, Mahewu
Bangladesh	Amitri, Jilapi, Pantavaat, Pauruti
Belgium	Lambic beer
Botswana	Bogobe
China	Ang-kak, Lao-chao, Miso, Shaosingjiu
Egypt	Bouza, Busa, Kishk
Ghana	Banku, Kenkey, Koko
India	Aara, Adai Dosa, Ahom, Ambali, Apong/ennog, Appam/kallappam/vellayppam, Ark/ara, Atingba, Bhaati jaanr, Bhang-chyang, Buza, Chakuli, Chhang, Chhuchipatra pitha, Chitou, Daru,

	Dekuijao, Dhokla, Dosa, Enduri pitha, Faapar ko jaanr, Gahoon ko jaanr, Hakua, Handia, Handwa, Haria, Idli, Imrati, Jann/jaan, Jao ko Jaanr, Jhara, Jou, Judima, Juharo, Juhning, Kiad, Koozh/koozhu, Lugri, Madhu, Makai ko jaanr, Mingari/lohpani, Munha pitha/poto pitha, Nduijao, Opo, Pachwai, Pazhaya sadham, Pona, Puda/Pudha, Rabadi, Raksi, Ruhi, Sez, Sujen, Sura, Themsing, Yu, Zu, Zutho/Zhuchu, Kanji, Pitha, Torani
Indonesia	Brem, Brembali, Tape, Lao-chao
Iran	Bread, Barbari Bread, Sangak Bread, Taftoon Bread, Lavash Bread, Tarkhineh, Kashk-e zard
Japan	Amazake, Miso, Koikuchi shoyu, Usukuchi shoyu, Saishikomi shoyu, Tamari shoyu, Shiro shoyu, Fukuyama pot vinegar, Bettara-zuke, Sagohachi-zuke, Sake, Shochu, Awamori, Mirin
Korea	Makgeolli, Yakju, Soju, Vinegar, Jeungpyeong, Kichudok, Takju
Mexico	Atole, Pozol,
Mongolia	Darassum
Nepal	Hyaun thon, Jaand, Jand, Imrati, Murcha, Rakshi, Thumba
New Zealand	Kaanga-kopuwai
Nigeria	Am-som, Burukutu, Kunuzaki, Ogi, Pito
Pakistan	Andrassay, Doli Ki Roti, Jalebi, Naan
Peru	Chicha
Philippines	Burong mustasa, Balao-balao, Burong isda, Burong kalabi, Burong babi, Puto, Bibingka, Tapuy, Pangasi
Romania	Braga
Sri Lanka	Idly, Thosai, Appa/appam
Sudan	Merissa
Tanzania	Togwa
Thailand	Sato, Khanomjeen,
Turkey	Tarhana
Vietnam	Banh men, Sour shrimp, Tuong, Me

Source: (Bhalla & Savitri, 2017; Tamang, 2016)

2. Cereal Grain-Fermented Products

2.1. Bread

During bread production, water, salt, yeast (*Saccharomyces cerevisiae*), sugar, enzymes, malt flour as an enzyme source, vital gluten and permitted additives are added to wheat flour, and this mixture is kneaded, shaped, fermented, and cooked in accordance with its technique (Anonymous, 2012). Bread production basically consists of six stages: obtaining the dough, first fermentation, cutting-weighing, second fermentation, shaping, and baking (Ünüvar, 2008). Bread is rich in iron, calcium, niacin, protein, B1 and B2 vitamins and is known to meet a certain part of the daily need (Tax, 2020).

S. cerevisiae, a baker's yeast, has been used for food and beverage production throughout humankind's recipe thanks to its fermentative power (Perez-Torrado et al., 2015) and is a unicellular eukaryote (Al-sahlany et al., 2020). *S. cerevisiae* is 5-10 μm in diameter, and circular or oval in shape (Çakmakçı et al., 2020; Walker & Stewart, 2016, p. 2). In order for *S. cerevisiae* to function, high water activity, temperature in the range of 20-30^{o}C, and pH in the range of 4.5-6.5 are required (Walker & Stewart, 2016, p. 2). Industrial strains are well adapted to stress conditions, such as temperature, osmotic pressure and ethanol toxicity, and to conditions present during different fermentation periods (Perez-Torrado et al., 2015, p. 102).

2.2. Boza

Boza is obtained from the fermentation of grains, such as wheat, barley, oats, millet, corn and rye, is a sweet unique to Turkey, Bulgaria, Albania, Macedonia, Romania and North Africa, and a viscous and low alcohol beverage with a slightly acidic taste (Arslan

et al., 2015; Ashaolu & Reale, 2020; Çelik et al., 2016; Kışla & Hancıoğlu Silili, 2020). Boza is a product rich in fat, protein, carbohydrates, fiber, vitamins, amino acids and lactic acid. It is also known that boza has positive effects on the intestinal microbiota and digestive tropism (Kışla & Hancıoğlu Şıklı, 2020). It is also known that boza accelerates blood circulation, reduces hypertension, helps induce a bowel movement, renews blood, and reduces fat (Aila et al., 2020).

In traditional production, the grains are washed, thinned and cooked in a steam boiler. The cooked mixture is cooled and filtered, and sugar or artificial sweetener is added. The mixture obtained is fermented at 30^{o}C for 24 hours by adding the previously produced boza, yeast or yoghurt as a starter. After the fermentation process, boza is cooled to +4^{o}C and bottled and stored under cold conditions. During the production of boza, lactic acid bacteria and yeasts are involved (Arslan et al., 2015; Kışla & Hancıoğlu Şıklı, 2020).

Boza includes *Lactobacillus plantarum, Leuconostoc brevis, Lactobacillus fermentum, Leuconostoc mesenteroides, Lactobacillus casei, Lactobasillus acidophilus* (Ashaolu & Reale, 2020; Baschali et al., 2017), *Lactobacillus coprophilus, Leuconostoc raffinolactis, Lactobacillus paracasei, Lactobacillus rhamnosus* and *Lactobacillus pentosus* as bacteria, while it includes *Sacchoromyces cerevisiae, Candida tropicalis, Candida glabrata, Geotrichum penicillatum* and *Geotrichum candidum* as yeast (Baschali et al., 2017).

2.3. Tarhana

Tarhana is a traditional product produced by fermentation of dough obtained by using wheat flour or cracked wheat flour and various vegetables (such as tomatoes, red peppers, onions), spices (such as mint, tarhana herb, salt) and yogurt (Özdemir et al., 2020). Tarhana contains many substances such as protein, fat, carbohydrates, iron,

copper, magnesium, calcium, potassium, and sodium (Çekal & Aslan, 2017; Özdemir et al., 2020).

Although the production of tarhana differs locally, it consists of four stages: mixing the ingredients, obtaining dough, fermentation, and drying and grinding (Özdemir et al., 2020). In tarhana production, organic acids, such as lactic acid, succinic acid, and acetic acid, are formed by the effect of LAB in lactic acid fermentation. In addition, in varieties where yeast (*S. cerevisia*) is used in tarhana production, tarhana has both an acidic and sour flavor (Şanlıbaba & Uymaz Tezel, 2019).

Tarhana production can contain microorganisms such as *Lactobacillus plantarum, Lactobacillus brevis, Lactobacillus fermentum, Pediococcus pentosaceus, Pediococcus acidilactici, Leuconostoc mesenteriodes, Leuconostoc pseudomesenteriodes, Leuconostoc citreum, Lactobacillus fabifermentas, Lactobacillus mindensis, Lactobacillus paralimentarius, Lactobacillus alimentarius, Lactobacillus namurensis, Lactobacillus pentosus, Lactobacillus farciminis* and *Lactobasillus casei* (Özdemir et al., 2020).

2.4. Idli

Idli is a traditional Indian rice-based fermented food (Saravanan et al., 2019; Shivangi et al., 2020). It is also consumed in countries such as Sri Lanka, Malaysia and Singapore. Idli is a steamed product known for its characteristic sour taste, spongy texture, and typical aroma. Idli is consumed by those with poor digestion, especially by infants and the elderly (Regubalan & Ananthanarayan, 2019). Idli is a food especially rich in vitamins (especially B-complex vitamin), protein, and calories (Kannan et al., 2015). In addition, it has been reported that there is an increase in free sugar, amino acid, nicotinic acid, methionine and choline contents during the fermentation of idli

dough (Regubalan & Ananthanarayan, 2019).

Microbiota formed in idli fermentation generally contains LAB and yeasts. It is known that idli contains lactic acid bacteria, such as *Lactobacillus brevis, Lactobacilllus lactics, Lactobacillus casei, Leuconostoc mesenteroides, Pediococcus pestosaceus, Pediococcus cerevisiae,* and *Enterococcus faecalis*, and yeasts, such as *Saccharomyces cerevisiae, Debaryomyces hansenii, Candida glabarata, Candida tropicals, Candida fragilola, Hansenula anomala, Torulopsis holmii, Geptrichum candidum* and *Trichosporon beigelli* (Regubalan & Ananthanarayan, 2019).

2.5. Dosa

Dosa is a traditional Indian fermented rice-based, thin and crunchy fermented food, and is also common in Sri Lanka, Malaysia and Singapore (Shivangi et al., 2020). Dosa is obtained by cooking the fermented dough in a thin layer with a small amount of oil in a pan and has a semi-soft and crunchy texture (Devi & Rajendran, 2021). Dosa is traditionally made with rice and black lentils. In the traditional method, rice and lentils are ground with water after soaking, which results in a smooth and consistent dough. The resulting dough is fermented overnight at room temperature. The leavened dough is baked in thin layers on a flat plate that has been greased and heated with a small amount of cooking oil. As a result of the cooking process, circular, semi-soft and crispy dosa is obtained. During dosa fermentation, total acid, free amino acids, vitamins B1 and B2, amylase, proteases, folic acid, amino nitrogen and diol are formed, while an increase is observed in the amount of antimicrobial and antioxidant substances (Ray et al., 2016).

Dosa's low glycemic load and glycemic index help against prediabetic and postdiabetic conditions. In addition, dosa is believed by some people to increase fertility, fetal weight, and breast milk.

While Dosa has enough energy for physical endurance, it is also a suitable vegan product for people with wheat allergy or gluten intolerance (Ray et al., 2016). Dosa includes LAB and yeasts, such as *Lactobacillus fermentum, Streptococcus faecalis, Leuconostoc mesenteroides, Debaryomyces hansenii, Trichosporon beigelli, Bacillus amyoiquefaciens,* and *Saccharomyces cerevisiae*, which are dominant during the fermentation process (Devi & Rajendran, 2021).

2.6. Dhokla

Dhokla is a traditional fermented food native to India (Shivangi et al., 2020). Dhokla is a soft and spongy acid-fermented cake produced from rice and Bengal beans (Ray et al., 2016; Ray et al., 2017), and is usually consumed for breakfast (Ray et al., 2016). Dhokla production begins with the dough, which is obtained by mixing the raw materials, by fermenting overnight at room temperature. Dhokla is obtained by cooking the fermented dough in a steamer in open conditions with a greased tray (Ray et al., 2016). Dhokla contains many components such as carbohydrates, free sugar, dietary fiber, protein, fat, sodium, potassium, calcium, iron, folic acid, and vitamins A and C (Ray et al., 2016). In addition, Dhokla has a low glycemic index, making it beneficial for patients with diabetes (Devi & Shetty, 2020; Ray et al., 2016). It is also known to help manage age-related diseases and degenerative diseases caused by oxidative stress (Devi & Shetty, 2020), reduce blood cholesterol and body weight, and protect from cardiovascular diseases (Ray et al., 2016).

When the microflora of Dhokla was examined, LAB and yeast were detected. Dhokla contains microorganisms such as *Lactobacillus fermentum, Pichia silvicola* (Ray et al., 2016; Ray et al., 2017), *Lactobacillus mesenteroides, Enterococcus faecalis* (*S. faecalis*) (Ray et al., 2016), *Leuconostoc mesenteroides* (Kumari et al., 2015; S. Ray et al., 2017), *Streptococcus faecalis, Torulopsis*

candida, Torulopsis pullulans (Kumari et al., 2015), *Pediococcus pentosaceus,* and *Saccharomyces cerevisiae* (Ray et al., 2017).

2.7. Kishk

Kishk is a fermented food produced with boiled, dried and crushed whole wheat grains (bulgur) and Zeer milk. Kishk is an important food for Egyptians with its taste and cultural value as well as being healthy and natural. Kishk is a food rich in many vitamins, growth factors and other nutrients (Mahmoud et al., 2020). In addition, Kishk is a food rich in starch, fiber, iron and magnesium. Kishk also contains high concentrations of phenylalanine, threonine, isoleucine and lysine (ElAttar et al., 2015). Kishk is produced in summer to be served in winter. Thanks to its low moisture content and acidic pH, Kishk is a safe food against the growth of pathogenic microorganisms (Chedid et al., 2018).

Kishk contains *Lactobacillus plantarum, Lactobacillus casei, Lactobacillus brevis, Bacillus subtilis* and various yeasts during fermentation (Azam et al., 2017). In addition to these, microorganisms such as *Bacillus licheniformis, Bacillus megatherium, Bacillus polymyxa, Bacillus coagulans, Bacillus cereus, Streptococcus thermophilus, Lactobacillus bulgaricus* were also found in Kishk content (Abou-Zeid, 2016).

2.8. Ogi

Ogi is a cereal-based fermented cereal porridge (Farinde, 2015; Ukeyima et al., 2019). Ogi can be made from maize, millet and sorghum (Farinde, 2015). Ogi is traditionally prepared by soaking the grains in cold water for three days, followed by wet grinding and wet sieving. The liquid obtained as a result of filtration is left to settle, the supernatant is added, and Ogi is obtained (Farinde, 2015). Ogi is a weaning food for infants and a breakfast food for children and adults

(Adesulu-Dahunsu et al., 2020; Ukeyima et al., 2019). Ogi is also known by various names such as eko, agidi, akamu, and koko (Ukeyima et al., 2019). Ogi can be consumed alone or together with other foods (Farinde, 2015; Ukeyima et al., 2019). Ogi contains lactic acid bacteria, and various yeasts, such as *Lactobacillus sp*. and *Saccharomyces cerevisiae*, during fermentation (Farinde, 2015).

2.9. Kenkey

Kenkey is a fermented product, which is widely consumed in Ghana, a West African country, and is prepared from fermented corn flour, similar to sour and hard bread (Atter et al., 2015). During Kenkey production, corn kernels are ground by soaking in water for about 2 days, and a dough with approximately 55% moisture content is kneaded. Afterwards, the dough is left to ferment for 2-4 days. Some of the sourdough obtained is made into aflata and mixed with an uncooked dough to obtain a sticky dough, and shaped into balls. The shaped dough is wrapped in leaves and cooked for 3 hours to obtain kenkey (Atter et al., 2015; Oduro-Yeboah et al., 2016). Kenkey is consumed as a ready-to-eat food with other foods due to its shelf life of a few days (Kohajdova, 2017).

As a result of the fermentation of Kenkey dough, LAB and yeasts are mixed. Kenkey contains microorganisms such as *Lactobacillus fermentum, Lactobacillus reuteri, Candida krusei, Saccharomyces cerevisiae, Lactobacillus plantarum, Lactobacillus brevis, Pediococcus pentosaceus, Lactobacillus mesenteroides, Pediococcus acidilactici* and *Geotrichum candidum* (Kohajdova, 2017).

2.10. Mahewu

Mahewu is a corn-based fermented food consumed both as a meal and as a beverage (Olusanya et al., 2020). Mahewu is a sour, non-

alcoholic beverage and is a popular food among the indigenous people of South Africa (Idowu et al., 2016). Mahewu can be consumed by all age groups and as a weaning food for babies. Although Mahewu contains sufficient amounts of protein, carbohydrates, fat, essential vitamins and minerals, it is insufficient in terms of essential amino acids and various micronutrients (Olusanya et al., 2020). Mahewu is prepared by fermenting cooked corn mash with millet or sorghum malt. Mahewu can be produced by uncontrolled fermentation or by adding starter cultures. Cooking the maize porridge in the production process neutralizes the microorganisms in the maize flour and water used, and no heating process is performed to inactivate the microorganisms found in millet or sorghum (Pswarayi & Ganzle, 2019).

The content of Mahewu, a refreshing drink, is usually dominated by LAB bacteria. Studies have found the presence of *Lactobacillus delbrueckii, Lactobacillus plantarum, Streptococcus thermophilus* and *Lactobacillus lactis* in Mahewu (Idowu et al., 2016).

2.11. Pozol

Pozol is a corn-based fermented soft drink native to Mexico. In Pozol production, corn kernels are cooked in approximately 1% lime solution and washed with water. After the washing process, a dough known as nixtamal is formed by grinding. Then, this dough is shaped into balls, wrapped in banana leaves and fermented at room temperature for 0.5 to 4 days. The fermented dough is kept in water, and this water is drunk. Since some fibrous components in the dough are not completely dissolved in this process, there is sediment in the water obtained. In order to reduce this residue, some people apply a second boiling process before the grinding process in production (Kaur et al., 2019; Kohajdova, 2017).

During Pozol fermentation, the presence of many classes of microorganisms, such as lactic acid bacteria, amylolytic lactic acid bacteria, other bacterial classes, yeast, and filamentous fungi, is observed. Although it is known that lactic acid bacteria constitute 90-97% of the microflora, it is known that the dominant species are *Lactobacillus, Streptococcus, Leuconostoc,* and *Weissella* (Ramirez-Guzman et al., 2019).

2.12. Chicha

Chicha is a clear, yellow and sparkling beverage produced from grains such as corn or rice (Grijalva-Vallejos et al., 2020; Pilo et al., 2018). Although the traditional method of chicha production is carried out by chewing and germinating corn, changes have occurred in the raw material and in the applied method over time. Boiling, cooling and fermentation processes are commonly used in Chicha preparation. In addition, optional sugar or various spices are added. Depending on the production method and the raw material used, the alcohol level of Chicha varies between 1% and 12%. Fermentation parameters have not yet been determined in chicha production, and the beverage is consumed when the sweetness is lost and the taste becomes semi-sharp (Grijalva-Vallejos et al., 2020).

Lactic acid bacteria, yeasts and some molds are dominantly observed in chicha fermentation. *Saccharomyces, Candida, Torulaspora, Henseniaspora, Dekkera, Rhodotorula* and *Pichia* are the common yeast varieties in Chicha (Grijalva-Vallejos et al., 2020). In addition, *Laltobacillus, Bacillus, Leuconostoc, Enterococcus, Streptomyces, Enterobacter, Acinetobacter, Escherichia, Cronobacter, Klebsiella, Bifidobacterium* and *Propioniobacterium* are observed in Chicha content (Jyoti P. Tamang et al., 2016).

3. Conclusion

There are many fermented grain products with different regional and ethnic characteristics that countries produce using main agricultural products. These products are developed by the fermentation method, which is based on different grains, and the usefulness, probiotic properties, health effects of foods are consequently increased, and aroma and flavor components are enriched. The number of traditional fermented cereal products bearing traces of different cultures is very large; therefore, limited information was included in this chapter. It is recommended that studies that examine the microbiological composition in the production of cereal-based fermented cereal products in more detail should be conducted in this field in order to contribute to the literature.

References

Abou-Zeid, N. A. (2016). Review of Egyptian Cereal-Based Fermented Product (Kishk). *International Journal of Agriculture Innovations and Research*, 4(4), 600–609.

Achi, O. K., & Ukwuru, M. (2015). Cereal-Based Fermented Foods of Africa as Functional Foods. *International Journal of Microbiology and Application*, 2(4), 71–83.

Adesulu-Dahunsu, A. T., Dahunsi, S. O., & Olayanju, A. (2020). Synergistic Microbial Interactions between Lactic Acid Bacteria and Yeasts During Production of Nigerian Indigenous Fermented Foods and Beverages. *Food Control*, 110, 106963.

Aila, R., Alim, A., Mahemuti, A., & Kelimu, A. (2020). Separation, Purification and Identification of Excellent Yeasts from the Natural Fermented Beverage of Boza. *Journal of Food and Nutrition Research*, 8(9), 450–458.

Akçelik, N., & Akçelik, M. (2019). Gıda Fermantasyonlarında Rol

Oynayan Mikroorganizmalar. R. E. Anlı & P. Şanlıbaba içinde, *Fermente Gıdalar: Mikrobiyoloji, Teknoloji ve Sağlık*, pp. 9–35.

Al-sahlany, S. T. G., Altemimi, A. B., Al-Manhel, A. J. A., Niamah, A. K., Lakhssassi, N., & Ibrahim, S. A. (2020). Purification of Bioactive Peptide with Antimicrobial Properties Produced by Saccharomyces cerevisiae. *Foods*, 9(3), 324.

Ali, J. B., Ek-Sisy, T. T., & Abdel-Salam, A. F. (2020). Impacts of Adding Rye, Sorghum and Their Mixtures on the Quality of Untraditional Egyptian Kishk. *European Journal of Nutrition and Food Safety*, 12(2), 56–72.

Anonymous. (2012). *Türk Gıda Kodeksi Ekmek ve Ekmek Çeşitleri Tebliği (Tebliğ No: 2012/2).* Mevzuat Bilgi Sistemi. accessed on 09.08.2021 https://www.mevzuat.gov.tr/Metin.Aspx?MevzuatKod=9.5.15746&MevzuatIliski=0&sourceXmlSearch=ekmek#

Arslan, S., Durak, A. N., Erbaş, M., Tanrıverdi, E., & Gulcan, U. (2015). Determination of Microbiological and Chemical Properties of Probiotic Boza and Its Consumer Acceptability. *Journal of the American College of Nutrition*, 34(1), 56–64.

Ashaolu, T. J., & Reale, A. (2020). A Holistic Review on Euro-Asian Lactic Acid Bacteria Fermented Cereals and Vegetables. *Microorganisms*, 8(8), 1176.

Atter, A., Ofori, H., Anyebuno, G. A., Amoo-Gyasi, M., & Amoa-Awua, W. K. (2015). Safety of a Street Vended Traditional Maize Beverage, Ice-Kenkey, in Ghana. *Food Control*, 55, 200–205.

Azam, M., Mohsin, M., Ijaz, H., Tulain, U. R., Ashraf, M. A., Fayyaz, A., Abadeen, Z. Ul, & Kamran, Q. (2017). Lactic Acid Bacteria in Traditional Fermented Asian Foods. *Pakistan Journal of Pharmaceutical Sciences,* 30(5), 1803–1814.

Bahgaat, W. K., & Ghani, S. A. El. (2017). Comparison of Amino Acids and Fatty Acids Profiles of Egyptian Kishk: Dried Wheat Based Fermented Milk Mixture as Functional Food. *American Journal of Food Technology*, 12(1), 43–50.

Baschali, A., Tsakalidou, E., Kyriacou, A., Karavasiloglou, N., & Matalas, A.-L. (2017). Traditional Low-alcoholic and Non-alcoholic Fermented Beverages Consumed in European Countries: A Neglecter Food Group. *Nutrition Research Reviews*, 30, 1–24.

Bhalla, T. C., & Savitri. (2017). Yeasts and Traditional Fermented Foods and Beverages. T. Satyanarayana & G. Kunze (eds) Yeasts Diversity in Human Welfare, pp. 53–82.

Blandino, A., Al-Aseeri, M. E., Pandiella, S., Cantero, D., & Webb, C. (2003). Cereal-based fermented foods and beverages. *Food Research International*, 36, 527–543.

Chedid, M., Tawk, S. T., Chalak, A., Karam, S., & Hamadeh, S. K. (2018). The Lebanese Kishk: A Traditional Dairy Product in a Changing Local Food System. *Journal of Food Research*, 7(5), 16–23.

Çekal, N., & Aslan, B. (2017). Gastronomik Bir Değer Olarak Tarhana ve Coğrafi İşaretlemede Tarhananın Yeri ve Önemi. *Güncel Turizm Araştırmaları Dergisi*, 1(2), 124–135.

Çelik, İ., Işık, F., & Yılmaz, Y. (2016). Effect of Roasted Yellow Chickpea (Leblebi) Flour Addition on Chemical, Rheological and Sensory Properties of Boza. *Journal of Food Processing and Preservation*, 40(6), 1400–1406.

Devi, P. B., & Shetty, P. H. (2020). Traditional Preserved and Fermented Foods and Their Nutritional Aspects. Prakash J., Waisundara V. & Prakash V. (eds) Nutritional and Health Aspects of Food in South Asian Countries, pp. 61–73.

Devi, P. B., & Rajendran, S. (2021). Impact of Starter Culture on

Nutraceutical and Functional Properties of Underutilized Millet-Legume Co-Fermented Indian Traditional Product. *LWT - Food Science and Technology*, 149, 111818.

ElAttar, A., Shehata, E., Awad, S., & Nawar, M. (2015). Physico-Chemical Properties of Homemade and Market Egyptian Laban Zeer and Kishk Samples, 12th Egyptian Conference of Dairy Science and Technology.

Farinde, E. O. (2015). Chemical and Sensory Properties of Sieved and Unsieved Fortified "Ogi.". *Nature and Science*, 13(1), 49–53.

Grijalva-Vallejos, N., Aranda, A., & Matallana, E. (2020). Evaluation of Yeasts from Ecuadorian Chicha by Their Performance as Starters for Alcoholic Fermentations in the Food Industry. *International Journal of Food Microbiology*, 317, 108462.

Idowu, O., Fadahunsi, I. F., & Onabiyi, O. (2016). Production and Nutritional Evaluation of Mahewu: A Non-Alcoholic Fermented Beaverage of South Africa. *International Journal of Research in Pharmacy and Biosciences,* 3(6), 27–33.

Iskakowa, J., Smanalieva, J., & Methner, F.-J. (2019). Investigation of Changes in Rheological Properties During Processing of Fermented Cereal Beverages. *Journal of Food Science and Technology*, 56(9), 3980–3987.

Kannan, D., Chelliah, R., Rajamanickam, E. V., Venkatraman, R. S., & Antony, U. (2015). Fermented Batter Characteristics in Relation with the Sensory Properties of Idli. *Croatian Journal of Food Technology, Biotechnology and Nutrition*, 10(1–2), 37–43.

Karaçıl, M. Ş., & Acar Tek, N. (2013). Dünyada Üretilen Fermente Ürünler: Tarihsel Süreç ve Sağlık ile İlişkileri. *Uludağ Üniversitesi Ziraat Fakültesi Dergisi*, 27(2), 163–173.

Karademir, E., Karasu Yalçın, S., & Yalçın, E. (2018). Tahıl ve Bakliyat Esaslı Gıdalarda Fermantasyon İşleminin Besinsel Özellikler ve Biyoaktif Bileşenler Üzerine Etkisi. *Gıda*, 43(1), 163–173.

Karahan Çakmakçı, A. G., Sağlam, H., & Çakmakçı, M. L. (2020). Endüstriyel Mikroorganizmalar. Erkmen O., Erten H. & Sağlam H. (eds) Fermente Ürünler Teknolojisi ve Mikrobiyolojisi, pp. 33–65.

Kaur, P., Ghoshal, G., & Banerjee, U. C. (2019). Traditional Bio-Preservation in Beverages: Fermented Beverages. Grumezescu A. & Holban A. M. (eds) Preservatives and Preservation Approaches in Beverages, pp. 69–113.

Kışla, D., & Hancıoğlu Sıkılı, Ü. (2020). Boza Üretimi. Erkmen O., Erten H. & Sağlam H. (eds) Fermente Ürünler Teknolojisi ve Mikrobiyolojisi, pp. 499–510.

Kohajdova, Z. (2017). Fermented Cereal Products. A. Pandey, M. A. Sanroman, G. Du, C. R. Soccol & C. Dussap içinde, Current Developments in Biotechnology and Bioengineering, pp. 91–117.

Kumari, S., Guleria, P., & Dangi, N. (2015). Cereal Based Beverages and Fermented Foods: A Review. *International Journal of Enhanced Research in Science, Technology and Engineering*, 4(10), 134–145.

Kumral, A. (2015). Nutritional, Chemical and Microbiological Changes During Fermentation of Tarhana Formulated with Different Flours. *Chemistry Central Journal*, 9(1), 16.

Mahmoud, E. A., Abd-Alla, A.-E. A., & Salman, K. H. (2020). Utilization of Cinnamon, Clove and Thyme Essential Oils as Antimicrobial and Bioactive Compounds in Kishk Manufacturing. *Journal of Food Sciences; Suez Canal University*, 7(1), 43–54.

Menis-Henrique, M. E. C., Scarton, M., Piran, M. V. F., & Clerici, M. T. P. S. (2020). Cereal Fiber: Extrusion Modifications for Food Industry. *Current Opinion in Food Science*, 33, 141–148.

Oduro-Yeboah, C., Mestres, C., Amoa-Awua, W., Fliedel, G., Durand, N., Matignon, B., Michodjehoun, V. L., Saalia, F. K., Sakyi-Dawson, E., & Abbey, L. (2016). Stepping Time and Dough Fermentation Affect the Milling Behaviour and Quality of White Kenkey (nsiho), a Sour Stiff Dumpling Prepared from Dehulled Maize Grains. *Journal of Cereal Science*, 69, 377–382.

Olusanya, R. N., Kolanisi, U., Onselen, A. van, Ngobese, N. Z., & Siwela, M. (2020). Nutritional Composition and Consumer Acceptability of Moringa Oleifera Leaf Powder (MOLP)-Supplemented Mahewu. *South African Journal of Botany*, 129, 175–180.

Özdemir, N., Şimşek, Ö., & Çon, A. H. (2020). Tarhana Üretimi. Erkmen O., Erten H. & Sağlam H. (eds) Fermente Ürünler Teknolojisi ve Mikrobiyolojisi, pp. 531–547.

Perez-Torrado, R., Gonzalez, S. S., Combina, M., Barrio, E., & Querol, A. (2015). Molecular and Enological Characterization of a Natural Saccharomyces uvarım and Saccharomyces cerevisia hybrid. *International Journal of Food Microbiology*, 204, 101–110.

Pilo, F. B., Carvajal-Barriga, E. J., Guaman-Burneo, M. C., Portero-Barahona, P., Dias, A. M. M., Freitas, L. F. D. de, Gomes, F. de C. O., & Rosa, C. A. (2018). Saccharomyces cerevisiae Populations and Other Yeasts Associated with Indigenous Beers (Chicha) of Ecuador. *Brazilian Journal of Microbiology*, 49, 808–815.

Pswarayi, F., & Ganzle, M. G. (2019). Composition and Origin of the

Fermentation Microbiota of Mahewu, a Zimbabwean Fermented Cereal Beverage. *Applied and Environmental Microbiology*, 85(15), e03130-18.

Ramirez-Guzman, K. N., Torres-Leon, C., Martinez-Medina, G. A., Rosa, O. de la, Hernandez-Almanza, A., Alvarez-Perez, O. B., Araujı, R., Gonzalez, L. R., Londono, L., Ventura, J., Rodriguez, R., Martinez, J. L., & Aguilar, C. N. (2019). Traditional Fermented Beverages in Mexico. Grumezesvu A. M. & Holban A. M. (eds) Fermented Beverages, pp. 605–635.

Ray, M., Ghosh, K., Singh, S., & Mondal, K. C. (2016). Folk to Functional: An Explorative Overview of Rice-Based Fermented Foods and Beverages in India. *Journal of Ethnic Foods*, 3(1), 5–18.

Ray, S., Saha, R., Raychaudhuri, U., & Chakraborty, R. (2017). Characterization and Analysis of Dhokla with Incorporated Tomato Powder. *Nutra Foods*, 16, 223–229.

Regubalan, B., & Ananthanarayan, L. (2019). Investigation of Biogenic Amines Content in Fermented Idli Batter During Storage. *Journal of Food Science and Technology*, 56(4), 1775–1784.

Saleh, A. S. M., Wang, P., Wang, N., Yang, S., & Xiao, Z. (2019). Technologies for Enhancement of Bioactive Components and Potential Health Benefits of Cereal and Cereal-Based Foods: Research Advances and Application Challenges. *Critical Reviews in Food Science and Nutrition*, 59(2), 207–227.

Saravanan, C., Kavitake, D., Kandasamy, S., Devi, P. B., & Shetty, P. H. (2019). Production, Partial Characterization and Antioxidant Properties of Exopolysaccharide α-D-glucan produced by Leuconostoc lactis KC117496 Isolated from an Idli Batter. *Journal of Food Science and Technology*, 56(1), 159–166.

Shivangi, S., Devi, P. B., Ragul, K., & Shetty, P. H. (2020). Probiotic Potential of Bacillus Strains Isolated from an Acidic Fermented Food Idli. *Probiotics and Antimicrobial Proteins*, 12, 1502–1513.

Şanlıbaba, P., & Uymaz Tezel, B. (2019). Tarhana. Anlı R. E. & Şanlıbaba P. (eds) Fermente Gıdalar: Mikrobiyoloji, Teknoloji ve Sağlık, pp. 543–552.

Tamang, Jyoti P., Watanabe, K., & Holzapfel, W. H. (2016). Review: Diversity of Microorganisms in Global Fermented Foods and Beverages. *Microbiology of Fermented Foods and Beverages*, 7.

Tamang, Jyoti Prahash (Ed.). (2016*).* Ethnic Fermented Foods and Alcoholic Beverages of Asia.

Ukeyima, M. T., Acham, I. O., & Awojide, C. T. (2019). Quality Evaluation of Ogi from Acha (Digitaria exilis), Soybean (Glycine max) and Carrot (Daucus carota L.) Composite Flour. *Asian Journal of Biotechnology and Bioresource Technology*, 5(2), 1–11.

Ünüvar, Ş. (2008). Ekmek ve Ekmek Çeşitleri Üretim Teknolojisi (Fırıncı Meslek Eğitimi). Savaş Kitap ve Yayınevi.

Vergi, H. (2020). *Ekmek İsrafında Tüketici Tercihlerinin Rolü: Bingöl İli Örneği.* Yüksek Lisans Tezi. Sosyal Bilimler Enstitüsü, İşletme Anabilim Dalı, Üretim Yönetimi ve Pazarlama Bilim Dalı, Bingöl Üniversitesi.

Walker, G. M., & Stewart, G. G. (2016). Saccharomyces cerevisiae in the Production of Fermented Beverages. *Beverages*, 2(4), 30.

CHAPTER IX

ENZYME CATALYZED BIOREMEDIATION IN FOOD INDUSTRY

Oya Irmak SAHIN

(Asst. Prof. Dr) Yalova University, Chemical Engineering Department, Yalova, Turkey

E-mail: isahin@yalova.edu.tr

Orcid: 0000-0003-2225-7993

1. Introduction

Currently, world's industrialization is progressively growing. Wastes from several industries including food, textiles, plastics and other petrochemicals are affecting the quality of life due to the pollution of water, soil, food and weather (Okino-Delgado et al., 2019). For the last 40 years, accelerated expansion and technological improvement of industries become a speeding up problem for the environment. Although many contaminant of these industries are responsible for this environmental problem, pesticides and fertilizers are the major sources (Thassitou & Arvanitoyannis, 2001).

Food industry wastes have gained importance in recent years and have been attracted by many environmental, social and economic authorities. Food waste (FW) is either edible or non-edible residual that is generated in any step of the food processing: manufacturing, storing, transporting and post-consumer (Bilal & Iqbal, 2019; Carmona-Cabello et al., 2018). At preharvest step many food losses

can occur due to climate impacts and pest infestations. It can be divided (Table 1) as avoidable and unavoidable. Also, European Union in 2003 described another classification for FW;

- Class 1: High risk to be incinerated
- Class 2: Materials unfit for human consumption
- Class 3: Material which is fit for but not destined for human consumption

Food supply chain wastes are generated during harvesting and processing stage, usually due to technological changes involving increased modernization, equipment faults and novel processing techniques (Kosseva, 2013). FW can be either liquid or solid waste, and 40% of the total municipal waste is FW (Tiwari et al., 2013). Approximately 90 million tons FW are generated from the food processing industry every year (Bilal & Iqbal, 2019). Nutrient composition of food waste is affecting the waste processing and management type. FWs exhibit variety of pH, composition diversity and different but high biological oxygen demand (BOD) and chemical oxygen demand (COD).

Table 1. Classification of FW according to Lebersorger and Schneider (Lebersorger & Schneider, 2011)

Classification	**Sources**
Non avoidable	Preparation residues
Possibly avoidable	Preparation residues
	Leftovers
Avoidable	Whole unused food
	Partly consumed food

As the food wastes have high water and nutritional content (Table 2), they provide microorganism contamination which will cause an urgent and serious environmental problem. Especially untreated FWs gas generation problems become more destructive than the greenhouse gases CO_2.

Because food processing processes involve many stages and because of the changing content of food, food waste is very difficult to recycle or process. Huge amount of waste that is generated during all "farm to fork", needs to be treated by advanced and effective waste management systems (Punnagaiarasi et al., 2017).

Bioremediation is a naturally occurring transforming process in which microorganisms or their enzymes involved, environmental pollutants or contaminants into harmless, non-noxious products (Thassitou & Arvanitoyannis, 2001). It represents an important environmental remediation strategy because it:

- harnesses naturally occurring biological processes,
- destroys or immobilises contaminants rather than transfers them from one environmental medium to another,
- saves financial resources due to shortened clean-up times and/or lower capital expenditures compared to many other remediation technologies.

Table 2. Food waste nutrient composition (Escamilla-Alvarado et al., 2014; Kobayashi et al., 2012; Kwon & Lee, 2004; Ohkouchi & Inoue, 2006; Pan et al., 2008; Van Dyk et al., 2013; Vavouraki et al., 2013; Wang et al., 2008)

FW composition according to food chain steps							
Dry Weight (%)	*Fruit & Vegetable*	*Oil*	*Cereal*	*Dairy*	*Meat*	*Fish*	
Pre-consumer	48	2	14	6	3	1	
Post-consumer	21	2	52	12	6	1	
Dry Weight (%)	*Carbohydrate*	*Fat*	*Protein*	*Starch*	*Hemicellulose*	*Cellulose*	*Lignin*
Potato waste	100			100			
Apple waste	48.1				24.4	7.2	23.5
Grape waste			6.1		21.0	30.3	17.4
Olive waste	31.0		24.0		26.8	36.4	26.0
Cherry waste					10.7	12.0	
Sugar beet waste			10.8		28.1	27.4	3.1
Food processing waste	10.2		4.05	7.06		41.2	
Food processing waste	19.1		19.10	15.6		2.26	
Food processing waste			6.62		21.7		9.2
Kitchen garbage	16.0	18.02	15.56			16.9	
Food processing waste	31.0	14.0	16.90	24.0	7.7		17.0

2. Enzymes

Enzymes in bioremediation have enormous potential for food industry as well as other industries. They have significant potential in waste management and developing the green environment. The potential advantages of enzymatic treatment as compared with conventional treatments include application to recalcitrant materials, operation at high and low contaminant concentrations.

For the last decades, enzymes are the most popular biocatalysts for the agro-industrial waste management and the food waste valorisation, with other industries. This increasing demand for enzymes creates new technological applications for enzyme applications and itself. Therefore, as Beniwal and Sharma (2014) dedicated the worldwide market for enzymes has increased threefold form 2008 to 2016.

As the food processing industry has its own classification; "*Fruit and Vegetable, Meat, Poultry and Fish, Oil, Dairy, Fermentation and Brewing*", enzymes that are used for the bioremediation of these processing departments' wastes are differs. Enzymes are classified as shown in Fig. 1, and mainly EC 1 and EC 3 are used as a biocatalyst for valorization.

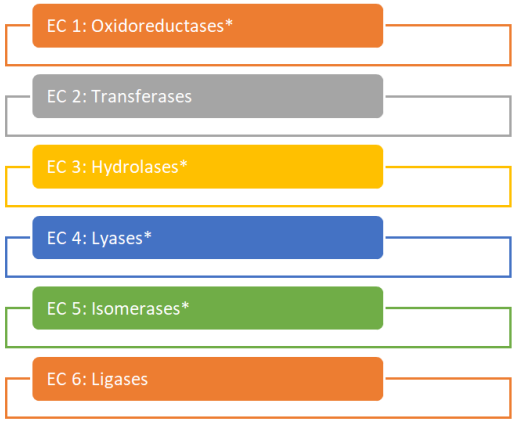

Figure 1. Classification of enzymes with their class names (*mostly used enzyme classes in food waste valorisation)

Treatments with oxidoreductases (oxygenase and peroxidase), oxidases (laccase) and hydrolases (protease and lipase) are the innovator enzymes for bioremediation. They are responsible for the transforming of phenols, aromatic hydrocarbons and amines, chlorinated compounds to simple and less reactive substances.

2.1. Oxidoreductases (EC 1)

They are the enzymes that catalyse electron transfer by oxidation-reduction reactions, and usually uses NADP as coenzyme. These enzymes can be produced by fungi, bacteria and higher plants, and capable to degrade pollutants, their toxic and heavy metal loads.

Oxygenases (EC 1.13, EC 1.14), as understood from the name, are catalyses the oxygen transfer, from molecular oxygen to an organic or an inorganic substrate with the coenzymes FAD, NADP. Their classes are named as the number of oxygen atoms used during oxidation, which EC 1.13 as monooxygenases and EC 1.14 as dioxygenases (Karigar & Rao, 2011). The degradation and detoxification mechanisms are going through with hydroxylation, dehydrogenation, cyclization, etc. (Okino-Delgado et al., 2019). Aromatic compounds (such as phenols) (Chakraborty et al., 2014), halogenated compounds (herbicides, fungicides, pesticides) (Sivaperumal et al., 2017), chlorinated compounds and aliphatic hydrocarbons (Okino-Delgado et al., 2019) are degraded by oxygenases.

Monooxygenases act on alkanes, fatty acids and aliphatic and aromatic hydrocarbons. Desulfurization, dehalogenation, denitrification, and hydroxylation are the mechanisms used by the enzyme. *Bacillus megaterium* BM3 is the main producer for monooxygenases (Karigar & Rao, 2011).

Laccases (EC 1.10) are a broad family of multicopper oxidases and can be obtained from higher plants and fungi. It

oxidizes polyphenols, methoxy-substituted phenols, diamines, polyamines and a considerable range of other compounds as well as some inorganic ions, except tyrosine.

The use of laccase has potential applications in bioremediation of food industry wastewater, especially act on lignin, cellulose and amin-contained wastes. Olive oil mill wastewaters can be treated with laccase to oxidize different phenolic compounds in it (Berrio et al., 2007; Osma et al., 2010).

Beyond these enzymes, peroxidases (EC 1.11) and glucose-oxidases (EC 1.1) are also used for the bioremediation of food wastes.

2.2. Hydrolases (EC 3)

This enzyme class hydrolysis the reaction of transferring functional groups to water. This transfer reactions benefit the toxicity reduction of organophosphate components like pesticides and herbicides (Beniwal & Sharma, 2014). Hydrolases act on chemical bonds of esters, peptides and carbons. This type of remediation is advantageous compared to other non-enzymatic treatments, for its safe, economical and controllable properties.

Amylases (EC 3.2) are one of the most important and a wide range of an enzyme group which is the 25% of the industrial enzyme market (Cotârleţ et al., 2011). *Streptomyces* sp. and *Bacillus* sp. are the sources for amylases with the fungi *Aspergillus* sp. α-amylases (EC 3.2.1.1), β-amylases (EC 3.2.1.2), glucoamylases (EC 3.2.1.3), isoamylases (EC 3.2.1.68) and pullulans (EC 3.2.1.41) are responsible for the hydrolysing glycosidic bonds simple starch and carbohydrate compounds to produce amylose and oligosaccharides. Mainly in vegetable processing wastewater treatments are carried out with this enzyme group.

Lipases (EC 3.1.1.3) are also named as, triacylglycerol acyl hydrolases, are the enzymes that hydrolyse and synthesise of fatty acids, esters and glycerides (Kumar et al., 2014). Generally, they are used to treat oil wastes for modifying the fatty acid chains and reducing the toxicity of the cooked-oil wastes (Okino-Delgado et al., 2019). Lipases from *Pseudomonas* sp. and *Aspergillus* sp. and *Penicillium* sp. are the most popular microbial lipases.

Proteases (EC 3.4.21.12) are present in all living microorganisms, plants and animals (Kuddus et al., 2013) mainly from marine sources. They are multifunctional enzymes that hydrolysis the peptide bonds and also catalyses the amide and esters synthesize reactions. They have a 60% worldwide enzyme market demand. Proteases have been utilised for being able to reduce pathogen counts, reduce the solids content, and increase deflocculation in sludge. They are classified as endopeptidases and exopeptidases (Fig.2)

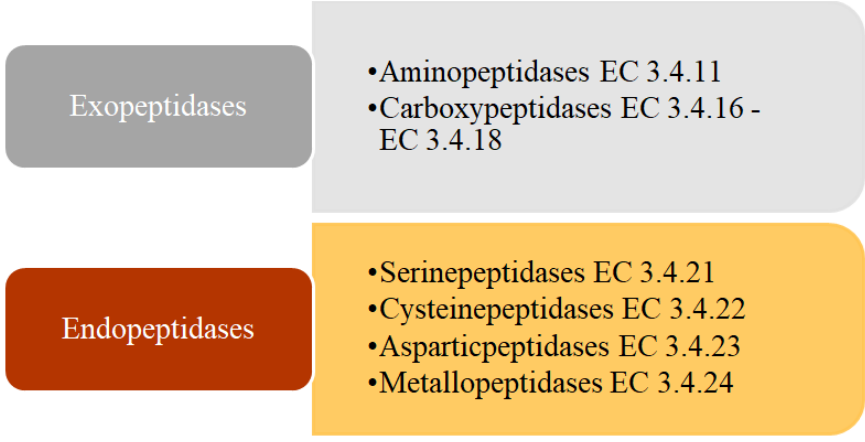

Figure 2. Classification and class numbers of proteases

2.3. Lyases (EC 4)

Lyases are catalyse the addition or removal of the elements of water (hydrogen, oxygen), ammonia (nitrogen, hydrogen), or carbon dioxide (carbon, oxygen) at double bonds. Especially the enzyme decarboxylase (EC 4.1.1) is used for the hydrolysis of the organic acids in FW.

2.4. Isomerases (EC 5)

Isomerases are a general class of enzymes that convert a molecule from one isomer to another. Isomerases facilitate intramolecular rearrangements in which bonds are broken and formed.

Glucose isomerase, which is also known as xylose isomerase (EC 5.3.1.5) is an enzyme that catalyses the interconversion of $_{D}$-xylose and $_{D}$-xylulose. It has a wide range of sources, including microorganisms, such as bacteria, fungi and actinomycetes, as well as plants and animals. Glucose isomerase is a key enzyme in the industrial production of high fructose corn syrup and fuel ethanol.

3. Enzymatic Valorization of FW

Valorization of FW as animal feed is the oldest and most known technique. On the other hand, various biological materials can be generated from FW using free or immobilized enzymes. Route for the valorization of several types of FW are shown in Fig 3.

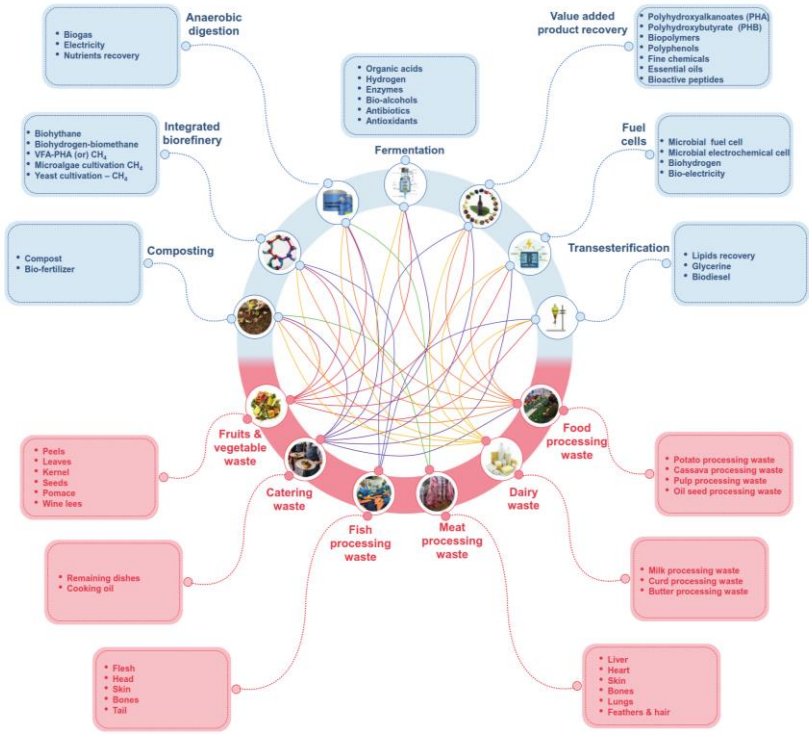

Figure 3. Type of FW and their valorization route (Banu et al., 2020)

3.1. Production of Polyhydroxy butyrate

Poly(3-hydroxybutyrate) (PHB) belongs to the group of polyhydroxyalkanoates (PHAs), which is a microbial short-chain polymer that is synthesised by more than 75 different bacteria (Reddy et al., 2003). This biopolymer is 100% biodegradable and nontoxic and has chemical properties compatible with polypropylene (Akpinar-Bayizit et al., 2010). Many valorization applications of FW types for PHB production is shown in Table 3.

3.2. Production of Biodiesel

Biodiesel is a biological product of transesterification of oil, lipid and grease wastes, transforming triglycerides into glycerol and fatty acids

by the enzyme “lipase” used as catalyst. Glycerol from cooked oil wastes, reacts with the catalyst lipase, to form fatty acid alkyl esters (biodiesel) and alcohol as by-product. This conversion is a sustainable and environmentally friendly process.

FW from spent coffee grounds using microbial lipase, biodiesel has been generated with an efficiency of 96% (Banerjee et al., 2013; Karmee et al., 2018). In these research solid-state and batch fermentations has been applied.

Starch-rich FW also is a good resource for biodiesel production, amylase from *Saccharomyces cerevisiae* in a solid-state fermenter has been degraded carbohydrates with a biodiesel efficiency of 93.86% (Yan et al., 2011).

3.3. Production of Bioethanol

Bioethanol, like biodiesel, is a biological alcohol generated during the microbial fermentation from carbohydrate-rich FWs. During this production, cellulase, hemicellulose and invertase are used as catalyst of the cellulose and sucrose hydrolysis by the breakdown of 1,4-β-glycosidic bonds. Under aerobic conditions this hydrolysis process produces ethanol. Many bioethanol productions from many FWs at different compositions were studied (Table 4).

3.4. Valorization by fermentation

Fermentation process is a metabolic system in which usually simple carbohydrates are converted to organic acids, alcohols and/or gases. So far, many researches and industrial applications have been made for the valorization of FW by fermentation for the products lactic acid, sweeteners, ethanol, butanol, PHB and some prebiotics (Moon et al., 2009; Pan et al., 2008; Uçkun Kiran & Liu, 2015; Wolf et al., 2018; Yan et al., 2011).

Table 3. Different FW sources for PHB production

FW type	Bioremediation Technique	Enzyme	Enzyme source	Application of enzyme	Ref.
Bakery waste and Seawater	Batch fermentation	Glucoamylase Protease	*Halomonas boliviensis*	Hydrolysis of carbohydrate and proteins	(Pleissner et al., 2014)
Whey	Fed-batch fermentation	Lactase	*E.coli CML3-1*	Lactose breakdown	(Pais et al., 2014)
Kitchen waste	Batch fermentation	Decarboxylase	*Cupriavidus necator CCGUG 52238*	Organic acid hydrolysis	(Omar et al., 2011)
Restaurant waste	Batch fermentation	Decarboxylase Oxidase	*E.coli pnDTM2*	Organic acid hydrolysis	(Eshtaya et al., 2012)
Pea shells	Batch fermentation	Protease	*Bacillus cereus EGU3*	Protein breakdown	(Ghate et al., 2011)

Table 4. Different FW sources for bioethanol production

FW type	Bioremediation Technique	Enzyme	Enzyme source	Application of enzyme	Ref.
Household wastes	Liquefaction	Amylolytic, Glycolytic enzymes	*Saccharomyces cerevisiae*	Sugar compounds hydrolysis	(Matsakas & Christakopoulos, 2015)
Grain processing wastes	Solid-state fermentation	Invertase	*Dry yeast*	Sugar compounds hydrolysis	(Moukamnerd et al., 2013)
Kitchen wastes	Batch fermenter	Glucose oxidase, pectinase, α-amylase	*Aspergillus sp.* *S. cerevisiae*	Sugar compounds hydrolysis	(Moon et al., 2009)
Restaurant wastes	Batch fermenter	Amylase Protease	*Candida sp.* *S. cerevisiae*	Sugar and protein hydrolysis	(Hafid et al., 2016)
Household wastes	Batch fermenter	Cellulase Hemicellulase	*Myceliophthora thermophila*	Cellulose degradation	(Matsakas & Christakopoulos, 2015)
Mixed food wastes	Solid-state fermentation	Cellulase, Hemicellulase, invertase	*Aspergillus sp.* *S. cerevisiae*	Cellulose, Xylene, Pectin degradation	(Uçkun Kiran & Liu, 2015)

The process mechanism is proceeded as, the choosing of microorganism that suitable to grow fast and controllable at the FW (FW is used as a feedstock) for the targeted enzyme desired to be produced. Then the microorganism synthesizes the targeted enzyme and the targeted enzyme hydrolyse or degrade the FW. This process can also use for the new enzyme production as well (Ushani et al., 2020).

The immobilization of enzymes is used to improve stability and extend the life of the enzyme, to work in a wide range of environmental conditions. The immobilization of an enzyme effectively changes the environment it is exposed to and therefore make it reactive at different temperatures and pH conditions than when not immobilized. These benefits have made them highly applicable to a range of evolving biotechnologies (Omay, 2014).

For the dairy processing wastes, enzyme-catalysed lactose transformation is a significant process. Even the lactose is not a valuable sweetener compared to sucrose, lactose-rich wastes can be a valuable resource for the enzymatic conversion of other sweeteners. For this conversion β-$_D$-galactosidase and glucose isomerase are used for the hydrolysis of lactose to glucose (Gennari et al., 2018; Panesar et al., 2018; Wolf et al., 2018).

Galactooligosaccharides (GOS) are known as the most important prebiotics. Enzyme catalysed transformation of lactose to GOS is a profound issue in food industry. For this transformation immobilized β-galactosidase enzyme is used in a continuous packed-bed reactor (Ushani et al., 2020). Dairy processing wastes, especially whey, conversion to GOS by glass or silica nanoparticles immobilized β-galactosidase increase the GOS production efficiency two-three times (Banjanac et al., 2016; Eskandarloo & Abbaspourrad, 2018).

Besides the lactose transformation to sweeteners or GOS, transglycosidation to" lactulose and lactosucrose" is also an important enzyme catalysed valorisation. Lactulose is a disaccharide formed from D-galactose and fructose, and a result of the transformation of lactose-rich wastes by β-galactosidase. It is a prebiotic substance that strengthens the growth of bifidobacteria and lactobacilli and metabolised by bacterial enzymes to short chain fatty acids mainly lactic and acetic acid as well as methane and hydrogen. This effect leads to a decrease of the pH-value and an increase of the osmotic pressure in the colon (Bilal & Iqbal, 2019).

Lactosucrose is a trisaccharide composed of glucose, galactose and fructose. Also, via enzyme-catalysed reactions (transfructosylation) of lactose and sucrose, it can be produced. Lactosucrose is used as a functional food, low-calorie, ingredient because it's indigestible in the human digestive tract and therefore low in calories(Bilal & Iqbal, 2019).

4. Conclusion

Food industry is a wide source of environmental pollutant which is a profound issue for the public. Its generated waste is determined by the factors of consumer population, consumption patterns and also the production seasons. Fruit and vegetable processing, dairy processing and meat, poultry and fish processing industries are the most waste generated parts of food industry. On the other hand, although these industries are generated huge amount of waste, these wastes are an important resource for the valuable compounds that can be recovered from.

Valorization of FW using the right technique can enhance the economical outputs in food industry. It is also believed to be a useful tool for environmental policies of food processing waste management all over the world.

This chapter is a brief of food waste and its composition, with the valorization of these wastes by enzyme catalysed reactions. Valorization of FW is also a part of bioremediation process, which is naturally occurring by microorganisms and their enzymes to valuable, safe products. Herein, numerous enzymes, used in food industry waste management either for free of immobilized, which involved in the production of biofuels, biogases, bioplastics (PHA, PHB) and functional food ingredients such as prebiotics and sweeteners.

Immobilized enzymes are the most attractive and efficient catalysts for the bioremediation of FWs, because of immobilization provides a continuous conversion of wastes. However, waste management and enzyme catalysed waste management need to be developed furthermore.

References

Akpinar-Bayizit, A., Ozcan, T., Sahin, O. I., & Yilmaz-Ersan, L. (2010). The utilisation of microbial poly-hydroxy alkanoates (PHA) in food industry. *RESEARCH JOURNAL OF BIOTECHNOLOGY*, *5*(3), 76–79.

Banerjee, A., Singh, V., Solanki, K., Mukherjee, J., & Gupta, M. N. (2013). Combi-protein coated microcrystals of lipases for production of biodiesel from oil from spent coffee grounds. *Sustainable Chemical Processes*, *1*(1), 14. https://doi.org/10.1186/2043-7129-1-14

Banjanac, K., Carević, M., Ćorović, M., Milivojević, A., Prlainović, N., Marinković, A., & Bezbradica, D. (2016). Novel β-galactosidase nanobiocatalyst systems for application in the synthesis of bioactive galactosides. *RSC Advances*, *6*(99), 97216–97225. https://doi.org/10.1039/C6RA20409K

Banu, J. R., Kumar, G., Gunaskaran, M., & Kavitha, S. (2020). *Food waste to valuable resources: Applications and management*. Academic Press.

Beniwal, V., & Sharma, A. K. (2014). *Industrial Enzymes: Trends, Scope and Relevance*. Nova Science Publishers, Incorporated.

Berrio, J., Plou, F. J., Ballesteros, A., Martínez, Á. T., & Martínez, M. J. (2007). Immobilization of *pycnoporus coccineus* laccase on Eupergit C: Stabilization and treatment of olive oil mill wastewaters. *Biocatalysis and Biotransformation*, *25*(2–4), 130–134. https://doi.org/10.1080/10242420701379122

Bilal, M., & Iqbal, H. M. N. (2019). Sustainable bioconversion of food waste into high-value products by immobilized enzymes to meet bio-economy challenges and opportunities – A review. *Food Research International*, *123*, 226–240. https://doi.org/10.1016/j.foodres.2019.04.066

Carmona-Cabello, M., Garcia, I. L., Leiva-Candia, D., & Dorado, M. P. (2018). Valorization of food waste based on its composition through the concept of biorefinery. *Current Opinion in Green and Sustainable Chemistry*, *14*, 67–79. https://doi.org/10.1016/j.cogsc.2018.06.011

Chakraborty, J., Jana, T., Saha, S., & Dutta, T. K. (2014). Ring-Hydroxylating Oxygenase database: A database of bacterial aromatic ring-hydroxylating oxygenases in the management of bioremediation and biocatalysis of aromatic compounds. *Environmental Microbiology Reports*, *6*(5), 519–523. https://doi.org/10.1111/1758-2229.12182

Cotârleţ, M., Negoiţă, T. Gh., Bahrim, G. E., & Stougaard, P. (2011). Partial characterization of cold active amylases and proteases of Streptomyces sp. From Antarctica. *Brazilian Journal of Microbiology*, *42*(3), 868–877.

https://doi.org/10.1590/S1517-83822011000300005

Escamilla-Alvarado, C., Ponce-Noyola, M. T., Poggi-Varaldo, H. M., Ríos-Leal, E., García-Mena, J., & Rinderknecht-Seijas, N. (2014). Energy analysis of in-series biohydrogen and methane production from organic wastes. *International Journal of Hydrogen Energy*, *39*(29), 16587–16594. https://doi.org/10.1016/j.ijhydene.2014.06.077

Eshtaya, M. K., Nor 'Aini, A. R., & Hassan, M. A. (2012). Bioconversion of restaurant waste into Polyhydroxybutyrate (PHB) by recombinant E. coli through anaerobic digestion. *International Journal of Environment and Waste Management*, *11*(1), 27–37. https://doi.org/10.1504/IJEWM.2013.050521

Eskandarloo, H., & Abbaspourrad, A. (2018). Production of galacto-oligosaccharides from whey permeate using β-galactosidase immobilized on functionalized glass beads. *Food Chemistry*, *251*, 115–124. https://doi.org/10.1016/j.foodchem.2018.01.068

Gennari, A., Mobayed, F. H., Volpato, G., & de Souza, C. F. V. (2018). Chelation by collagen in the immobilization of Aspergillus oryzae β-galactosidase: A potential biocatalyst to hydrolyze lactose by batch processes. *International Journal of Biological Macromolecules*, *109*, 303–310. https://doi.org/10.1016/j.ijbiomac.2017.12.088

Ghate, B., Pandit, P., Kulkarni, C., Mungi, D. D., & Patel, T. S. (2011). PHB production using novel agro-industrial sources from different Bacillus species. *International Journal of Pharma and Bio Sciences*, *2*(3). https://www.cabdirect.org/cabdirect/abstract/20113339900

Hafid, H. S., Rahman, N. A., Shah, U. K. M., Baharudin, A. S., & Zakaria, R. (2016). Direct utilization of kitchen waste for

bioethanol production by separate hydrolysis and fermentation (SHF) using locally isolated yeast. *International Journal of Green Energy*, *13*(3), 248–259. https://doi.org/10.1080/15435075.2014.940958

Karigar, C. S., & Rao, S. S. (2011). Role of Microbial Enzymes in the Bioremediation of Pollutants: A Review. *Enzyme Research*, *2011*, 1–11. https://doi.org/10.4061/2011/805187

Karmee, S. K., Swanepoel, W., & Marx, S. (2018). Biofuel production from spent coffee grounds via lipase catalysis. *Energy Sources, Part A: Recovery, Utilization, and Environmental Effects*, *40*(3), 294–300. https://doi.org/10.1080/15567036.2017.1415394

Kobayashi, T., Xu, K.-Q., Li, Y.-Y., & Inamori, Y. (2012). Evaluation of hydrogen and methane production from municipal solid wastes with different compositions of fat, protein, cellulosic materials and the other carbohydrates. *International Journal of Hydrogen Energy*, *37*(20), 15711–15718. https://doi.org/10.1016/j.ijhydene.2012.05.044

Kosseva, M. R. (2013). Chapter 3—Sources, Characterization, and Composition of Food Industry Wastes. In M. R. Kosseva & C. Webb (Eds.), *Food Industry Wastes* (pp. 37–60). Academic Press. https://doi.org/10.1016/B978-0-12-391921-2.00003-2

Kuddus, M., Singh, P., Thomas, G., & Al-Hazimi, A. (2013). Recent Developments in Production and Biotechnological Applications of C-Phycocyanin. *BioMed Research International*, *2013*. https://doi.org/10.1155/2013/742859

Kumar, V., Punesh Sangwan, Dharmendra Singh, & Prabhjot Kaur Gill. (2014). *Global scenario of industrial enzyme market*. https://doi.org/10.13140/2.1.3599.0083

Kwon, S.-H., & Lee, D.-H. (2004). Evaluation of Korean food waste composting with fed-batch operations I: Using water extractable total organic carbon contents (TOCw). *Process Biochemistry*, *39*(10), 1183–1194. https://doi.org/10.1016/S0032-9592(03)00233-4

Lebersorger, S., & Schneider, F. (2011). Discussion on the methodology for determining food waste in household waste composition studies. *Waste Management*, *31*(9), 1924–1933. https://doi.org/10.1016/j.wasman.2011.05.023

Matsakas, L., & Christakopoulos, P. (2015). Ethanol Production from Enzymatically Treated Dried Food Waste Using Enzymes Produced On-Site. *Sustainability*, *7*(2), 1446–1458. https://doi.org/10.3390/su7021446

Moon, H. C., Song, I. S., Kim, J. C., Shirai, Y., Lee, D. H., Kim, J. K., Chung, S. O., Kim, D. H., Oh, K. K., & Cho, Y. S. (2009). Enzymatic hydrolysis of food waste and ethanol fermentation. *International Journal of Energy Research*, *33*(2), 164–172. https://doi.org/10.1002/er.1432

Moukamnerd, C., Kawahara, H., & Katakura, Y. (2013). Feasibility Study of Ethanol Production from Food Wastes by Consolidated Continuous Solid-State Fermentation. *Journal of Sustainable Bioenergy Systems*, *3*(2), 143–148. https://doi.org/10.4236/jsbs.2013.32020

Ohkouchi, Y., & Inoue, Y. (2006). Direct production of l(+)-lactic acid from starch and food wastes using Lactobacillus manihotivorans LMG18011. *Bioresource Technology*, *97*(13), 1554–1562. https://doi.org/10.1016/j.biortech.2005.06.004

Okino-Delgado, C. H., Zanutto-Elgui, M. R., do Prado, D. Z., Pereira, M. S., & Fleuri, L. F. (2019). Enzymatic Bioremediation: Current Status, Challenges of Obtaining

Process, and Applications. In P. K. Arora (Ed.), *Microbial Metabolism of Xenobiotic Compounds* (pp. 79–101). Springer. https://doi.org/10.1007/978-981-13-7462-3_4

Omar, F. N., Norrsquo, Rahman, A. A., Hafid, H. S., Mumtaz, T., Yee, P. L., & Hassan, M. A. (2011). Utilization of kitchen waste for the production of green thermoplastic polyhydroxybutyrate (PHB) by Cupriavidus necator CCGUG 52238. *African Journal of Microbiology Research*, *5*(19), 2873–2879. https://doi.org/10.5897/AJMR11.156

Omay, D. (2014). Immobilization of lipase onto a photo-crosslinked polymer network: Characterization and polymerization applications. *Biocatalysis and Biotransformation*, *32*(2), 132–140. https://doi.org/10.3109/10242422.2014.894027

Osma, J. F., Toca-Herrera, J. L., & Rodríguez-Couto, S. (2010). Uses of Laccases in the Food Industry. *Enzyme Research*, *2010*, 1–8. https://doi.org/10.4061/2010/918761

Pais, J., Farinha, I., Freitas, F., Serafim, L. S., Martínez, V., Martínez, J. C., Arévalo-Rodríguez, M., Auxiliadora Prieto, M., & Reis, M. A. M. (2014). Improvement on the yield of polyhydroxyalkanotes production from cheese whey by a recombinant Escherichia coli strain using the proton suicide methodology. *Enzyme and Microbial Technology*, *55*, 151–158. https://doi.org/10.1016/j.enzmictec.2013.11.004

Pan, J., Zhang, R., El-Mashad, H. M., Sun, H., & Ying, Y. (2008). Effect of food to microorganism ratio on biohydrogen production from food waste via anaerobic fermentation. *International Journal of Hydrogen Energy*, *33*(23), 6968–6975. https://doi.org/10.1016/j.ijhydene.2008.07.130

Panesar, P. S., Kaur, R., Singh, R. S., & Kennedy, J. F. (2018). Biocatalytic strategies in the production of galacto-

oligosaccharides and its global status. *International Journal of Biological Macromolecules*, *111*, 667–679. https://doi.org/10.1016/j.ijbiomac.2018.01.062

Pleissner, D., Lam, W. C., Han, W., Lau, K. Y., Cheung, L. C., Lee, M. W., Lei, H. M., Lo, K. Y., Ng, W. Y., Sun, Z., Melikoglu, M., & Lin, C. S. K. (2014, July 20). *Fermentative Polyhydroxybutyrate Production from a Novel Feedstock Derived from Bakery Waste* [Research Article]. BioMed Research International; Hindawi. https://doi.org/10.1155/2014/819474

Punnagaiarasi, A., Elango, A., Rajarajan, G., & Prakash, S. (2017). Application of Bioremediation on Food Waste Management for Cleaner Environment. In M. Prashanthi, R. Sundaram, A. Jeyaseelan, & T. Kaliannan (Eds.), *Bioremediation and Sustainable Technologies for Cleaner Environment* (pp. 51–56). Springer International Publishing. https://doi.org/10.1007/978-3-319-48439-6_5

Reddy, C. S. K., Ghai, R., Rashmi, & Kalia, V. C. (2003). Polyhydroxyalkanoates: An overview. *Bioresource Technology*, *87*(2), 137–146. https://doi.org/10.1016/S0960-8524(02)00212-2

Sivaperumal, P., Kamala, K., & Rajaram, R. (2017). Bioremediation of Industrial Waste Through Enzyme Producing Marine Microorganisms. *Advances in Food and Nutrition Research*, *80*, 165–179. https://doi.org/10.1016/bs.afnr.2016.10.006

Thassitou, P. K., & Arvanitoyannis, I. S. (2001). Arvanitoyannis, bioremediation: A novel approach to food waste management. Trends Food Sci. *Technol.,* 185–196.

Tiwari, B. K., Norton, T., & Holden, N. M. (Eds.). (2013). *Sustainable Food Processing*. John Wiley & Sons, Ltd. https://doi.org/10.1002/9781118634301

Uçkun Kiran, E., & Liu, Y. (2015). Bioethanol production from mixed food waste by an effective enzymatic pretreatment. *Fuel*, *159*, 463–469. https://doi.org/10.1016/j.fuel.2015.06.101

Ushani, U., Sumayya, A. R., Archana, G., Rajesh Banu, J., & Dai, J. (2020). Chapter 10—Enzymes/biocatalysts and bioreactors for valorization of food wastes. In J. R. Banu, G. Kumar, M. Gunasekaran, & S. Kavitha (Eds.), *Food Waste to Valuable Resources* (pp. 211–233). Academic Press. https://doi.org/10.1016/B978-0-12-818353-3.00010-9

Van Dyk, J. S., Gama, R., Morrison, D., Swart, S., & Pletschke, B. I. (2013). Food processing waste: Problems, current management and prospects for utilisation of the lignocellulose component through enzyme synergistic degradation. *Renewable and Sustainable Energy Reviews*, *26*, 521–531. https://doi.org/10.1016/j.rser.2013.06.016

Vavouraki, A. I., Angelis, E. M., & Kornaros, M. (2013). Optimization of thermo-chemical hydrolysis of kitchen wastes. *Waste Management*, *33*(3), 740–745. https://doi.org/10.1016/j.wasman.2012.07.012

Wang, Q., Ma, H., Xu, W., Gong, L., Zhang, W., & Zou, D. (2008). Ethanol production from kitchen garbage using response surface methodology. *Biochemical Engineering Journal*, *39*(3), 604–610. https://doi.org/10.1016/j.bej.2007.12.018

Wolf, M., Gasparin, B. C., & Paulino, A. T. (2018). Hydrolysis of lactose using β-d-galactosidase immobilized in a modified Arabic gum-based hydrogel for the production of lactose-

free/low-lactose milk. *International Journal of Biological Macromolecules*, *115*, 157–164. https://doi.org/10.1016/j.ijbiomac.2018.04.058

Yan, S., Li, J., Chen, X., Wu, J., Wang, P., Ye, J., & Yao, J. (2011). Enzymatical hydrolysis of food waste and ethanol production from the hydrolysate. *Renewable Energy*, *36*(4), 1259–1265. https://doi.org/10.1016/j.renene.2010.08.020

CHAPTER X

A REVIEW ON NON-DESTRUCTIVE TESTING METHODS FOR ENGINEERING MATERIALS

Aziz Barış BAŞYİĞİT[1] & Engin ERGÜL[2] & Halil İbrahim KURT[3] & [4]Necip Fazıl YILMAZ

[1] *(Asst. Prof. Dr.) Materials Science and Engineering Department, Engineering Faculty, Kırıkkale University,*
e-mail: abbasyigit@kku.edu.tr
Orcid: 0000-0003-1544-3747

[2] *(Dr.) Mechanical Department, Izmir Vocational High School, Dokuz Eylul University, e-mail: engin.ergul@deu.edu.tr*
Orcid: 0000-0003-3347-5400

[3] *(Assoc. Prof. Dr.) Materials Science and Engineering Department, Engineering Faculty, Gaziantep University,*
e-mail: hikurt@gantep.edu.tr
Orcid: 0000-0002-5992-8853

[4] *(Prof. Dr.) Mechanical Engineering Department, Engineering Faculty, Gaziantep University, e-mail: nfyilmaz@gantep.edu.tr*
Orcid: 0000-0002-0166-9799

1. Introduction

Engineering materials are increasingly demanded by various industries. These materials consist mainly of metals and their alloys, ceramics, polymers and composites (Vlack, 1994; Kurtz et.al., 1998). As these materials are widely used in

engineering applications especially in automotive, aviation and defense industries, bridges etc. the service life of these materials must be taken into account carefully for technical reliability considerations. These materials can have various types of defects originating from raw material itself or arising after an operation such as welding, heat treating, coating, machining, forging and forming as simply defined by irregularities, discontinuities or flaws that can be used interchangeably meaning the same. Hence the confirmations of these materials that are free from such defects have to be provided by accredited types of testing methods. These methods are basically divided in two groups as destructive and non-destructive testing methods. By applying non-destructive tests, parts can be used without any performance losses throughout the material however after applying destructive tests they cannot be used again. The quality of products or mechanical parts depends on many factors such as design criteria, raw material properties and fabrication methods. The defects that exist in industrial parts have to be detected before the service conditions for technical security and human life considerations. Detection of these defects or discontinuities is essential to provide an acceptable or satisfactory level of production quality. Hence there are needs of detecting such these defects in materials without affecting their performance of usage.

Non destructive testing (NDT), non destructive evaluation (NDE) and non destructive inspection (NDI) are the expressions to identify the methods about determining the properties of materials and detecting the discontinuities and detrimental defects without damaging the materials engineering properties. However there are various approaches about defining NDT, NDE and NDI. Testing is commonly defined as ‘determining the properties of a substance and to exhibit a given characteristic when subjected to a test’ whether the evaluation is explained by examining and judging carefully; also

expressed in ASTM E-1316 as 'a review following interpretation of the indications noted, to determine whether they meet specified acceptance criteria'. Inspection is also described as examination. Nevertheless these three terms refer approximately the same meanings in industrial applications (Hellier, 2003; ASM Vol.17, 1997). Non destructive testing is seriously important about the quality control of the finished products and throughout the several phases of semi finished parts during manufacturing processes. NDT methods can also be used for predicting the remaining life of industrial parts. As compared with destructive tests there are some limitations, advantages and disadvantages about non destructive testing. The comparison is summarized in Table 1 (Raj et.al., 2002).

Table 1: Comparison of destructive and non-destructive test methods

Destructive Tests	***Non-destructive tests***
● The results are more reliable and precise	● Reliability needs verification by another method (or methods)
● Commonly quantitative measurements	● Usually qualitative measurements but sometimes quantitative test results
● Relation can be easily established directly between measurements and material properties	● Experience is needed for making relation between results and material properties
● Tests are not applied directly on parts but only on representative samples or materials	● Tests can safely be applied directly on original parts
● A test method can only measure just one or a little amount of material properties	● A test method can measure various types of material properties
● Testing while in service is not possible	● Testing during service is possible
● Samples cannot be re-tested	● Samples can be tested again many times
● Test sample preparation is expensive and time consuming	● Test sample preparation is usually rapid and inexpensive

There are many non-destructive testing methods for investigating defects that applied on materials and industrial mechanical parts (Ida and Meyendorf, 2019; Omar, 2012). However, only a few of these

methods are applied on materials commercially. Traditionally widespread techniques consist of Magnetic Particle Testing (MT or MPT), Penetrant Testing (PT), Ultrasonic Testing (UT), Radiographic Testing (RT), Visual Testing (VT) and Eddy-Current Testing (ET). Some of these methods are applied very quickly, practically and easily while some of them are much more complicated. Another grouping is made by detection of discontinuities that exists on only surface and/or inner regions of the inspected samples. Generally; MT, PT, VT and ET methods investigate surface and near surface defects while RT and UT focuses on inner type defects (Dwivedi S.K. et.al, 2018; ASM Handbook Vol. 17, 1997).

However developing technology produces new and advanced investigation methods for non-destructive testing. (Omar, 2012; Ida and Meyendorf, 2019). These methods are used in various industries (Schabovicz, 2019; Pecur, 2009; Peta, 2018). But in order to maintain safe, reliable and validated test results, non destructive testing methods have to be verified by accredited independent parts of organizations worldwide. Hence PT, VT, MT, UT, RT and ET tests are accredited via standard documents including personnel training, application, test acceptance and reject criterias (ASTM E165, 2018; ASTM A802, 2019, ASTM E1444, 2016; ASTM E1001, 2016; ASTM E1742, 2018; ASTM A309, 2016).

2. Basic NDT Methods

2.1. Visual Testing

Visual testing (or inspection) is the most widespread and firstly used method among the other non-destructive tests due to its easiness, fast results and low costs (Hellier, 2003). Visual testing has to be applied firstly whether using with supplementary non destructive testing methods for preventing unnecessary expenses.

Visual testing can determine flaws, defects that exist directly upon the surface of the investigated materials. Therefore the method cannot reveal the inside defects in materials. Method uses at least a healthy naked human eye and adequate amount of light in order to determine defects. When naked eye is insufficient; magnifier is frequently preferred as given in Figure 1-(a). However with the support of the recent developments in visual inspection technology such as high resolution cameras, borescopes and endoscopes, results become more reliable and faster (ASM Handbook Vol. 17, 1997; Raj et al., 2002).

Common application areas include;

(a) Surface flaws, discontinuities, defects, cracks, general view of paints, coatings, welding regions especially tears, porosities, excess weld areas
(b) Inspection of inner bore regions of complicated geometrical shaped parts via endoscopes or borescopes
(c) Surface corrosion, erosion and fracture behavior of materials
(d) Controlling the leakage of pressure vessels and complex assembly systems

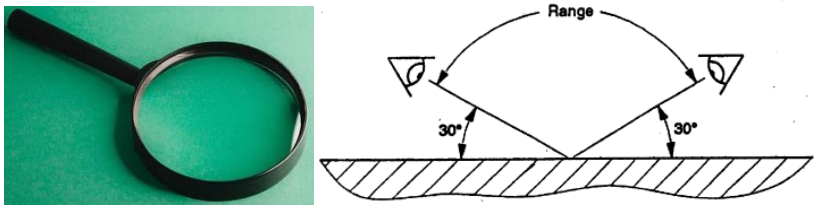

(a) (b)

Figure 1: (a) magnifier (b) examination angles

Operators must consider the standard documents that regulate their own test conditions. Minimum 30 degrees of examination angle must be adjusted as shown in Figure 1-(b). Surface cleanliness is very important in VT. Rust, oil, scale and any kind of dirt must be

removed from the surface of the tested material for more correct results.

Visual inspection is not advised to be replaced with other NDT methods. When direct visual inspections cannot be made, sophisticated optical instruments can often be used to provide remote viewing of critical areas (Paul, 2005).

The basic limitation of visual testing is the access problem. Operator has to reach the investigation area and get the discontinuities easily revealed by the eyes.

Basic test operation order

Pre-cleaning
Drying if necessary
Investigation for defects and marking
Reporting

2.2. Penetrant Testing

Penetrant testing method reveals the surface discontinuities that just open to the surface of the nonporous materials by making a colorful florescent or paint contrast by filling the vacancies. The method is not productive on porous materials so that porosities can be misdefined like a surface discontinuity resulting incorrect test reports. (Raj et al., 2002) Basic test operation arrangement is schematically given in Figure 2.

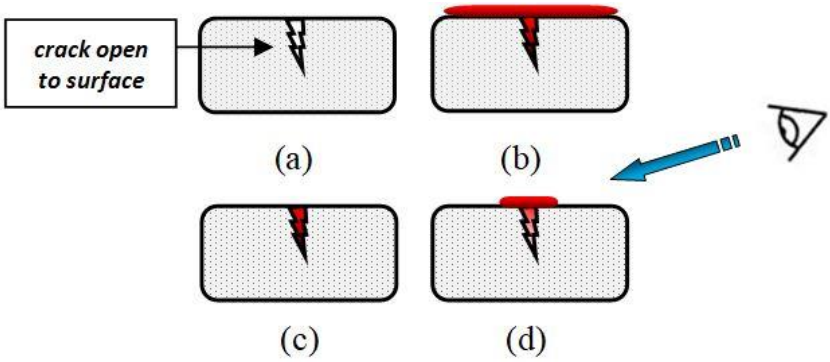

Figure 2: Schematic view of penetrant testing (a) defect open to surface (b) penetrant application throughout the surface (c) excess penetrant cleaned (d) developer application takes out the penetrant from the crack and provides easily inspection by eyes

Basic test operation order

Pre-cleaning for surface preparation
Drying (if necessary)
Penetrant (dye or fluorine type) application
Waiting for a while depending on type of the inspected material
Draining
Developer application
Waiting for a while depending on type of the inspected material
Investigation for defects and marking
Reporting and final cleaning (ASM Handbook Vol. 17, 1997; Raj et al., 2002).

PT method is examined in two groups as fluorine light and dye penetrant inspection. The main difference is using fluorine instead of dye paint types hence ultraviolet light is used. The fluorine light penetrant method is more sensitive in revealing defects as compared to dye penetrant method (ASM Handbook Vol. 17, 1997; Raj et al., 2002).

In case of applying fluorine PT the ambient lighting amplitude (darkness) must be smaller than 50 lux value, whether in paint PT this value has to be minimum 500 lux.

Common application temperatures must be between +5 and +50, -16 and +52 celsius degrees due to the possible decomposition of chemical agents depending on the ASTM and EN standards that used in tests (ASTM E165, 2018; ASTM E1417, 2016; EN ISO 3452-1, 2013). Whether the temperature of the parts to be inspected is out of this range, special type of penetrant test chemicals have to be used. The reliability of tests should be verified by the standard certified reference blocks.

In penetrant testing, irregularity type can be bigger in size or on the contrary in fact little than seems from outside in PT as given in Figure 3-a, b, c and d. This is a serious problem for reliable testing. However some types of deep and/or closed flaws cannot be detected that given in Figure 3-e.

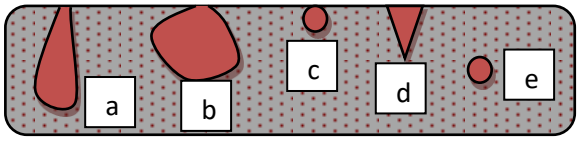

Figure 3: Flaw types in Penetrant Testing

2.3. Magnetic Particle Testing

MT or MPT is a method for detecting the surface or near subsurface flaws due to the fact that when the ferromagnetic material or part under the test is magnetized, magnetic discontinuities that lay throughout a direction that transverse to the magnetic field causing a leakage in magnetic field. This leakage in magnetic field resulted in revealing the location of the possible flaws. A mixture of ferromagnetic powder, liquid carrier, paint or fluorine and anti corrosion material is used during the test for occupying the flaws by the help of the magnetic field.

Non-ferromagnetic materials like aluminum, magnesium, lead, titanium, copper and their alloys, austenitic stainless steels cannot be inspected by MT. These types of materials have to be inspected with alternative methods such as VT, PT or ET (ASM Handbook Vol. 17, 1997). An efficient magnetic particle inspection can only be done whether the relative magnetic permeability of a tested material is greater than 100 μr value.

The flaws that exist in a depth of maximum 0.2 mm from the surface of parts with minimum dimensions of 1x10μm can be safely detected by MT. The elongation of a discontinuity must be transverse to the direction of magnetic field lines to be detected as given in Figure 4-a and b.

Optimum flaw detection angle is 90 degrees (right angle) away from the surface normal according to the magnetic field line directions. The flaws that exist up to 30 degrees away from the surface normal cannot be efficiently detected. Whether testing an alloy that has two or more types of phases or structures by MT, one of the phases have to satisfy adequate magnetization ability otherwise it cannot be inspected by MT.

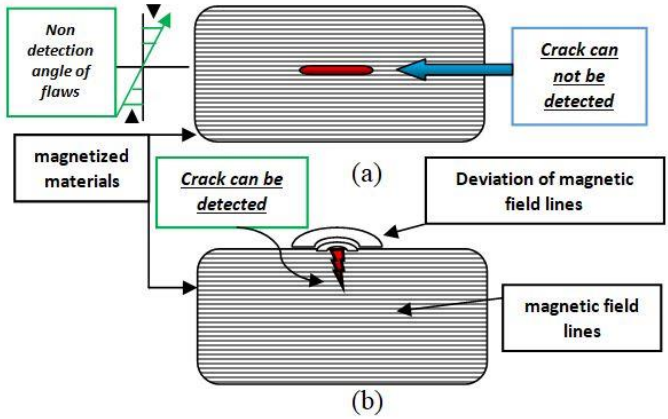

Figure 4: Schematic view of magnetic particle testing.

MT can be applied in two ways as fluorine and paint tests. Fluorine MT is more sensitive than paint MT for detecting smaller size flaws and ultraviolet light is used. In case of applying fluorine MT the ambient lighting amplitude (darkness) must be smaller than 50 lux value, whether in paint MT, this value has to be minimum 500 lux.

Basic test operation order

Pre-cleaning

Demagnetization due to previous possible magnetizing operations such as welding, machining, heat treating etc. if needed,

Magnetization according to material type and depth of flaws,

Spraying the mixture of iron powder, carrier fluid, fluorine or paint, anti-corrosion material to inspected parts during magnetization,

Proceeding to magnetization minimum 2 seconds after spraying operation finishes,

Investigation for defects and marking,

Reporting,

Demagnetization,

Final cleaning.

Magnetization of parts can be applied by 4 common ways depending on applicability;

- hand yoke (portable method)
- magnetizing coil
- directly magnetizing
- combined methods.

The iron powder that used in MT varies with average grain size depending on flaw size. Three different average size types of magnetizable iron powder can be applied.

Fine type ($d \leq 8\mu m$)

Middle type ($8<d<16\mu m$)

Coarse type ($d\geq16\mu m$)

Decreasing average grain size results in detecting smaller sizes of flaws and testing becomes more sensitive.

Both direct and alternating currents are used in MT. Direct current is used when possible deeper located flaws need to be investigated. Alternating current is preferred when shallow located flaws within parts are in concern. However AC current type is more sensitive to surface flaw detection as compared to DC currents (ASM Handbook Vol. 17, 1997; Raj et al., 2002).

2.4. Ultrasonic Testing

UT can be applied on various types of materials whether metallic or non metallic. UT is efficient especially in detecting internal (volumetric) flaws but at the present time by using special designed instruments and probes, near surface defects of materials can also be detected. Access from one side of the material is adequate for testing. Sound frequencies of more than 20 kHz are used in testing but typical values are between 1 to 10MHz in many industrial applications.

In UT, sound beam is transmitted from a specific sound generating probe directly to test material. The probe includes a crystal having a piezo-electrical property that is capable of transforming the electrical energy into the mechanical energy and also mechanical energy into the electrical energy reciprocally.

Each industrial material has ability for sound waves to let travelling throughout themselves depending on materials physical and chemical specific properties such as chemical composition, density, crystal structure, hardness etc. The sound velocities of materials are constant whether physical or chemical properties are also kept constant. If a sound wave encounters a discontinuity in a

material that means a void, the velocity of sound wave changes too. The difference in sound velocity that refers to travel speed can be detected by ultrasonic testing instrument so that operator can be sure whether flaws existing or not in tested material. Ultrasonic testing can provide quantitative data about the sizes of discontinuities and locations very precisely. Ultrasonic testing instrument and screen view of method is given in Figure 5. The definition 'back echo' means the full thickness of the tested material and 'flaw echo' means the depth of discontinuity from the surface of the material.

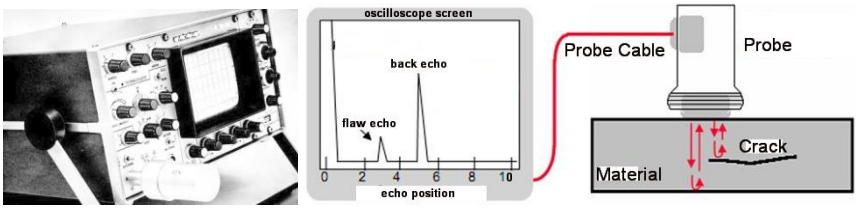

Figure 5: Ultrasonic testing instrument and screen view

Ultrasonic transducers (probes) are classified in two main groups: normal and angle probes as given in Figure 6. In normal probes; ultrasonic sound is transferred at a direct angle to test piece whether in angle probe it is transferred by a desired angle according to the discontinuities angles in materials.

Normal probes produce longitudinal sound waves while angle probes produce transverse waves. Longitudinal waves travel generally faster than transverse waves throughout the same material. All probes must be in good contact with the tested materials for better viewing results (ASM Handbook Vol. 17, 1997; Raj et al., 2002).

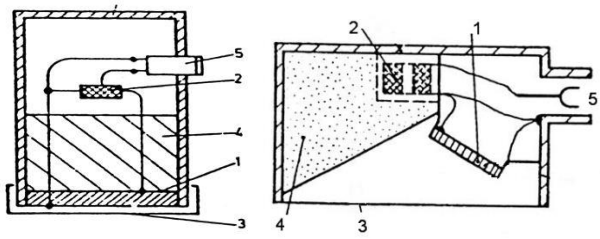

(a) (b)

Figure 6: Ultrasonic probes; (a) normal probe, (b) angle probe
1: crystal, 2: coil, 3: protective cover, 4: damping material, 5: connector

Ultrasonic inspection methods

There are two types of ultrasonic inspection methods commonly named as pulse-echo and through-transmission methods. In pulse-echo testing; there is only one probe that acts both as a transmitter and a receiver in single crystal. In through-transmission method; there are two separate probes opposing each other having two different crystals, one of them acting as a transmitter so that it generates ultrasonic sounds while the other probe receives sounds and converts into the electrical signals for ultrasonic test estimations.

The location and sizes of discontinuities can be precisely determined in pulse-echo method while it cannot be displayed and estimated in through-transmission method. Through-transmission method is preferred especially in materials that weaken the sound travelling ability such as plastic based materials and composites etc. but accessing the opposite two sides of tested material is needed (ASM Handbook Vol. 17, 1997; Raj et al., 2002).

Ultrasonic inspection is highly operator dependent. The reliability of results is related to operators' skills, experience and also calibration quality. The testing instrument has to be calibrated according to related standard documents and material type to be tested. Standard certified calibration blocks with abbreviations of K_1

and K_2 are used according to agreements between parties (EN ISO 2400, 2013).

There have been also new developments in Ultrasonic Testing asserted by scientists like laser generated ultrasonic testing. The technique uses low cost, completely non-contact type probes providing high precision especially where traditional piezoelectric ultrasonic probes are hard to apply (Luo S.T. et.al., 2011; Hass K. et.al.; 2019).

2.5. Radiographic Inspection

The basis of the RT method depends on using of short wavelength electromagnetic radiations like *x* or gamma rays while focused on objects, after the penetration due to the absorbance of rays by the material the remaining radiations pass throughout the test piece and results in casting an image on a recording media located behind the object named as a film.

The image density differences or contrast of images on the film proves there are flaws or not in correspondence to matrix views. Schematic view of radiographic inspection is given in Figure 7.

The sizes of images are always greater than the real flaw sizes in consequence of the distances between the radiation source and the tested material physically.

Whether a flaw exists in tested material, its image will form on the film media. The greater volume of the flaw means the darker contrast regions of the image.

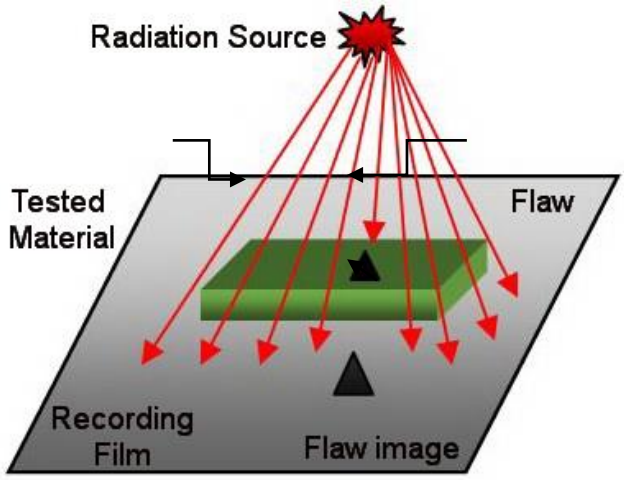

Figure 7: Schematic explanation of radiographic inspection.

Radiation sources

X-rays

X-rays are short-wave length electromagnetic waves (Brandes E.A and Brook G.B, 1992). They are frequently used for structure determination and the study of defects (Cahn R.W and Haasen P.,1996). X-rays are produced by x-ray tubes depending on their power defined in terms of kilo Volts.

X-ray tubes consist of a glass bulb inside the vacuum media and electrodes for electrical current emitting electrons from one side to target plate. Acceleration of electrons to target plate results in formation of x-rays and they are focused by optical instruments for transferring outside of the x-ray tubes directly on testing materials.

Electrical energy is used in x-ray tubes so that it is practically safer when they shut down no radiation danger occur. X-ray tubes need a professional cooling system for heating problems arising from electron bombardments on target plates.

450kV powered x-ray tube is adequate for testing many types of materials up to satisfactory thicknesses.

Gamma rays

Radiography by gamma rays presents a practical way of application, compactness, free from electrical power, however the most important incident is, the method should be so much dangerous to living things when precautions are not well taken into account by responsible staff.

Gamma rays are generated from a few kinds of radioisotopes that previously produced in a nuclear reactor. Commonly there are 4 widespread radioisotopes preferred in industrial radiography. The power densities and half life of radioisotopes play important roles on selection of them.

Radioisotopes are selected according to type and thickness of the tested material. The main properties of radioisotopes used in industrial radiography are summarized in Table 2.

Table 2: Types of gamma ray isotopes

Feature	***Cobalt-60***	***Iridium-192***	***Caesium-137***	***Thulium-170***
Half Life	5.27 years	74.3 days	30.1 years	129 days
Energy value (MeV)	1.33-1.17	0.3-0.6	0.66	0.08-0.05
Test piece maximum thickness (steel-mm)	200	75	100	10
Source thickness (mm)	10	30	75	50

Radiographic imaging

The efficiency of radiographic imaging depends on a few factors.

a. Source spot size must be as smaller as possible.
b. The distance between the testing object and radiation source must be as large as possible.
c. The radiograph film should be as closer as possible to testing object.
d. Radiation source should be located without missing scanning the whole part.

Image quality indicators (penetrameters) are used for testing whether the test parameters are correct or not in radiographic inspection. There are many types of penetrameters prepared according to the tested materials due to the standard documents.

Radiographic inspection techniques

● ***Single wall-single image technique***

This technique is preferred whether the material can be reached from two sides of plates, cylinders and large diameter pipes. There are two possibilities; the radiation source is located inside or outside of the tested object as given in Figure 8. Panoramic technique can also be applied in this technique by locating the radiation source in the central of the hollow sample allowing 360 degrees of imaging at one time.

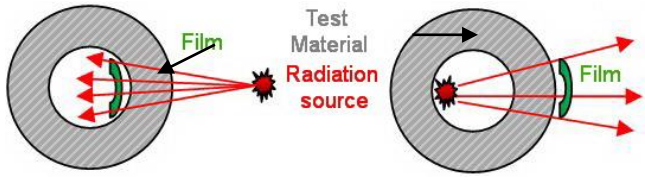

(a) (b)

Figure 8: Single wall single image method, radiation source is located (a) outside (b) inside of the tested sample

● Double wall penetration technique

This method is preferred especially when there is no access to parts inner sides. Double wall penetration technique is applied in three different ways as double wall with single and double images and super-imposing image. These methods are illustrated in Figure 9.

Double wall-single image

The radiation source is located very close to test piece as given in Figure 9-a. Close regions cannot be tested. Only film side can be imaged effectively. This technique is applied to the pipes with diameters more than 90mm.

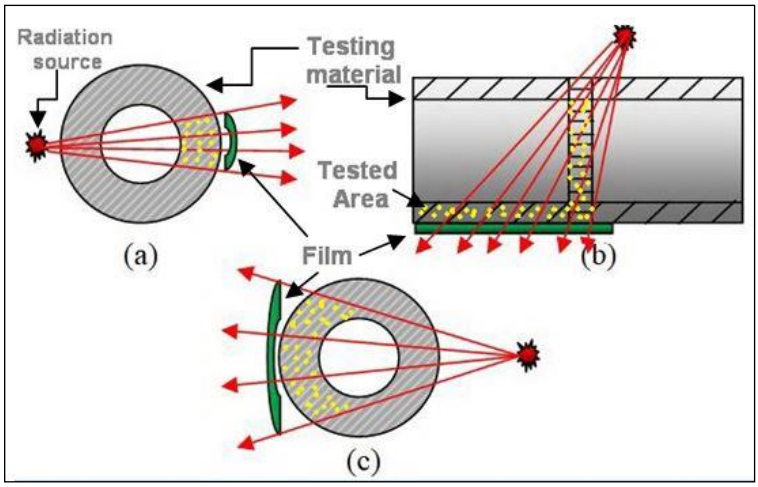

Figure 9: Double wall penetration method; (a) single image (b) double image (c) super imposing image

Double wall-double image

This method is especially preferred for weldments of pipes diameters up to 90mm. By this application, either far away to source or the near film sides can be tested at once. However minimum two posing is needed to scan the complete weld regions as illustrated in Figure 9-b.

Super-imposing technique

Super-imposing method is applied when double image could not be possible in consequence of the regional limitations for the pipe type weldments up to diameters of 90mm. Hence minimum 3 exposures are needed for whole regions of the weld as an example given in Figure 9-c.

● ***Double Film Method***

Double film method provides imaging of two different cross-sectioned complex shaped parts at only single exposure. The principle idea can be explained as faster films for thick sections and slower films for thin sections. Therefore two different thicknesses of a material can be investigated at just one exposure simultaneously.

There are many other radiographic inspection techniques asserted by scientists worldwide like real time radiography, neutron radiography and etc. (ASM Handbook Vol. 17, 1997; Raj et al., 2002). But in fact the other specified methods are not so common among the industrial radiography imaging in consequence of very high costs and also high investment prices.

The operators and/or employers in radiography sector must be aware of government regulations arranging public health because of the radiation risks. Ferrous and non-ferrous and also metallic and non-metallic materials can be tested by radiographic imaging. Almost whole cross sections of the parts or materials can be successfully inspected.

2.6. Eddy-Current Testing

Eddy-current is an alternating electrical current with frequencies ranging from 1 kHz to 2 MHz passes through a coil and generating an alternative magnetic field around the coil. When this coil is brought very closer (almost touching but no contact) to an electrically conductor material, an Eddy current is formed on

material in consequence of the electromagnetic induction.

Whether any discontinuity or a flow exists close to the surface of the tested material these Eddy currents disturbs and alters the characteristics of current flow. The changes in impedance provide important data detected by primary (original) coil or as a voltage change by a secondary coil.

Eddy currents are in parallel direction with the coils winding direction. The change in impedance can be effected by; the distance between coil and the tested part, test frequencies, electrical conductivity and magnetic permeability, geometrical factors and temperature of tested material. Schematic representation of Eddy-Current Testing is given in Figure 10.

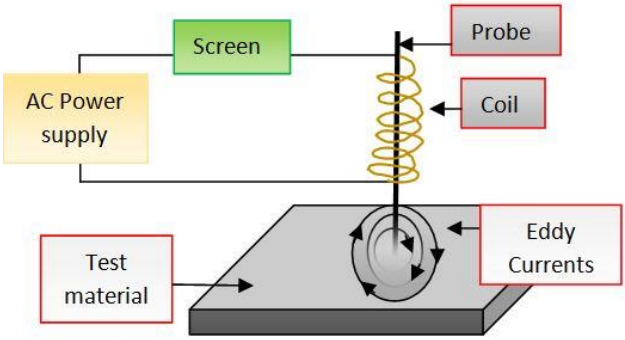

Figure 10: Schematic representation of Eddy-Current Testing.

Operator adjusts the frequencies for efficient inspections. Higher frequencies give lower depth of penetration besides accelerates the inspection speed and presents better sensitivities. The geometry and dimensions of probes can be designed according to the parts to be tested. However a probe can investigate many types and shapes of materials whether suitable.

There are numerous traditional and advanced Eddy Current testing methods and instruments. Eddy current testing is also used for evaluating conductivity, hardness and strength of materials. Besides

dimensions, heat treatment conditions and coating thicknesses of materials can also be investigated. Metallic based materials flaws approximately up to 6mm in depths from the surface can be effectively inspected (Raj. et al., 2002).

The materials to be tested by Eddy currents must be electrically conductive and no matter they are ferromagnetic or non-ferromagnetic (García-Martín J. et.al, 2011). The method is not extensively used as compared to other non destructive inspection methods because of the very high investment costs of complicated instruments.

3. Conclusions

In this study, a review was carried out on non-destructive testing methods including visual test, ultrasonic test, magnetic particle inspection, radiographic inspection and Eddy-current testing. Basic principles, application areas, advantages, disadvantages and comparison of these non-destructive techniques were briefly explained.

There are numerous non destructive testing methods either still being used by many industrial sectors or not used but still going on being a research field by many scientists.

Among them just a few are applied within standard accredited documents such as ASTM and EN norms worldwide especially in serious industrial fields like aerospace, railways, defense and automotive.

The operators have to get training courses from accredited organizations about application of methods, reporting and taking important responsibilities.

Each NDT method has a specific application field. One method can be replaced by another or cannot be used instead of another however applying more than one method can be a requisite

due to the technical security needs of the parts or materials. Substitution of a method by another depends on technical requirements and types of the tested parts.

In general; MT, PT, VT and ET methods are efficiently suitable for detecting only surface and/or near defects while RT and UT are better in inspection of volumetric inner flaws.

Selection or designing of an NDT method depends mainly on varieties of expected discontinuities, types of materials or alloys, production processes, test duration times, instruments, finance and costs, geometric factors of parts.

Non destructive testing allows reducing costs in manufacturing processes saves time and profits needless subsequent tests.

References

ASM Metals Handbook, The committee of ASM Handbook, Volume 17, Non destructive evaluation and quality control, (1997), pp: 87-94, 136-259, 339-407, 486-763, ASM International, The Materials Information Company, ISBN 0-87170-007-7.

ASTM A802, Standard practice for steel castings surface acceptance standards, visual examination, (2019) ASTM International, USA.

ASTM E165/E165M, Standard practice for liquid penetrant testing for general industry, (2018), ASTM International, USA.

ASTM E309-16, Standard practice for eddy current examination of steel tubular products using magnetic saturation, (2016), ASTM International, USA.

ASTM E1001-16, Standard practice for detection and evaluation of discontinuities by the immersed pulse echo ultrasonic method using longitudinal waves, (2016), ASTM International, USA.

ASTM E1417/E1417M, (2016), Standard practice for liquid penetrant testing, ASTM International, USA.

ASTM E1444/E1444M-16e1, Standard practice for magnetic particle testing, (2016), ASTM International, USA.

ASTM E1742/E1742M-18, Standard practice for radiographic examination, (2018), ASTM International, USA.

Brandes E.A., Brook G.B., (1992), Smithells Metals Reference Book, 7th edition, Butterworth Heinemann, p. 4-1, ISBN: 0 7506 3624 6, Great Britain.

Büyüköztürk O., et.al., (2013), Non destructive testing of materials and structures, Proceedings of NDTMS, Springer, Doi: 10.1007/978-94-007-0723-8.

Cahn R. W., Haasen P, (1996), Physical Metallurgy Volume 2, p.1119, 4th edition, North Holland Publications, Elsevier Science, The Netherlands, ISBN: 0 444 89875 1.

Dwivedi S.K., Vishwakarma M., Soni A, Advances and researches on non-destructive testing: A review, (2018), Materials today, Proceedings, pp: 3690-3698, Elsevier.

EN ISO 2400, Non destructive testing-ultrasonic testing, specification for calibration block No: 1, (2013), International Standards Organization.

EN ISO 3452-1, (2013), Non destructive testing, penetrant testing, Part 1: General Principles, International Standards Organization.

García-Martín, J.; Gómez-Gil, J.; Vázquez-Sánchez, E. Non-Destructive Techniques Based on Eddy Current Testing. Sensors, (2011), 11, 2525-2565. https://doi.org/10.3390/s110302525

Hass K., Riobo L.M., Gonzales G., Veiras F.E., Quintian F.P., (2019), Software defined laser ultrasonics: non-destructive

testing, 22nd annual conference on novel optical systems methods and applications, San Diego CA., USA.,

Hellier C.J., (2003), Handbook of non-destructive evaluation, McGraw-hill Publications, Doi: 10.1036/007139947X.

Ida N., Meyendorf N., (2019), Handbook of advanced non destructive evaluation, Springer, USA. Doi: 10.1007/978-3-319-26553-7

Kurtz M., (1998). Mechanical Engineers Handbook, 2nd Edition, Volume 1, Materials and Mechanical Design, p. 3,A Wiley Interscience Publication, USA.

Luo S.T., Tan X.L., Pan M.C. Fan C.G., (2011), Progress of Laser-generated Ultrasonic Non-destructive Testing Technology, Proceedings of SPIE, International symposium on photoelectric detection and imaging, Book series, Volume 8192, Part1, ISBN: 978-0-81948-833-6.

Mordfin L., (2002), Handbook of reference data for non destructive testing, ASTM International, USA. ISBN 0-8031-2092-3.

Omar M., (2012), Non destructive testing methods and new applications, Intech Publications, ISBN: 978-953-51-0108-6, Crotia.

Paul E.M., (2005), Introduction to non destructive testing, a training guide, 2nd edition, Wiley interscience publications. New Jersey, USA, ISBN: 13 978-0-471-42029-3.

Pecur I.B., Stirmer N., Galic J., (2009), Testing polymer modified concrete by non-detructive methods, Gradevinar, Volume 61., issue: 7, pp: 655-662.

Peta K., Zurek J., Patalas A., (2018), Non destructive testing of automotive heat exchangers, 3rd International Scientific Conference on Innovative Technologies in Engineering Production (ITEP), Slovakia.

Schabovicz K., (2019), Non destructive testing of materials in civil engineering, Materials, Volume 12, issue: 19.

Vlack, L.H.V, (1994). Elements of Material Science and Engineering Sixth Edition, p. 13, *Addison Wesley Publishing Company*.

Wang, L., Liu, Y., Yang, C., & Gao, M. (2021). Study of porosity suppression in oscillating laser-MIG hybrid welding of AA6082 aluminum alloy. *Journal of Materials Processing Technology*, 292(May 2020), 117053. Retrieved from https://doi.org/10.1016/j.jmatprotec.2021.117053